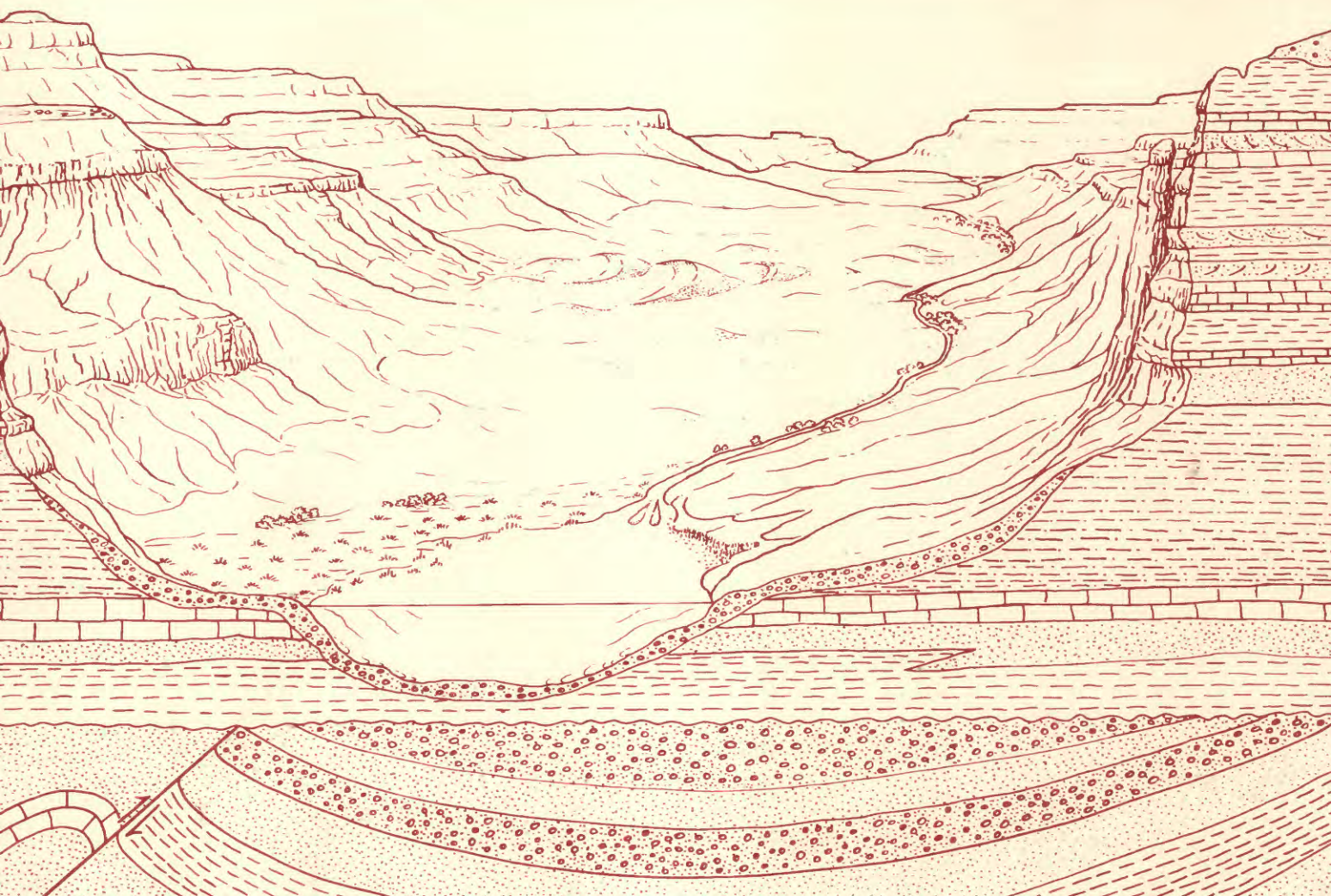


Surface Vitrinite Reflectance Study of the
Uinta and Piceance Basins and Adjacent
Areas, Eastern Utah and Western Colorado—
Implications for the Development of
Laramide Basins and Uplifts

U.S. GEOLOGICAL SURVEY BULLETIN 1787-DD



Chapter DD

Surface Vitrinite Reflectance Study of the Uinta and Piceance Basins and Adjacent Areas, Eastern Utah and Western Colorado—Implications for the Development of Laramide Basins and Uplifts

By RONALD C. JOHNSON and VITO F. NUCCIO

A multidisciplinary approach to research studies of sedimentary rocks and their constituents and the evolution of sedimentary basins, both ancient and modern

U.S. GEOLOGICAL SURVEY BULLETIN 1787

EVOLUTION OF SEDIMENTARY BASINS—UINTA AND PICEANCE BASINS

U.S. DEPARTMENT OF THE INTERIOR
MANUEL LUJAN, JR., Secretary

U.S. GEOLOGICAL SURVEY
Dallas L. Peck, Director



Any use of trade, product, or firm names in this publication is for descriptive purposes only and does not imply endorsement by the U. S. Government

UNITED STATES GOVERNMENT PRINTING OFFICE: 1993

For sale by
USGS Map Distribution
Box 25286, Building 810
Denver Federal Center,
Denver, CO 80225

Johnson, Ronald Carl, 1950—

Surface vitrinite reflectance study of the Uinta and Piceance basins and adjacent areas, eastern Utah and western Colorado—implications for the development of Laramide basins and uplifts / by Ronald C. Johnson and Vito F. Nuccio.

p. cm.—(U.S. Geological Survey Bulletin ; 1787-DD)

(Evolution of sedimentary basins—Uinta and Piceance basins ; ch. DD)

Includes bibliographical references (p.).

Supt. of Docs. no.: I 19.3:1787-DD

1. Geology, Stratigraphic—Cretaceous. 2. Geology, Stratigraphic—Tertiary.
3. Geology, Structural—Colorado—Piceance Creek Basin. 4. Geology,
Structural—Uinta Basin (Utah and Colo.). I. Nuccio, Vito F. II. Title.
III. Series. IV. Series: Evolution of sedimentary basins—Uinta and Piceance
basins ; ch. DD.

QE75.B9 no. 1787-DD

[QE688]

557.3 s—dc20

[551.7'7'09792]

92-10230
CIP

CONTENTS

Abstract	DD1
Introduction	DD1
Previous vitrinite reflectance studies	DD4
Estimating overburden removed using stratigraphic projections and geologic inference	DD4
Estimating overburden removed using surface vitrinite reflectance	DD10
Sampling and analytical techniques	DD10
Results	DD11
Pre-Cretaceous rocks	DD11
Dakota Sandstone, Mowry Shale, and Frontier Formation	DD11
Mancos Shale	DD11
Mesaverde Group	DD12
North Horn, Fort Union, Colton, and Wasatch Formations	DD13
Green River Formation	DD14
Uinta and Duchesne River Formations	DD14
Estimating overburden removed by extrapolating vitrinite reflectance versus depth profiles	DD15
Estimating overburden removed using burial reconstructions of surface samples	DD18
Implications for the structural development of Laramide uplifts using surface vitrinite reflectance samples	DD22
Summary	DD24
References cited	DD27
Appendix—Location, formation, age, and vitrinite reflectance data for surface samples from the Uinta, Piceance, and Eagle basins, Utah and Colorado	DD30

PLATES

[Plates are in pocket]

1. Map showing general geology, selected vitrinite reflectance values, and locations of surface samples and drill holes used to construct vitrinite reflectance profiles, Uinta and Piceance basins and adjacent areas, eastern Utah and western Colorado.
2. Generalized time-stratigraphic cross section for Mississippian and younger strata in the Uinta and Piceance basins and adjacent areas, eastern Utah and western Colorado.

FIGURES

- 1–5. Maps showing:
 1. Generalized geology and structure of Uinta and Piceance basins and surrounding uplifts DD2
 2. Elevation of 0.73-percent Rm thermal maturity level, Piceance basin and eastern Uinta basin DD5
 3. Elevation of 1.10-percent Rm thermal maturity level, Piceance basin DD6
 4. Temperatures at 0.73-percent Rm level during maximum burial, Piceance basin DD7
 5. Temperatures at 1.10-percent Rm level during maximum burial, Piceance basin DD8

- 6-16. Vitrinite reflectance profiles using:
 6. Subsurface data from Mobil T-52-19G well and estimated surface Rm value **DD15**
 7. Subsurface data from Chancellor 398-10-1 well and estimated surface Rm value **DD16**
 8. Subsurface data from MWX site and surface sample 86-2G **DD16**
 9. Subsurface data from Barrett A-2 Crystal Creek well **DD17**
 10. Subsurface data from Chorney 1-14 oil and gas test well and USGS CH-9A shallow oil-shale corehole **DD17**
 11. Subsurface data from Tipperary 1-30 F Bear Gulch oil and gas test well and Skyline Hydrocarbon 2 shallow oil-shale corehole **18**
 12. Subsurface data from Tenneco 20-4 well and surface sample 86-1B **DD18**
 13. Subsurface data from TRW Sunlight Federal 2 well and surface samples at Fourmile Creek along Grand Hogback **DD19**
 14. Subsurface data from Mid-America 1 Unit well and surface sample 85-97B **DD19**
 15. Subsurface data from Mountain Fuels 1 and 3 Island Unit wells and surface sample 86-9D **DD20**
 16. Subsurface data from Shell 1-11-B4 Brotherson well and surface sample 85-97J **DD20**
- 17-19. Graphs showing burial curves for:
 17. Sample of Cameo-Fairfield coal zone, Mobil T-52-19G well **DD21**
 18. Typical surface sample of Mesaverde Group on Douglas Creek arch **DD21**
 19. Surface sample of Duchesne Formation collected in area of Altamont-Bluebell oil field **DD21**
- 20, 21. Graphs showing:
 20. Overburden and geothermal gradients needed to explain observed vitrinite reflectance values, Uinta and Piceance basins and Douglas Creek arch **DD22**
 21. Excess overburden and excess thermal gradient above present-day needed to explain observed vitrinite reflectance values, Uinta and Piceance basins and Douglas Creek arch **DD23**
- 22, 23. Graphs showing burial curves for surface samples of Mesaverde Group collected:
 22. Along Piceance Creek water gap **DD24**
 23. From Harvey Gap **DD25**
24. Geologic cross section across Grand Hogback at Piceance Creek water gap **DD25**
25. Graph showing burial curve for area of samples 86-5G and 86-5H, northeast flank of San Rafael Swell **DD26**

Surface Vitrinite Reflectance Study of the Uinta and Piceance Basins and Adjacent Areas, Eastern Utah and Western Colorado—Implications for the Development of Laramide Basins and Uplifts

By Ronald C. Johnson and Vito F. Nuccio

Abstract

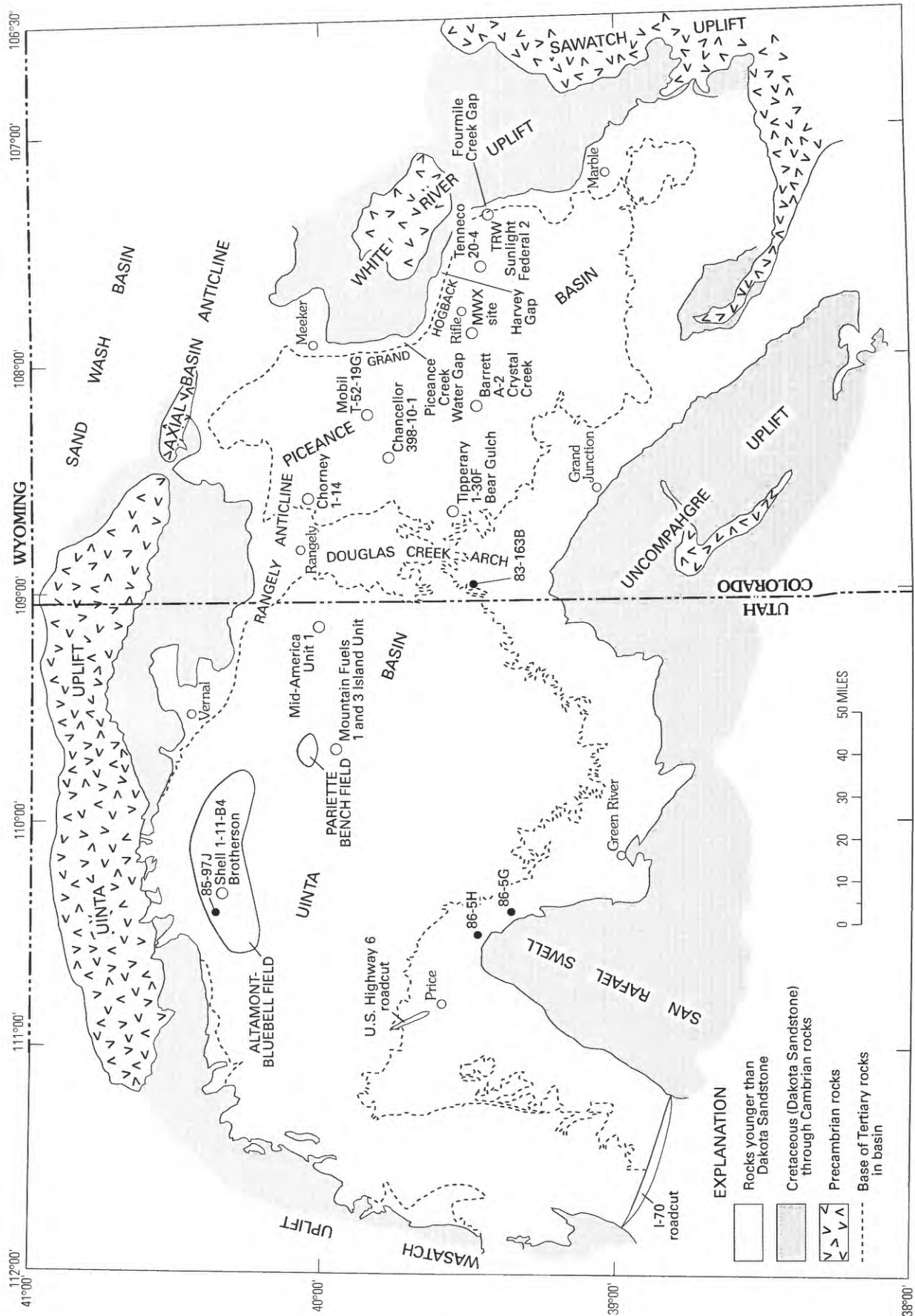
A study of mean random vitrinite reflectance (R_m) of surface and near-surface samples was conducted in western Colorado and eastern Utah in order to better understand the subsidence and thermal histories of the Laramide (Late Cretaceous through Eocene)-age Uinta and Piceance basins and to estimate the thickness of overburden removed from the two basins. The history of uplift on some of the adjacent Laramide uplifts was also studied. In the first part of the study, surface vitrinite reflectance information was combined with subsurface information to create R_m versus depth plots; these plots were extrapolated to R_m values of 0.20 and 0.30 percent, which are believed to be R_m values for vitrinite near the surface in a basin that has not undergone erosion. In the second part of the study, comparisons were made between measured vitrinite reflectance values and reflectance values predicted by applying coalification models to burial curves constructed from geologic inference. Estimates of overburden removed in the Piceance basin made by extrapolating eight R_m versus depth plots to R_m 0.20 and 0.30 percent generally bracket estimates made from geologic inference, whereas estimates for the Uinta basin made by extrapolating the three R_m versus depth plots vary widely. Coalification models generally underpredict surface vitrinite reflectance values in the two basins using burial curves constructed from geologic inference. Coalification models also markedly underpredict reflectance values on the White River uplift east of the Piceance basin. These results contrast with those from previous investigations of deep subsurface coals in the Piceance basin in which coalification models tended to overpredict vitrinite values using similar burial curves and similar assumptions. The problems with interpreting surface vitrinite reflectance data are substantial, but nevertheless our results suggest that the thermal regime in the Piceance basin may have been significantly different in the past. Our results can be explained if convective flow of hot

fluids into shallow areas of the basin was a significant heat-transferring mechanism in the past.

INTRODUCTION

Mean random vitrinite reflectance (R_m) is used extensively to reconstruct the subsidence and thermal histories of sedimentary basins. This paper presents results of a surface vitrinite reflectance study of the Uinta and Piceance basins and adjacent areas of eastern Utah and western Colorado, herein referred to as the Uinta-Piceance basin area. The study area is rectangular in shape and extends from about lat 38° to 41° N. and from about long 106° to 113° W. (plate 1). The boundaries of the study area were chosen to include two Laramide sedimentary basins—the Uinta basin of eastern Utah and western Colorado and the Piceance basin of western Colorado—and parts of the surrounding Laramide uplifts.

The Piceance basin is bounded on the north by the Axial basin anticline, on east by the White River and Sawatch uplifts, on the south by the San Juan Volcanic Field, and on the southwest by the Uncompahgre uplift. The Uinta basin is bounded on the north by the Uinta uplift, on the south by the Uncompahgre uplift and the San Rafael anticline, and on the west by the Wasatch uplift. The basins are separated by the Douglas Creek arch, a broad, low-amplitude structural arch that acted as a hingeline between the two subsiding basins during the Laramide orogeny (Johnson and Finn, 1986). The purposes of this study were (1) to estimate the thickness of overburden removed from the Uinta-Piceance basin area by extrapolating vitrinite reflectance versus depth



profiles, (2) to estimate overburden removed by using burial reconstructions of surface vitrinite reflectance samples, and (3) to reconstruct the structural history of Laramide uplifts by using surface vitrinite reflectance data. These reconstructions are an important tool in understanding how sedimentary basins form and determining when and where hydrocarbon generation has occurred.

Vitrinite is derived from the metamorphism of woody plant material and is a common organic component in sedimentary rocks. Vitrinite reflectance is a measure of the proportion of the light reflected from a polished vitrinite grain. It is directly related to the degree of metamorphism of the vitrinite grain and can be directly converted to coal rank. Vitrinite reflectance values have been correlated with oil and gas generation for potential source rocks (Dow, 1977; Waples 1985). For example, Waples (1985) stated that oil generation begins over a range of vitrinite reflectance values depending on the type of kerogen; oil generation begins at about 0.45–0.50 percent Rm for high sulfur kerogen, 0.60 percent Rm for type II kerogen, and 0.65 percent Rm for type III kerogen. Oil generation also ends over a range of vitrinite reflectance values, but 1.35 percent Rm is commonly accepted as the value at which oil begins to break down to shorter chain hydrocarbons. Dow (1977) stated that oil generation by liptinitic-rich source rocks begins between 0.50 and 1.35 percent Rm. Wet gas is generated from mixed organic matter and by the breakdown of oil between 0.80 and 2.0 percent Rm, and dry gas or methane is generated from humid organic matter and by the breakdown of wet gas between about 1.0 and 3.0 percent Rm. The vitrinite reflectance method is commonly supplemented by other types of analysis of organic matter such as Rock-Eval pyrolysis.

Models have been developed that predict vitrinite reflectance values based on the integrated time-temperature history of a rock. These models fall into two general categories, time-dependent models and time-independent models. Time-dependent models assume that vitrinite metamorphism is a first-order chemical reaction, or that time and temperature are interchangeable factors in changing its reflectance (Karweil, 1955; Lopatin, 1971; Hood and others, 1975; Waples, 1980). In these models, the entire burial history of a sample is integrated to predict the level of thermal maturity. Time-independent models suggest that vitrinite equilibrates fairly rapidly, a million years or less, to a given temperature and will not metamorphose further until the temperature is raised (Suggate, 1982; Barker and Pawlewicz, 1986a;

Barker, 1989). In other words, vitrinite reflectance is, in most geologic instances, a paleothermometer that records the maximum burial temperature to which the vitrinite was subjected. Both models are calibrated using reconstructed burial and thermal histories from sedimentary basins, and the considerable amount of uncertainty in these reconstructions results in a tremendous amount of scatter in the data. Recently, attempts to test the models have been made using nonorganic recorders of thermal history such as apatite annealing (Naeser, 1979, 1981), fluid inclusions (Roedder, 1984), and clay transformations (Pollastro and Barker, 1986), but a complete discussion of the merits of these models is beyond the scope of this paper. For this study we used the time-dependent model of Lopatin (1971) and the maximum-temperature-only-dependent model of Barker (1989).

Several problems with using vitrinite reflectance analysis have been identified. (1) Vitrinite is not totally uniform, and different types of vitrinite give slightly different vitrinite reflectance values under the same geologic conditions. (2) Fusinite or fossil charcoal formed by natural burning prior to deposition is commonly incorporated into sediments and can be difficult to distinguish from high-rank vitrinite. (3) In dispersed kerogen samples, other macerals (exinite, inertinite, and semifusinite) and organic particles such as solid bitumen, chitinozoans, graptolites, and scolecodonts are sometimes mistaken for vitrinite (Goodarzi, 1984; Goodarzi and Norford, 1985; Bertrand and Heroux, 1987). (4) Weathering, which is not always easy to detect, can raise or lower the vitrinite reflectance reading such as at Bell Creek field, Montana, where coaly organic matter from surface samples above the field shows significant increases in apparent vitrinite reflectance related to alteration of the coal in an environment of petroleum microseepage (Barker and Pawlewicz, 1986b). (5) Solar heating of a sample exposed on the surface for an extended period of time could conceivably raise the vitrinite reflectance value. (6) Vitrinite reflectance can be influenced by the chemical composition of associated organic matter or by diagenetic events; these influences cause vitrinite to undergo a physiochemical change that lowers the reflectance. Reflectance suppression can be caused by the association of vitrinite and hydrogen-rich organic matter (Hutton and Cook, 1980; Price and Barker, 1984) or by impregnation of bitumen in the vitrinite (Walker and others, 1983). Because bitumen and zooclasts mature at different rates than vitrinite, misidentification can lead to erroneous interpretation of the level of maturation.

It is likely that effects of groundwater and (or) meteoric water can also influence organic matter in surface and near-surface samples. Simple weathering of coals does not generally influence vitrinite reflectance if oxidized vitrinite pieces are avoided. Chandra (1962) concluded that mean random vitrinite reflectance does not vary significantly between weathered and unweathered coal samples from the same

Figure 1 (facing page). Generalized geology and structure of Uinta and Piceance basins and surrounding uplifts. Areas where no geologic contacts are shown were not sampled extensively for this study. Rocks younger than latest Eocene–early Oligocene are not shown. Locations of vitrinite reflectance extrapolations and burial reconstructions discussed in text are shown. Modified from Johnson (1985).

seam. Marchioni (1983) reported that weathering effects in bituminous coal (0.90–1.50 percent Rm) caused a decrease in vitrinite reflectance by 0.10–0.20 percent, but that such effects in low-rank coal (0.50 percent Rm) caused an increase in vitrinite reflectance of about 0.05–0.10 percent. In a similar study, Ingram and Rimstidt (1984) concluded that vitrinite reflectance is a reliable indicator of rank if measurements are taken away from weathered features. If, however, the grain(s) of vitrinite is totally oxidized or weathered, the “weathered features” (commonly a halo around the grain) will be unidentifiable and the grain(s) mistaken for unweathered.

PREVIOUS VITRINITE REFLECTANCE STUDIES

A considerable amount of subsurface vitrinite reflectance information and a minor amount of surface information has been published for the Uinta-Piceance basin area. Vitrinite reflectance maps have been generated for the Cameo-Fairfield coal zone of the Upper Cretaceous Mesaverde Group (plate 2) in the Piceance basin (Freeman, 1979; Nuccio and Johnson, 1983) and for coals above the Castlegate and Sego Sandstones of the Mesaverde Group in the Uinta basin (Nuccio and Johnson, 1986). Several vitrinite reflectance profiles (Bostick and Freeman, 1984; Nuccio and Johnson, 1984a; Johnson and Nuccio, 1986; Law and others, 1989) and cross sections showing variations of vitrinite reflectance with depth in both basins (Nuccio and Johnson, 1983, 1986, 1989a; Chancellor and Johnson, 1986, 1988; Johnson and Nuccio, 1986) also have been published. Johnson and others (1987) estimated the positions of the 0.73- and 1.1-percent Rm thermal maturity levels in the Piceance basin and used these thermal maturity levels to approximately define the limits of the low-permeability Mesaverde gas accumulation.

Vitrinite reflectance levels in the two basins probably are controlled by both structure and variations in thermal gradients. In general, planes of equal vitrinite reflectance dip toward the structural troughs of the Uinta and Piceance basins but at a gentler dip than the structure. This relationship is shown on figure 2, which shows the elevation of the 0.73-percent Rm thermal maturity level in the Piceance basin and eastern part of the Uinta basin, and figure 3, which shows the elevation of the 1.10-percent Rm thermal maturity level in the Piceance basin. An exception to this general relationship between planes of equal vitrinite reflectance and basin structure is on the White River Dome in the north-central part of the Piceance basin between Meeker and Rangely, Colorado (plate 1). Planes of equal vitrinite reflectance appear to pass through the White River Dome and are not deflected upward over the dome. A change in thermal gradient near the dome (Johnson and Nuccio, 1986) may be responsible.

Maps showing estimated temperatures at the 0.73- and 1.10-percent Rm levels prior to the onset of downcutting about 10 Ma for the Piceance basin (figs. 4, 5) were generated by overlaying the present-day thermal gradient map of the Piceance basin (Johnson and Nuccio, 1986) on figures 2 and 3 and assuming a present-day 10,000-ft level for the surface of maximum basin aggradation. These maps are very important because the burial reconstructions used later in this report assume that the present-day 10,000-ft level approximates the surface of maximum basin aggradation. The maps show that even if variations in present-day thermal gradients are factored in, there is a strong relationship between basin structure and the positions of these two vitrinite reflectance levels. Temperatures at the 0.73-percent Rm level prior to downcutting varied from about 140°F (60°C) along the Grand Hogback and southern margin of the basin to more than 280°F (138°C) near the structural trough in the northern part of the basin. Temperatures at the 1.10-percent Rm level prior to downcutting varied from about 160°F (71°C) in the southern part of the basin to more than 320°F (160°C) in the northern part.

ESTIMATING OVERBURDEN REMOVED USING STRATIGRAPHIC PROJECTIONS AND GEOLOGIC INFERENCE

The thickness of overburden removed from the Uinta and Piceance basins has previously been estimated using stratigraphic projections and geologic inference. Isopach maps can be used to estimate thicknesses of intervals that are still at least partly preserved in the basins, but estimates of thicknesses of units that have been totally removed by erosion must also be made. The area of the Uinta and Piceance basins was uplifted regionally starting about 10 Ma and a spectacular system of canyons cut through the region by the Colorado River system. Downcutting has been so extensive throughout the study area that only scattered remnants of the pre-uplift surface can be identified. Remnants of this surface are preserved beneath 9.7-million-year-old basalt flows in the south-central part of Piceance basin and beneath basalt flows as old as 24 million years on the White River uplift east of the Piceance basin. This pre-uplift surface presently is at an elevation of about 10,000 ft in both the south-central Piceance basin

Figure 2 (facing page). Approximate elevation (in feet) of 0.73-percent Rm thermal maturity level in Piceance basin and eastern Uinta basin. Constructed using information from Johnson and others (1987) and surface vitrinite reflectance information from this report. Areas where no geologic contacts are shown were not sampled extensively for this report. Rocks younger than latest Eocene–early Oligocene are not shown.

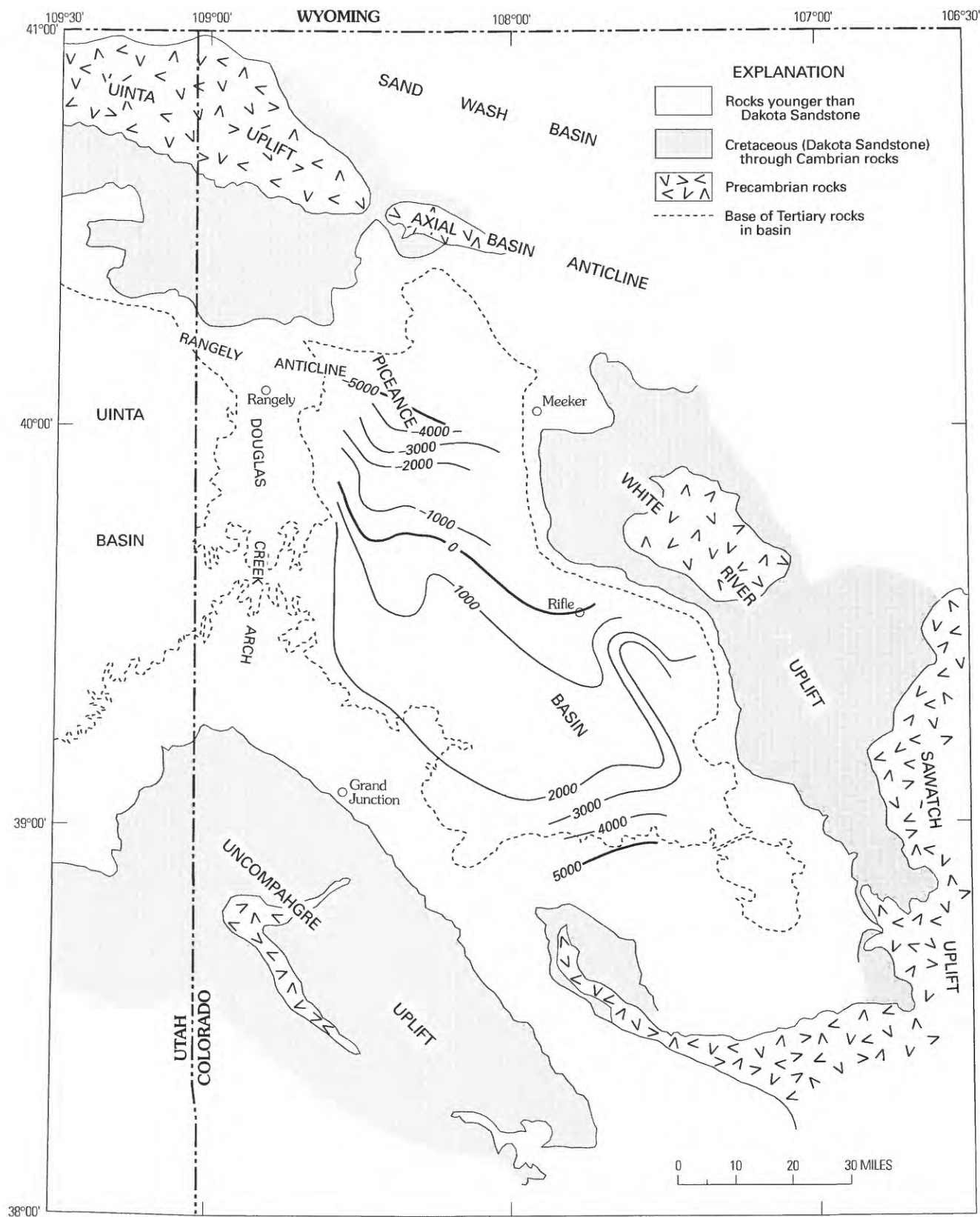


Figure 3. Approximate elevation (in feet) of 1.10-percent R_m thermal maturity level in Piceance basin. Constructed using information from Johnson and others (1987). Areas where no geologic contacts are shown were not sampled extensively for this report. Rocks younger than latest Eocene–early Oligocene are not shown.

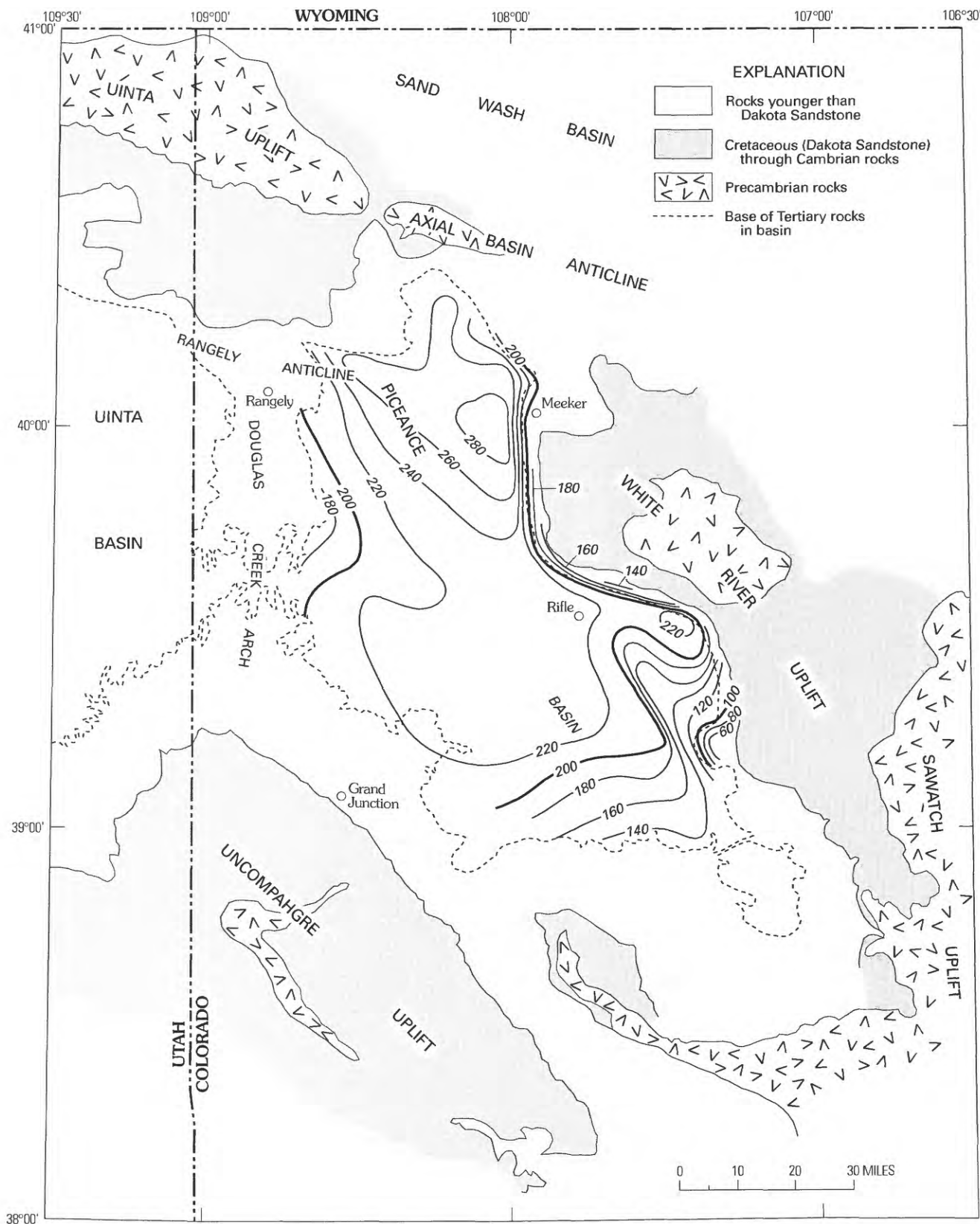


Figure 4. Temperatures in degrees Fahrenheit (°F) at 0.73-percent Rm level in Piceance basin during maximum burial assuming present-day geothermal gradients and present-day 10,000-ft level as the level of maximum burial.

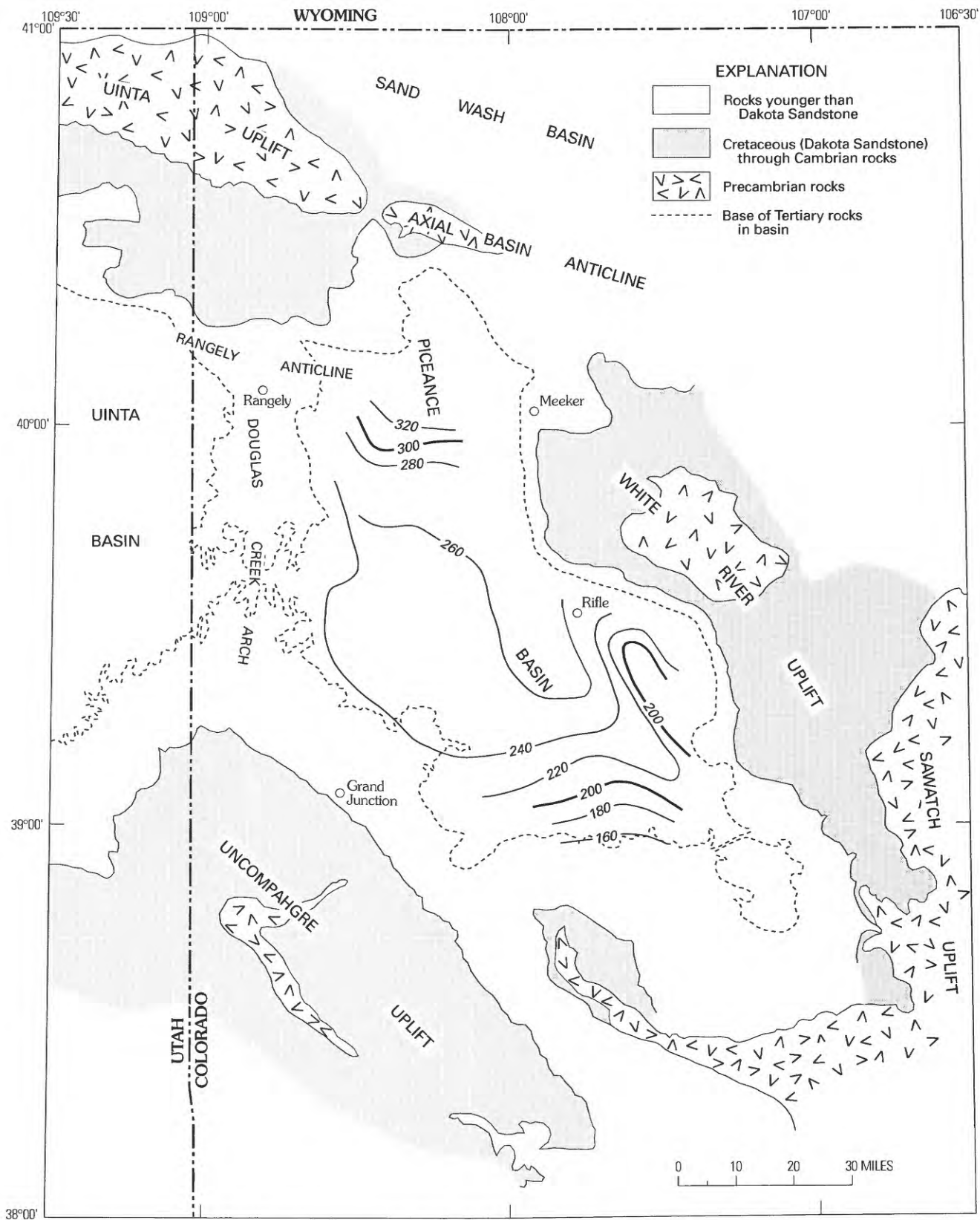


Figure 5. Temperatures in degrees Fahrenheit (°F) at 1.10-percent Rm level in Piceance basin during maximum burial assuming present-day geothermal gradients and present-day 10,000-ft level as the level of maximum burial. Areas where no geologic contacts are shown were not sampled extensively for this report. Rocks younger than latest Eocene–early Oligocene are not shown.

and on the White River uplift; perhaps the uplift had been eroded to about the same elevation as the Piceance basin prior to deposition of the basalts at 24 Ma. This surface clearly truncates upper Eocene rocks toward the southwestern margin of the Piceance basin and may have begun to form in the late Eocene during the final stages of the Laramide orogeny (Johnson and Nuccio, 1986). Johnson and Nuccio suggested that this surface covered much of Piceance basin prior to regional uplift and downcutting about 10 Ma, and they used this surface to estimate the thickness of overburden removed during the last 10 million years. The thickness of section removed beneath this surface is unknown but probably increases toward the margins of the Laramide-age Piceance basin. Johnson and Nuccio reconstructed burial curves only near the structural trough of the Piceance basin, where the thickness of section removed was probably minimal.

Significant deposition and erosion may have occurred in the Uinta and Piceance basins between the development of the late Eocene–early Oligocene erosion surfaces and the onset of regional uplift and downcutting about 10 Ma. The southern part of the Piceance basin was buried under an unknown thickness of volcanic debris following an Oligocene igneous event. Shallow intrusions of intermediate composition were emplaced in the southern part of the Piceance basin from about 34 to 29 Ma. Exposed plutons today are as high as 14,000 ft. Venting of some of these intrusions produced extensive layers of ash and breccia over the southern Piceance basin, but only remnants of this ash layer remain. Gravels and variegated claystones as thick as 900 ft are locally preserved beneath basalt flows on Grand Mesa in the south-central part of the Piceance basin (Yeend, 1969). Clasts in this unit probably were derived from Oligocene plutons to the south.

An east-west-trending valley was cut across the northern part of the study area prior to 25 Ma and partly filled by sediments of the upper Oligocene and Miocene Browns Park Formation (plate 1) (Sears, 1924; Bradley, 1936; Hansen, 1965; Izett, 1975). Tributaries from this valley could have extended southward into the Uinta and Piceance basins, removing a significant thickness of strata. The Piceance Creek drainage system in the north-central part of the Piceance basin (plate 1) flows north into the present-day White River and follows geologic structure to a remarkable degree; thus, the system may have developed prior to the end of structural movement near the end of the Laramide orogeny (Whitney and Andrews, 1983; Whitney and others, 1984). The ancestral Piceance Creek could have drained north into this east-west-trending valley, and a significant amount of erosion may have occurred in the ancestral Piceance Creek drainage system during this period. Another broad valley, possibly cut by the ancestral Gunnison River, is preserved beneath the West Elk Breccia, an

Oligocene volcanic breccia in the southernmost part of the Piceance basin (plate 1) (Hunt, 1969). This valley presently ranges in elevation from about 10,000 to less than 8,200 ft.

A similar late Eocene to Oligocene erosion surface, the Gilbert Peak erosion surface, is preserved along the flanks of the Uinta Mountains. This surface has been used to reconstruct post-Laramide collapse of the eastern part of the Uinta Mountains (Hansen, 1984). Laramide uplifts such as the Uinta Mountains are held up by crustal strength rather than buoyancy and are susceptible to collapse (Sales, 1983). Post-Laramide collapse occurred along roughly the same fault zones that brought the mountains up during the Laramide orogeny (Hansen, 1984). Unfortunately, the Gilbert Peak erosion surface is not preserved in the Uinta basin, and it is unclear how the collapse of the eastern part of the Uinta Mountains affected the adjacent basin.

This lack of a definable base level prior to the onset of downcutting about 10 Ma has resulted in widely varying estimates of the thickness of overburden removed during the last 10 million years from the Uinta basin. The present land surface in the Uinta basin is roughly bowl shaped, rising gently from about 5,000 ft in the center of the basin to more than 10,000 ft along both the north and south rims. In the southern half of the basin, the present-day topography and secondary streams generally follow structural dip and flow to the north, northeast, and northwest; however, this relationship probably formed since downcutting began about 10 Ma. The course of the Green River, which predates the onset of downcutting at 10 Ma, is not influenced by present-day topography. The Green River flows southwest across the eastern end of the Uinta Mountains, veers south across the Uinta basin, and then exits through the high south rim of the basin (plate 1). The remarkable course of the Green River has fascinated geologists since the days of John Wesley Powell; theories of the origin of the Green River have been described by Hansen (1969).

Tissot and others (1978) estimated that 5,840 ft of overburden was eroded from the site of the Shell 1–23–B4 Brotherson well in the Altamont-Bluebell field near the trough of the Uinta basin (plate 1) but did not explain how they arrived at their estimate. This amount of erosion would put the basin surface prior to downcutting at a present-day elevation of about 12,100 ft. Narr and Currie (1982) analyzed fluid inclusions from fractures in the Altamont-Bluebell area and produced widely varying estimates of overburden removed, from 1,112 to 9,482 ft. Pitman and others (1982) used projected thicknesses in the Pariette Bench field in the eastern Uinta basin to estimate that no more than 3,300 ft of overburden has been removed; this would put the basin surface prior to downcutting at the present-day elevation of about 8,800 ft.

Pitman and others (1987) estimated that 3,300 ft of overburden was removed from the Natural Buttes field area in the eastern Uinta basin for a present-day elevation of about 8,200 ft.

ESTIMATING OVERBURDEN REMOVED USING SURFACE VITRINITE REFLECTANCE

Surface vitrinite reflectance data can be used to estimate original depth of burial for both sedimentary basins and uplifts, providing an alternative to the traditional method of estimating overburden removed by stratigraphic projection from uneroded sections. There are two ways in which vitrinite reflectance can be used to estimate the thickness of overburden removed. First, surface vitrinite reflectance values can be combined with subsurface information from a nearby well to create a R_m versus depth curve, and, second, vitrinite reflectance data can be used directly to calculate overburden. Using the first method, the R_m versus depth information generally plot on a semilogarithmic scale as either a straight line (Dow, 1977) or a series of straight-line segments having somewhat different slopes (Law and others, 1989). The plot can then be extrapolated above the present-day ground surface to an assumed vitrinite reflectance value near the surface of a basin under maximum burial. It is very important to recognize changes in slope or "kinks" in the R_m versus depth plots when extrapolating to the surface of maximum burial. Buried erosion surfaces (unconformities) can cause breaks in the R_m versus depth plot (Katz and others, 1988). The discontinuous R_m versus depth profile at an unconformity can be completely overprinted by increased heating beyond that which occurred before exhumation. Both variations in thermal conductivity (Nuccio and Johnson, 1989b) and convective fluid flow (Law and others, 1989) can cause changes in slope. Law and others (1989) suggested that convective fluid flow during development of the Mesaverde low-permeability gas accumulation in the Piceance basin created near-vertical segments in R_m versus depth plots.

Extrapolations are difficult to make for uplifts, where little drilling has occurred and tens of thousands of feet of section have been removed, but can sometimes be made for the flanks of the uplifts, where much of the sedimentary section is still preserved. For our study, vitrinite reflectance samples were collected from the east flank of the Wasatch uplift in the western part of the study area, from the San Rafael Swell south of the Uinta basin, and from the west flank of the White River uplift east of the Piceance basin (plate 1).

Differing estimates of the point of intersection of the R_m versus depth curve and the surface under maximum burial are an important source of error and apparently arise because vitrinite does not form at the surface but at several hundred

feet depth. The depth of formation varies depending on the surface temperature and thermal regime of the area. For example, Bustin (1986) reported a near-surface rank of 0.15 percent R_m for Arctic lignites in an area of generally average to high thermal gradients. It is generally believed, however, that shallow occurrences of vitrinite have initial measured reflectance values of about 0.20–0.30 percent in coal and kerogen (Dow, 1977; Hunt, 1979; Robert, 1988), similar to values (as high as 0.29 percent) estimated from temperature- R_m models (Barker and Pawlewicz, 1986a). Obviously, the surface vitrinite reflectance value to which the R_m versus depth curve is projected can have a strong effect on the estimate of erosion. It is important, therefore, to check the surface value used in an extrapolation when possible and to realize that the difference between using surface values of 0.20 and 0.30 percent R_m can be substantial.

The second method for reconstructing the thickness of overburden removed is to use surface vitrinite information directly. In this method, a burial curve for surface samples is constructed, with the thickness of overburden removed as an unknown. A thermal gradient is assumed and the thickness of the removed overburden is solved for by using one of the models for vitrinite metamorphism. Assuming a thermal gradient for a thickness of rock that has been removed is risky at best. The lithology of the removed section is seldom known. Basin subsidence is in many cases caused by a thermal event, and thus present-day thermal gradients in basins such as the Uinta and Piceance, which are no longer subsiding, may differ considerably from thermal gradients during active subsidence. Igneous events such as the emplacement of shallow intrusions of intermediate composition in the southern part of the Piceance basin from 34 to 29 Ma and the extrusion of extensive basalt flows in the central Piceance basin starting about 10 Ma were almost certainly accompanied by some change in regional heat flow and thermal gradients. Surface water recharge from the Uinta Mountains has been cited as a possible cause for the unusually low present-day thermal gradients along the northern margin of the Uinta basin (Chapman and others, 1984). Changes with time in plumbing systems such as the one proposed by Chapman and others can thus produce changes in thermal gradients.

SAMPLING AND ANALYTICAL TECHNIQUES

Several hundred samples were collected from strata in the study area (plate 1, appendix). Dark-gray or black (color is commonly used as a possible indicator of organic richness) mudstone, shale, fine-grained sandstone, limestone, and coal were collected after digging 1–2 ft into an outcrop to obtain relatively fresh, unweathered samples. Buff to white samples were collected where dark-gray or black rocks were not available. Coal was prepared by crushing the

sample, mounting it in epoxy on a microscope slide, planing it off when hardened, and polishing it. In samples of other rock types kerogen was concentrated before analysis by crushing the sample, removing carbonate material using HCl, and separating the kerogen from the remaining mineral matter using aqueous solutions of zinc bromide (specific gravity 2.0 g/cm³). The kerogen concentrate was mounted in epoxy on a microscope slide, planed off, and polished. For all samples, mean random vitrinite reflectance from randomly oriented indigenous vitrinite grains was determined using plane-polarized incident white light, with a 546-nm monochromatic filter, in immersion oil on a nonrotating stage (Bostick, 1979; Bustin and others, 1983) on a Zeiss Universal microscope. The number of readings per sample varied widely depending on the quality of the sample (the amount of indigenous vitrinite in the sample). For samples containing abundant organic matter, the number of readings was higher; hence, the mean vitrinite reflectance value is statistically more valid than that for samples containing a paucity of vitrinite grains. As a rule of thumb, if the number of readings for a sample is greater than 30, and the standard deviation relatively small, then the mean vitrinite reflectance value is considered valid.

RESULTS

Rocks exposed on the surface in the study area are Precambrian to Holocene in age. Although units as old as Mississippian were sampled (plate 2), this study concentrated on Cretaceous and Tertiary units. The pre-Cretaceous geologic history of the study area is very complex, and no attempt was made to reconstruct burial histories for this period. It was also difficult to find suitable rock types for vitrinite reflectance studies in pre-Cretaceous units; hence, the results presented here are spotty at best.

Pre-Cretaceous Rocks

Pre-Cretaceous rocks crop out on all of the uplifts that surround the Uinta and Piceance Creek basins (plates 1, 2). In the Utah part of the study area, pre-Cretaceous rocks are exposed on the Uinta, Sawatch, and San Rafael uplifts and on scattered outcrops in the eastern part of the Basin and Range province. In the Colorado part of the study area, pre-Cretaceous rocks are exposed mainly on the White River, Sawatch, and Uncompahgre uplifts.

Twenty-seven samples were collected in Utah from pre-Cretaceous units, but only three samples, from Triassic and Jurassic units, gave satisfactory results. Two dark-gray shale samples (86-3Y, 86-3Z) from the Middle Jurassic San Rafael Group on the Wasatch uplift near Nephi, Utah, gave Rm values of 0.84 and 0.65 percent, respectively. The third

sample (86-4U), from the Lower Jurassic Glen Canyon Group on the San Rafael Swell, gave an Rm value of 1.43 percent. Many of the barren samples are from Paleozoic marine limestone formations. In these units conodont alteration index (CAI) may be a more useful tool with which to measure thermal maturity.

The thermal maturity of Lower Cretaceous and older units on the White River and Sawatch uplifts in Colorado has been measured and discussed (Nuccio and Schenk, 1986, 1987), and these units were not resampled. Pre-Cretaceous units also were not sampled from the Uncompahgre uplift.

Dakota Sandstone, Mowry Shale, and Frontier Formation

The Lower to Upper Cretaceous Dakota Sandstone, Mowry Shale, and Frontier Formation crop out along the margins of the Uinta and Piceance basins and on many of the uplifts in the study area. Strata of these units were deposited in marine, marginal-marine, and coastal-plain settings during the early history of the Cretaceous epeiric seaway (plate 2). These are the oldest strata that commonly contain carbonaceous intervals suitable for vitrinite reflectance analysis.

Nine samples of Dakota Sandstone and one sample of Frontier Formation were analyzed from the Utah part of the study area and all gave satisfactory results. Most samples are from the San Rafael and Uncompahgre uplifts south of the Uinta basin. Thirteen samples of Dakota Sandstone and one sample of Mowry Shale were sampled from the Colorado part of the study area, and ten gave satisfactory results.

Three samples of Dakota Sandstone from the San Rafael uplift area gave Rm values of from 0.50 to 0.57 percent. Thirteen samples of Dakota Sandstone from the Uncompahgre uplift and adjacent areas of the Uinta and Piceance basins gave values of from 0.55 to 1.14 percent; all but two values are between 0.50 and 0.94 percent. One sample of Frontier Formation (86-3H) from northeast of the Uinta uplift in the southwestern corner of the Bridger basin gave a value of 0.35 percent. One sample of Dakota Sandstone from beneath volcanic debris flows near Gunnison, Colorado (86-8M), near the boundary between the Piceance basin to the north and the San Juan Volcanic Field to the south, yielded a value of 0.47 percent. Two samples from the Grand Hogback near the boundary between the Piceance basin and the White River uplift in Colorado gave satisfactory results: a sample of the Dakota (87-67) gave a value of 0.90 percent, and a sample of Mowry-Frontier undifferentiated (87-70) gave a value of 0.40 percent.

Mancos Shale

The Mancos Shale is an offshore marine shale that was deposited in the Cretaceous epeiric seaway during the Late

Cretaceous (plate 2). It is generally several thousand feet thick and crops out over vast areas in the study area forming broad valleys between the topographically higher and more resistant rocks exposed in the Uinta and Piceance basins and on the surrounding uplifts.

Twenty samples of Mancos Shale were analyzed from the Uinta part of the study area. Sixteen of these samples were organic-rich shale from which kerogen was concentrated; four were coal samples. Nineteen of the samples were from the flanks of the San Rafael anticline south of the Uinta basin and gave consistent Rm values in a narrow range from 0.43 to 0.64 percent. Four of these samples were from the Interstate 70 roadcut on the Wasatch Plateau (fig. 1). Two of these samples (86-4P, 86-4Q) are coals that gave values of 0.51 and 0.54 percent, and two samples are organic-rich shale from the same stratigraphic interval (86-4O, 86-4R) that gave somewhat lower values of 0.43 and 0.45 percent.

Thirty-one organic-rich shale samples were collected from the Mancos Shale in the Colorado part of the study area, and most gave satisfactory results. Nine samples from the south flank of the Piceance basin (86-14D to 86-14H, 86-8D to 86-8F, 86-8H) gave values of from 0.31 to 0.67 percent. Ten samples from a complete section of Mancos Shale exposed near Marble, Colorado (87-98 to 87-108), gave values that varied widely from 1.25 to 4.82 percent. This section is in the Elk Mountains along the southeastern margin of the Piceance basin, an area containing extensive intrusive and extrusive rocks of Oligocene age, and the Mancos was likely metamorphosed by this igneous activity. Eight samples from the Grand Hogback, which forms the boundary between the Piceance basin and the White River uplift to the east (87-63, 87-64, 87-66, 87-68, 87-69, 87-71, 87-72, 87-76), gave values of from 0.42 to 0.68 percent.

Mesaverde Group

The Upper Cretaceous Mesaverde Group crops out throughout the Uinta and Piceance basins and is from about 2,000–2,500 ft thick in much of the Uinta basin and the Douglas Creek arch to more than 6,500 ft thick in the eastern part of the Piceance basin. The Mesaverde Group has been subdivided into formations and members of formations in most parts of the study area; however, a complete discussion of Mesaverde nomenclature is beyond the scope of this paper. In general, the Mesaverde Group can be subdivided into two major units, a lower unit consisting of several regressive marine cycles that intertongue with the underlying marine Mancos Shale and an upper, mostly fluvial unit (plate 2). Economically important coal zones are present in many of the regressive marine cycles, and some coal and carbonaceous shale are present throughout the fluvial part of the Mesaverde as well. Coal rank maps based on vitrinite reflectance have been generated for coal zones

associated with marine regressive cycles (Freeman, 1979; Nuccio and Johnson, 1983, 1986), and many vitrinite reflectance profiles through the Mesaverde are available (Bostick and Freeman, 1984; Chancellor and Johnson, 1986, 1988; Johnson and Nuccio, 1986; Nuccio and Johnson, 1989a). The position of several key vitrinite reflectance levels has also been generally determined in the Piceance basin (Johnson and others, 1987).

Twenty-three samples of Mesaverde coals were analyzed from the Uinta basin, and all but two yielded satisfactory results. Many of these samples were collected from the flanks of Laramide structures in order to study the development of these uplifts. Eight samples of Mesaverde coal and carbonaceous shale from along the Interstate 70 roadcut where it cuts through the Mesaverde Group on the Wasatch Plateau south of the town of Emery, Utah, gave Rm values of from 0.40 to 0.57 percent, with no significant increase through about 1,500 ft of section. Four samples collected from where U.S. Highway 6 cuts through the Mesaverde Group along the Wasatch Plateau, about 60 mi to the north of the previous locality, showed a slight increase in vitrinite reflectance from top to bottom through about 2,400 ft of section, from 0.49 to 0.61 percent. The last value is somewhat higher than the values of 0.55 and 0.59 percent from two samples of the underlying Mancos Shale, and vitrinite reflectance in the Mancos Shale may be somewhat suppressed. Seven Mesaverde coal samples from the Book Cliffs along the southern margin of the Uinta basin gave values of from 0.58 to 0.70 percent, or again somewhat higher than the values of from 0.43 to 0.64 percent obtained from the underlying Mancos Shale.

Sixty-one samples of Mesaverde coal and carbonaceous shale were analyzed from the Piceance basin, and all but five yielded satisfactory results. Fifteen Mesaverde coal samples from the northern part of the Douglas Creek arch, Rangely anticline, and adjacent northeastern corner of the Uinta basin area (2 from Utah and 13 from Colorado) gave consistently low results of from 0.36 to 0.56 percent. Seven Mesaverde samples from the south part of the Douglas Creek arch gave somewhat higher results of from 0.57 to 0.65 percent. The Mesaverde Group was sampled at three locations along the Grand Hogback in Colorado: the Piceance Creek water gap, Harvey Gap, and Fourmile Creek (plate 1). The underlying and overlying formations were also sampled. The Mesaverde Group has a near-vertical orientation along the Grand Hogback, which follows the western flank of the White River uplift east of the Piceance basin. Samples from the three Mesaverde profiles through the hogback are similar to those through the Mesaverde on the Wasatch Plateau in that vitrinite reflectance values are generally quite low and show surprisingly little increase from top to bottom through several thousands of feet of Mesaverde. Four Mesaverde samples from the Piceance Creek water gap gave values from 0.41 to 0.50 percent with no increase through about 5,000 ft of section.

Six Mesaverde samples from Harvey Gap increase slightly from top to bottom, from 0.59 to 0.66 percent through 4,500 ft of section, but this increase is barely distinguishable from the scatter. Vitrinite reflectance values of from 0.42 to 0.68 percent from the underlying Mancos Shale in the vicinity of Harvey Gap again suggest that vitrinite in at least some of the Mancos samples analyzed is suppressed. Five Mesaverde coal samples from the Mesaverde section at Fourmile Creek show an increase in Rm values from 0.33 to 0.65 percent through about 3,000 ft of section. Again, two samples of the underlying Mancos Shale (87-76, 87-77) gave somewhat lower values of 0.48 and 0.56 percent. Reflectance values for fourteen Mesaverde samples from the southern part of the Piceance basin vary widely from 0.46 to 4.24 percent. Oligocene magmatism in this area probably had a widely varying affect on thermal maturity.

North Horn, Fort Union, Colton, and Wasatch Formations

The mostly fluvial North Horn, Colton, and Wasatch Formations (plate 2) unconformably overlie the Mesaverde Group throughout most of the study area and were deposited in the Laramide Uinta and Piceance basins after the breakup of the Cretaceous foreland basin during Laramide uplift in latest Cretaceous and Paleocene time (plate 2). The formations are Paleocene to Eocene in age except for the lower part of the North Horn Formation in the western part of the Uinta basin and the Wasatch Plateau, which is Maastrichtian (Fouch and others, 1983).

The North Horn Formation is a mixed fluvial and lacustrine unit of Late Cretaceous Maastrichtian to late Paleocene age that overlies the Mesaverde Group and underlies the Flagstaff Member of the Green River Formation in the western part of the Uinta basin and along the Wasatch Plateau (Fouch and others, 1983). The Paleocene Fort Union Formation is a mixed fluvial, paludal, and lacustrine unit in the northern and central parts of the Piceance basin. The Colton Formation is a Paleocene to middle Eocene, variegated, mostly fluvial unit that overlies the Flagstaff Member of the Green River Formation and underlies the main body of the Green River Formation in the western part of the Uinta basin. The Wasatch Formation is a similar, upper Paleocene to lower Eocene, variegated, mostly fluvial unit in the eastern Uinta basin and Piceance basin. In the eastern Uinta basin it overlies the Mesaverde Group or the Flagstaff Member of the Green River Formation and interfingers with the overlying Green River Formation. In the southern part of the Piceance basin it directly overlies the Upper Cretaceous Mesaverde Group, whereas in the northern Piceance basin it overlies the Paleocene to lower Eocene Fort Union Formation. This difference is not considered geologically important because in the southern Piceance basin rocks similar in lithology and age to the Fort Union Formation are included

in the Wasatch Formation (Donnell, 1969). In the Piceance basin the Wasatch Formation interfingers with the overlying Green River Formation.

A single North Horn sample from the Wasatch Plateau (U86-KF-1VR) gave an Rm value of 0.49 percent, identical to the value obtained from a coal in the upper part of the underlying Blackhawk Formation (Upper Cretaceous) in the same area. A single sample in the western part of the Uinta basin ((U86-KF-1RC) gave an value of 0.52 percent, or slightly lower than the values of 0.59–0.70 percent for coals in the underlying Mesaverde Group. Two coaly fragments from the base of fluvial channel sandstones in the North Horn Formation were collected from the Interstate 70 road-cut through the Wasatch Plateau (86-4E, 86-4F), but neither gave satisfactory results. One was weathered and one contained almost all fusinite.

Rocks suitable for vitrinite reflectance analysis are rare in the Colton Formation; however, two samples of dark-gray mudstone from the Colton Formation, collected from where U.S. Highway 6 cuts across the Wasatch Plateau (86-5R, 86-5X), gave values of 1.46 and 0.40 percent, respectively. A wide range of reflectance populations in sample 86-5R suggests reworking.

Thirty-one samples of Wasatch Formation from the Piceance basin were analyzed. These samples can be divided into three general categories: pieces of coalified wood fragments from the base of fluvial channels, coaly stringers in mudstone or siltstone, and organic-rich mudstone and siltstone. Because coaly stringers and organic-rich mudstone and siltstone are rare in the Wasatch Formation, most of the samples collected were pieces of coalified wood fragments from the base of fluvial channels. Although most of these coalified wood fragments gave satisfactory analysis, many of the results are geologically unreasonable and possible causes for this will be discussed later. Few of the mudstone and siltstone samples gave satisfactory results.

Samples of the Wasatch collected from the southern part of the Piceance basin gave widely varying results. Vitrinite reflectance values for four samples from thin coal beds in the Wasatch (86-2D, 86-2G, 86-2K, 86-7Q) varied narrowly from 0.45 to 0.60 percent; however, values obtained from ten samples of coalified fragments from the base of fluvial channels varied widely from 0.53 to 2.01 percent. In several cases, samples from two closely spaced channels gave very different results. A few thin basaltic dikes are present in the area, but heating from these minor intrusions would have only metamorphosed a narrow zone of rock (Dow, 1977). At this time we feel that a most likely explanation is that many of these coaly fragments oxidized during diagenesis. Two samples of Wasatch shale from the southern part of the Piceance basin (86-7N, 86-8A) gave Rm values of 0.77 and 0.71 percent. One carbonaceous shale sample from the Wasatch in the northern part of the basin (85-64) gave a value of 0.62 percent, or slightly higher than values from the overlying Green River Formation in the area. One Wasatch

shale sample from the Sand Wash basin to the north gave a value of 1.07 percent, which seems anomalously high. Two small intrusions have been mapped about 3 mi northeast of the sample locality, but it is unlikely that these could have affected the reflectance of the samples.

Green River Formation

The Green River Formation was deposited in Lake Uinta, which covered much of the Uinta and Piceance basins and the Wasatch Plateau during the Eocene (plate 2). Lake Uinta formed during the Paleocene in the western Uinta basin and along the Wasatch Plateau to the south (Fouch, 1976) but did not expand to cover most of the area of the Uinta and Piceance basins until the Eocene. The upper Paleocene to lower Eocene lacustrine rocks in the western Uinta basin and Wasatch Plateau were originally called Flagstaff Limestone but subsequently defined as a member of the Green River Formation (Fouch, 1976). The Green River Formation consists of offshore lacustrine marlstone and oil shale and various marginal lacustrine rock types including sandstone, siltstone, ostracodal, oolitic and stromatolitic limestone, carbonate-rich mudstone, and carbonaceous shale containing thin coal beds. Limestone deposited during the early stages of Lake Uinta is commonly fossiliferous.

Thirteen samples of the Green River Formation in the Uinta basin and Wasatch Plateau were analyzed. Four of these were from the Flagstaff Member, and none gave satisfactory results. Five samples (86-5S to 86-5W) were collected in the westernmost part of the basin near Soldier Summit (fig. 1), but none gave satisfactory results. Of the four Green River samples collected in the remaining part of the Uinta basin, only two (U86-KF-2VR, 86-9D) gave satisfactory results. Sample U86-KF-2VR gave an Rm value of 0.49 percent, and sample 86-9D from the south-central part of the Uinta basin gave a value of 0.35 percent.

Thirteen samples of Green River Formation were analyzed from the Piceance basin. Seven samples (C-299, USGS CH-2, USGS CH-3, USGS CH-3A, USGS CH-4, USGS CH-9, and USGS CH-9A) were coalified fragments in lacustrine marlstone collected at shallow depths from coreholes drilled for oil-shale assessment, and all gave satisfactory values of from 0.31 to 0.51 percent. Sample 83-144P, a wood fragment collected from a rich oil-shale bed exposed on the surface, gave a value of 0.35 percent, or similar to other Green River samples in the area despite evidence that vitrinite is suppressed in rich oil shales in the Piceance basin (Nuccio and Johnson, 1984b). Three samples of thin coal beds in the lower part of the Green River Formation were analyzed. Samples 84-27G and VN-6C contained enough vitrinite to give satisfactory results (0.32 and 0.43 percent, respectively), but sample 84-36A would not take a polish and the reflectance value measured is probably low. Four samples of Green River mudstone were also analyzed,

but only one (86-7Z) contained enough vitrinite to give a satisfactory value of 0.55 percent, or slightly lower than the value of 0.71 percent obtained from a nearby sample from the underlying Wasatch Formation (sample 86-8A). Three Green River samples were also analyzed from the southern part of the Sand Wash basin because it is inside the boundary of the study area. One sample of gray silty shale from the Tipton Shale Member of the Green River Formation (sample 85-117M) contained enough vitrinite to give a satisfactory value of 0.45 percent. Two coal samples from the Luman Tongue of the Green River Formation (samples 85-177Q, 85-177R) yielded values of 0.53 percent.

Uinta and Duchesne River Formations

The Uinta and Duchesne River Formations are mixed fluvial and lacustrine units deposited during the final stages of subsidence and infilling in the Uinta and Piceance basins (plate 2). The Uinta Formation is late Eocene in age and crops out throughout much of the central areas of the Uinta and Piceance basins. It intertongues with the underlying Green River Formation and consists mainly of sandstone and some siltstone and mudstone deposited in a variety of lacustrine, marginal-lacustrine, and fluvial environments. The sandstones contain a high percentage of volcanic grains in the Piceance basin and eastern part of the Uinta basin. The Duchesne River Formation is an upper Eocene to possibly lower Oligocene, mostly fluvial unit that overlies and intertongues with the Uinta Formation in the central part of the Uinta basin. It consists predominantly of varicolored mudstone encasing lenticular sandstone bodies.

Sixteen samples of Uinta Formation in the Uinta basin were collected, but only four yielded satisfactory results. The Uinta Formation in the Uinta basin contains a highly variable array of rocks including thick sequences of lacustrine marl and oil shale, lacustrine volcanoclastic sandstone, and variegated fluvial rocks. Outcrops of lacustrine sandstone were examined throughout the Uinta basin for carbonized plant debris and wood fragments but finding unweathered outcrops was difficult. Three of the samples that gave satisfactory results were wood fragments (samples 85-74, 85-97B, 85-97E). Samples 85-74 and 85-97E from the central part of the Uinta basin yielded similar Rm values of 0.58 and 0.47 percent, respectively, and sample 85-97B, from the eastern part of the basin, gave a value of 0.41 percent. Sample 85-77 from a 1-in.-thick coal bed in a carbonaceous shale sequence gave a value of 0.48 percent.

Suitable rock types for a vitrinite reflectance study are rare in the variegated shale and lenticular sandstone of the overlying Duchesne River Formation. Six samples were collected. Five samples are from varicolored mudstone, and only one (85-73A) contained enough vitrinite to yield a satisfactory Rm value of 0.45 percent. The remaining sample (85-97J) is from a coaly carbonaceous shale about 6 in.

thick, and it also yielded a value of 0.45 percent. These two samples were from the Altamont-Bluebell oil field area and are the only reasonably reliable data points from near the deep trough of the Uinta basin.

Ten samples of Uinta Formation in the Piceance basin were collected, and eight gave satisfactory results. All were small coalified wood fragments in volcanoclastic sandstone. These fragments are generally less than an inch in diameter and less than about 4 in. long. Three samples (samples C-144, C-153, C-155) are from coreholes drilled to assess the underlying oil-shale reserves and one sample (Bar-A-2) was from an oil and gas test. The remaining six samples are from surface outcrops. Only outcrops that were well cemented with carbonate were sampled, and most of the wood chips collected had an unweathered appearance. Rm values for the eight good samples varied from 0.38 to 0.56 percent, or similar to values from nearby Green River Formation outcrops. An area of somewhat higher values of 0.47 to 0.56 percent can be discerned using both the Uinta and Green River data. This area runs northwest from the Piceance Creek dome to T. 1 S., R. 98 W. (plate 1), is close to the structural trough of the basin, and was previously defined using less data (Johnson and Nuccio, 1986).

ESTIMATING OVERBURDEN REMOVED BY EXTRAPOLATING VITRINITE REFLECTANCE VERSUS DEPTH PROFILES

Eleven vitrinite reflectance profiles are presented that were created using surface or near-surface vitrinite reflectance information (fig. 1): eight from the Piceance basin (figs. 6-13) and three from the Uinta basin (figs. 14-16). Some of these profiles have been published previously. All of the profiles are extrapolated above the present-day land surface to vitrinite reflectance values of 0.20 and 0.30 percent, giving a range of values for overburden removed. An unacceptably large range in thicknesses of overburden removed resulted from this extrapolation. In the Piceance basin, for example, extrapolation for the Mobil T-52-19G well from the central part of the basin (fig. 6) indicates that 3,700 ft of overburden has been removed using an Rm value of 0.30 percent and 7,200 ft using 0.20 percent. This would put the surface of maximum aggradation in this area at a present-day elevation of between 10,600 and 14,100 ft. A major problem in these extrapolations is large data gaps in the Rm profile that

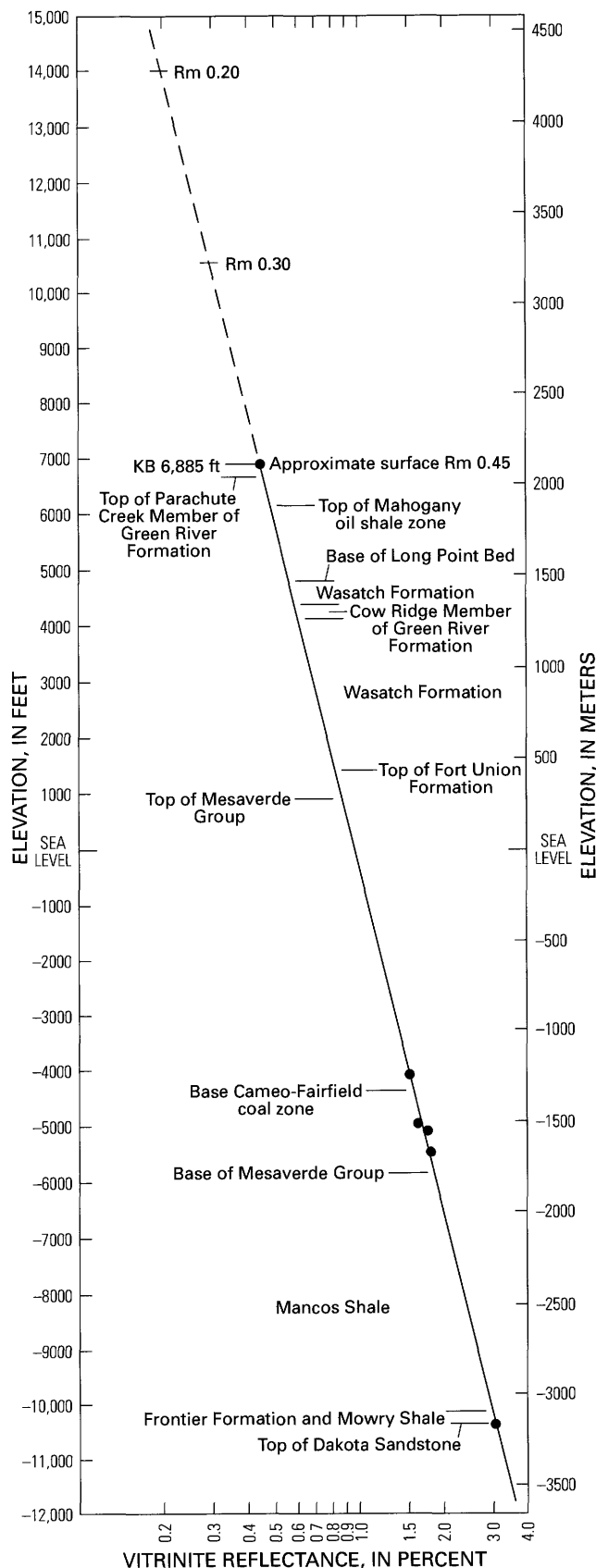


Figure 6 (facing column). Vitrinite reflectance profile using subsurface data from Mobil T-52-19G well (sec. 19, T. 2 S., R. 96 W.) (fig. 1, plate 1) and estimated surface Rm value of 0.45 percent. Selected geologic contacts and extrapolations (dashed line) to vitrinite reflectance values of 0.20 and 0.30 percent are shown.

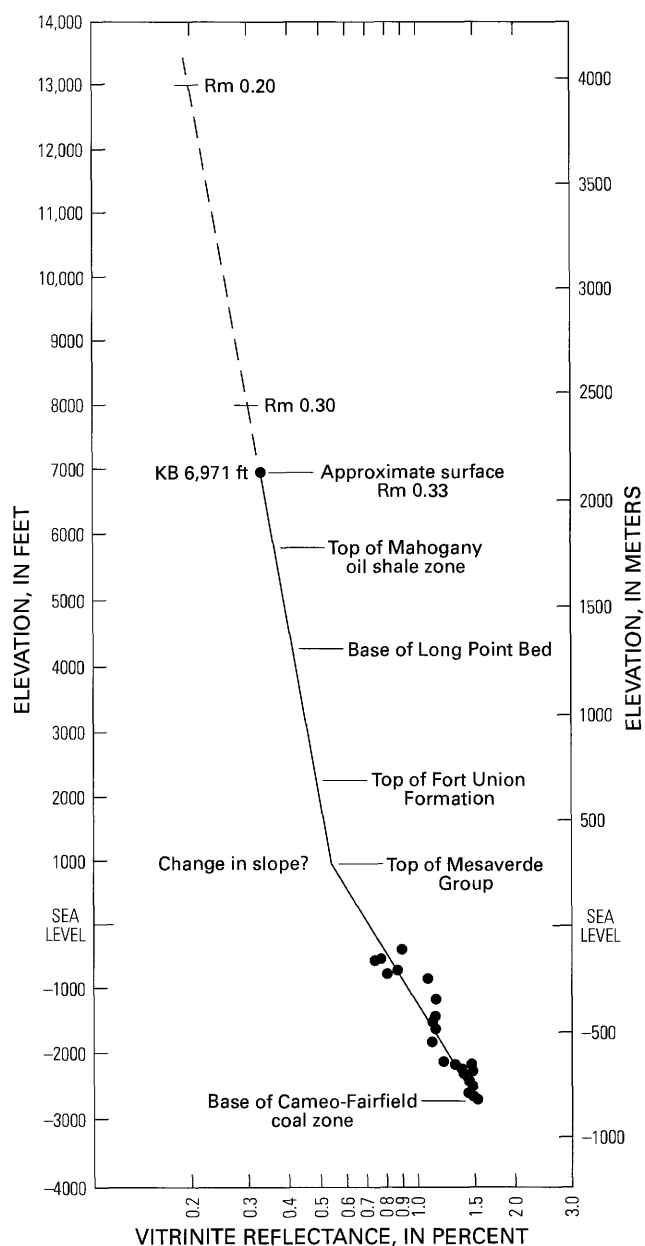


Figure 7. Vitritine reflectance profile using subsurface data from Chancellor 398-10-1 well (sec. 10, T. 3 S., R. 98 W.) (fig. 1, plate 1) and estimated surface Rm value of 0.33 percent. Selected geologic contacts and extrapolations (dashed line) to vitritine reflectance values of 0.20 and 0.30 percent are shown.

make it impossible to detect changes in slope. There is an 11,000-ft gap between the subsurface data and the surface data, and it is impossible to detect near-surface changes in slope in the Rm profile. Changes in slope almost certainly occur in the profile for the nearby Chancellor 398-10-1 well (fig. 7). Such changes in slope are common in the Piceance basin and can be detected in profiles that contain no major gaps in data, such as those for the

MWX (fig. 8) and Barrett A-2 Crystal Creek (fig. 9) wells. Three major segments having different slopes and possibly several less important changes in slope are shown in these two profiles. These changes in slope do not coincide very well with formational boundaries and have been attributed to convective fluid flow during the development of the thick, low-permeability Mesaverde gas pocket at these two locations (Law and others, 1989). Extrapolation to the 0.20-percent Rm level in the A-2 Crystal Creek well suggests that about 1,700 ft of overburden has been removed for a present-day elevation of

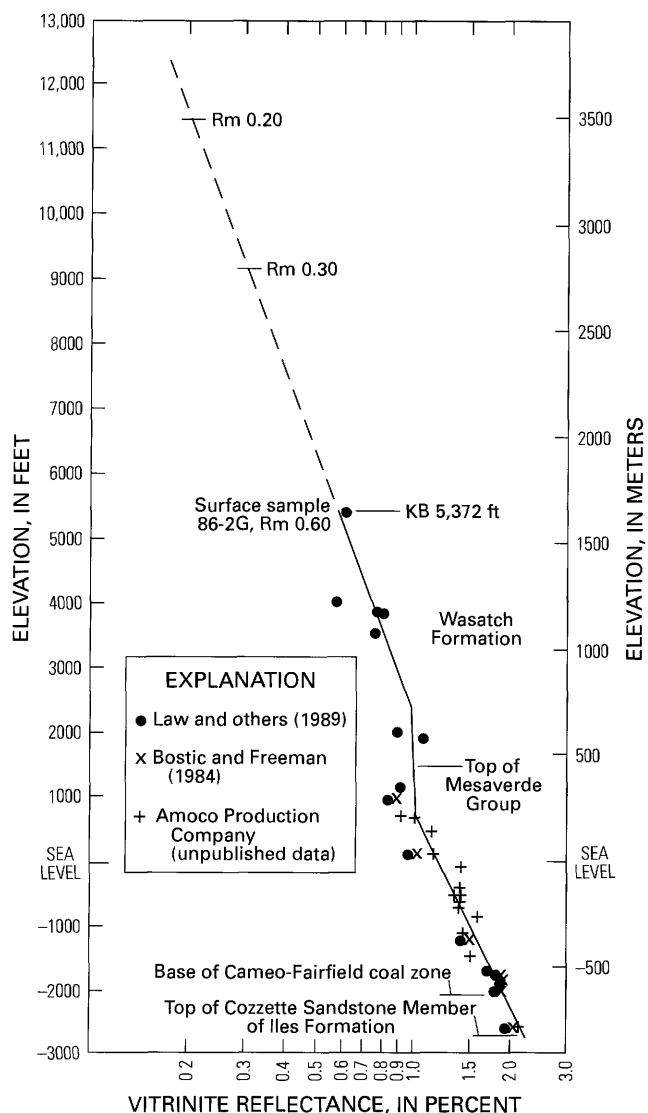


Figure 8. Vitritine reflectance profile using subsurface data from Multiwell Experiment (MWX) site (sec. 34, T. 6 S., R. 94 W.) and surface sample 86-2G (Law and others, 1989) (fig. 1, plate 1). Selected geologic contacts and extrapolations (dashed line) to vitritine reflectance values of 0.20 and 0.30 percent are shown.

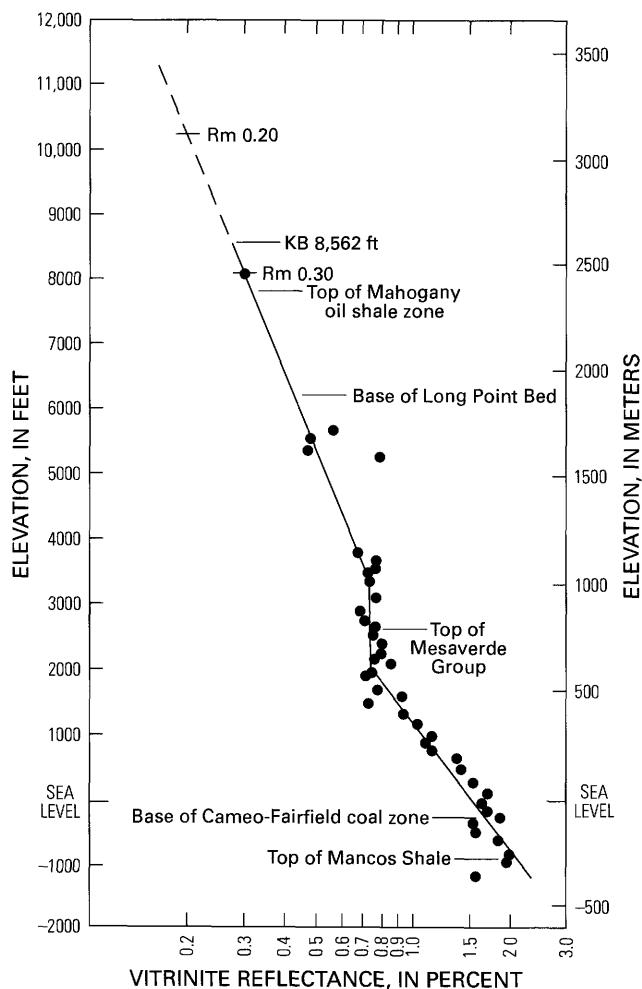


Figure 9. Vitritine reflectance profile using subsurface data from Barrett A-2 Crystal Creek well (sec. 23, T. 6 S., R. 97 W.) (Law and others, 1989) (fig. 1, plate 1). Selected geologic contacts and extrapolations (dashed line) to vitritine reflectance values of 0.20 and 0.30 percent are shown.

about 10,250 ft, close to the 10,000-ft level suggested by Johnson and Nuccio (1986). Extrapolation to the 0.30-percent Rm level is at a depth of about 500 ft in the well. Extrapolation to the 0.20-percent level in the MWX well suggests that about 6,100 ft of overburden has been removed for a present-day elevation of about 11,500 ft. Extrapolation to the 0.30-percent level suggests that about 3,800 ft of overburden has been removed for a present-day elevation of about 9,200 ft.

The three profiles from the Uinta basin give a wide range for thickness of strata removed (figs. 14–16). Again, large data gaps in the profiles make it difficult to detect changes in slope. Extrapolating the Mid-America 1 Unit profile to an Rm value of 0.30 percent (fig. 14) gives a thickness of overburden removed of about 4,000 ft for a present-day elevation of about 9,500 ft. Extrapolation to

0.20 percent gives a thickness of overburden removed of about 9,000 ft for a present-day elevation of about 14,500 ft. These values contrast markedly with extrapolations of the profile for the combined Mountain Fuels 1 and 3 Island Unit wells (fig. 15). In this profile a kink at approximately the middle of the Mesaverde Group changes the extrapolation and points out the importance of recognizing kinks in the profiles. Extrapolation to 0.30 percent yields a depth of about 900 ft below the surface, whereas extrapolation to 0.20 percent gives a thickness of only about 2,300 ft of overburden removed for a present-day elevation of about 7,200 ft. For the Shell 1–11–B4 Brotherson well (fig. 16), extrapolations resulted in unreasonable estimates of the thickness of overburden removed of from 6,200 ft for an Rm value of 0.30 percent to more than 11,000 ft for 0.20 percent, possibly because there is an 11,000-ft gap in the profile.

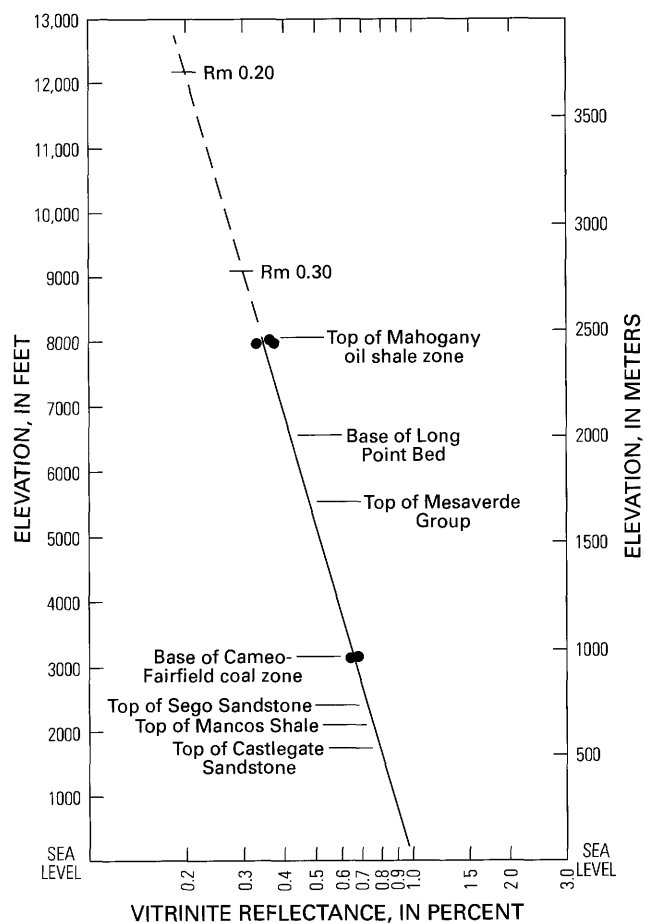


Figure 10. Vitritine reflectance profile using subsurface data from Chorney 1–14 East Rangely Govt. (sec. 14, T. 1 N., R. 100 W.) oil and gas test well and USGS CH–9A (sec. 12, T. 1 N., R. 100 W.) shallow oil-shale corehole (fig. 1, plate 1). Selected geologic contacts and extrapolations (dashed line) to Rm values of 0.20 and 0.30 percent are shown.

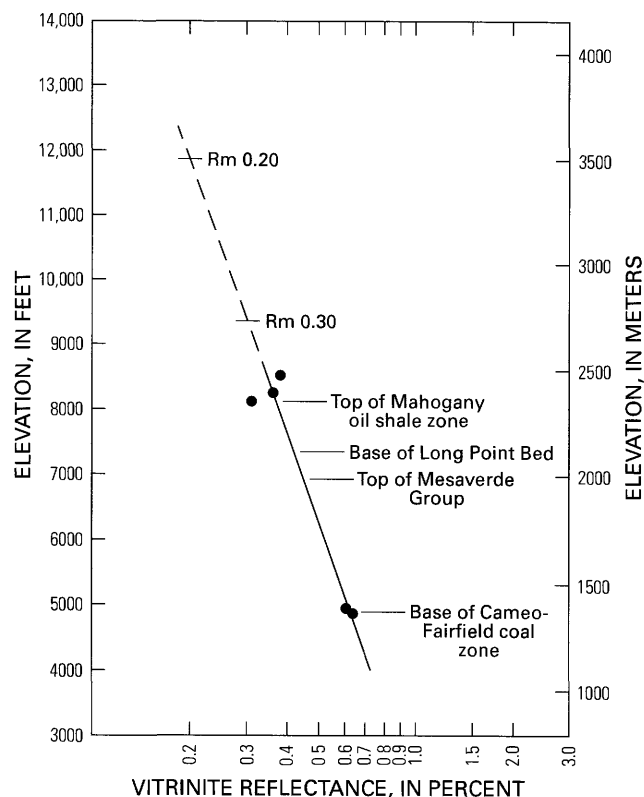


Figure 11. Vitrinite reflectance profile using subsurface data from Tipperary 1-30 F Bear Gulch (sec. 30, T. 5 S., R. 100 W.) oil and gas test well and Skyline Hydrocarbon 2 (sec. 13, T. 5 S., R. 100 W.) shallow oil-shale corehole (fig. 1, plate 1). Selected geologic contacts and extrapolations (dashed line) to vitrinite reflectance values of 0.20 and 0.30 percent are shown.

ESTIMATING OVERBURDEN REMOVED USING BURIAL RECONSTRUCTIONS OF SURFACE SAMPLES

Estimates of overburden removed can also be made directly by constructing a burial curve for a surface vitrinite reflectance sample and using either the time-temperature model of Lopatin (1971) or the time-independent model of Barker and Pawlewicz (1986a) and Barker (1989). This method previously had been applied to a surface sample near the MWX site that has an Rm value of 0.60 percent (Nuccio and Johnson, 1989b). The results suggested that the observed value of 0.60 percent could not be explained assuming present-day thermal gradients and a maximum basin surface elevation prior to downcutting of 10,000 ft. In contrast, however, we found that the models predicted higher than observed reflectance values for the Mesaverde coals at depth in the MWX well. These differences may be the result of incorrectly estimating the thermal conductivity of the over-

burden removed since downcutting began or the result of changes in heat flow and thermal gradients through time.

Burial curves were constructed for the vicinity of the Mobil T-52-19G well in the central Piceance basin (fig. 17), the Douglas Creek arch area (fig. 18), and the deep trough of the Uinta basin near the Shell 1-11-B4 Brotherson well (fig. 19). The Douglas Creek arch is a broad low-amplitude structure that separates the Uinta and Piceance basins and acted as a hingeline between the two subsiding basins during the Laramide orogeny (Johnson and Finn, 1986). Two burial curves were constructed for the Mobil T-52-19G well, one for the average surface Rm value of 0.45 percent in the vicinity of the well and one for a coal sample from the Cameo-Fairfield coal zone at a depth of 10,900 ft in the well. For the reconstruction the thicknesses of Cretaceous and Tertiary units were obtained from drill-hole information. The age of the Cameo-Fairfield zone is estimated at 73.8 Ma. The time interval represented by the unconformity at the top of the Upper Cretaceous Mesaverde Group is

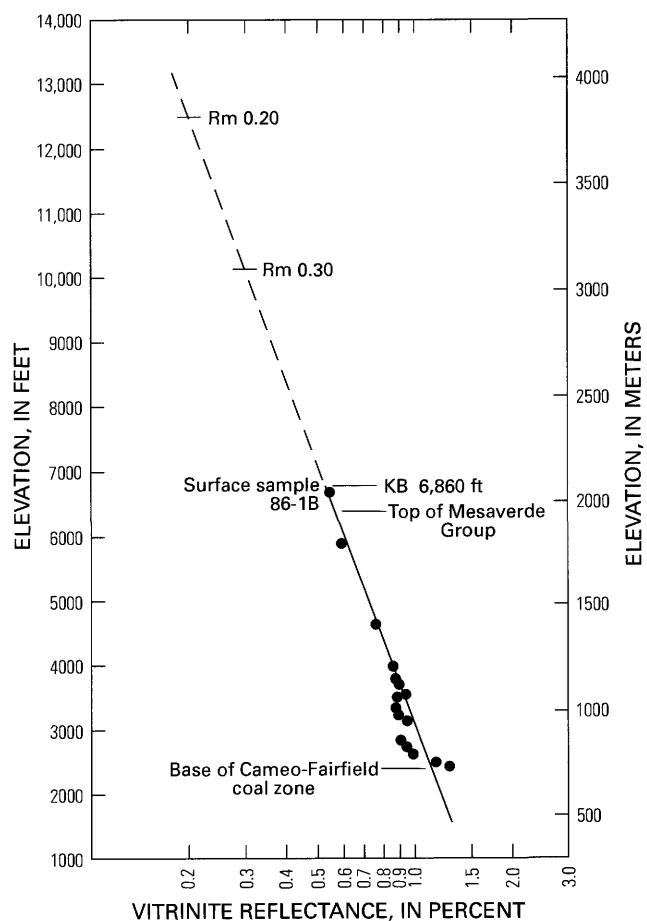


Figure 12. Vitrinite reflectance profile using subsurface data from Tenneco 20-4 well (sec. 20, T. 7 S., R. 91 W.) and surface sample 86-1B (fig. 1, plate 1). Selected geologic contacts and extrapolations (dashed line) to vitrinite reflectance values of 0.20 and 0.30 percent are shown.

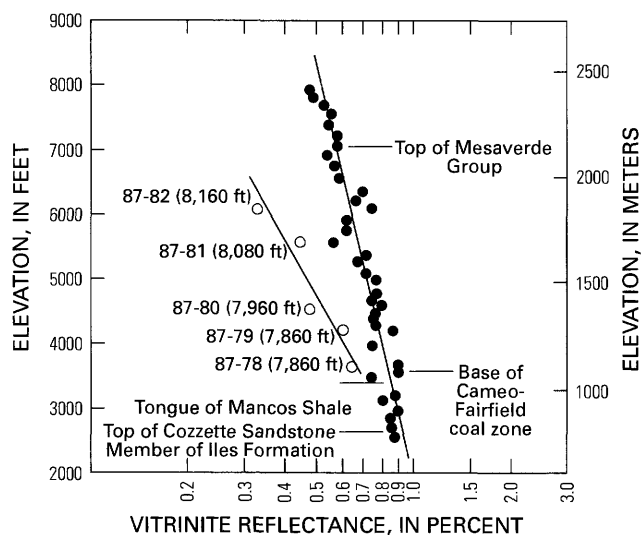


Figure 13. Vitritine reflectance profile using subsurface data from TRW Sunlight Federal 2 well (sec. 32, T. 7 S., R. 89 W.) (solid circles) and surface samples at Fourmile Creek along the Grand Hogback east of the well (open circles) (fig. 1, plate 1). Surface samples plotted at same stratigraphic positions as the TRW well; elevations of surface samples given in parentheses.

estimated to be 4 million years (from 66 to 62 Ma), and we assumed that no erosion occurred during this period. We also assumed that the area was under maximum burial from the end of the Laramide orogeny about 37 Ma to the onset of regional uplift and downcutting about 10 Ma and that the maximum basin surface during this period is represented by the present-day 10,000-ft level. We then solved for a geothermal gradient for the removed overburden. Using the Lopatin model a geothermal gradient of $3.20^{\circ}\text{F}/100\text{ ft}$ ($57^{\circ}\text{C}/\text{km}$) is needed, whereas using the Barker and Pawlewicz model a gradient of $3.13^{\circ}\text{F}/100\text{ ft}$ ($56^{\circ}\text{C}/\text{km}$) is needed. These gradients are considerably higher than the geothermal gradient of about $2.00^{\circ}\text{F}/100\text{ ft}$ ($37^{\circ}\text{C}/\text{km}$) in the area today (Johnson and Nuccio, 1986). In contrast, the Rm value of 1.56 percent for a subsurface coal sample from the Cameo-Fairfield coal zone in the T-52-19G well requires a gradient of $1.65^{\circ}\text{F}/100\text{ ft}$ ($30^{\circ}\text{C}/\text{km}$) for the Lopatin model and $2.37^{\circ}\text{F}/100\text{ ft}$ ($43^{\circ}\text{C}/\text{km}$) for the Barker and Pawlewicz model, both of which are much closer to the present-day thermal gradient.

Both models also seriously underpredicted the Rm value of 0.63 percent of Mesaverde surface sample 83-163B from the Douglas Creek arch (fig. 18). The burial curve again assumes that no erosion occurred during the Cretaceous-Tertiary hiatus, that the sample was under maximum burial from 37 to 10 Ma, and that the present-day 10,000-ft level is the surface of maximum burial. Using the Lopatin model a geothermal gradient of $3.90^{\circ}\text{F}/100\text{ ft}$ ($71^{\circ}\text{C}/\text{km}$) is needed, whereas using the Barker and Pawlewicz model a gradient of $4.32^{\circ}\text{F}/100\text{ ft}$ ($79^{\circ}\text{C}/\text{km}$) is required. These values compare

with a present-day gradient of about $2.30^{\circ}\text{F}/100\text{ ft}$ ($42^{\circ}\text{C}/\text{km}$) for the area (Johnson and Nuccio, 1986). If the present-day gradient of $2.30^{\circ}\text{F}/100\text{ ft}$ ($42^{\circ}\text{C}/\text{km}$) gradient is assumed instead, then 2,650 ft more overburden above the 10,000-ft level is needed for the Lopatin model and about 4,950 ft more overburden for the Barker and Pawlewicz model. These numbers are probably not geologically reasonable. Assuming that erosion occurred during the Cretaceous-Tertiary hiatus does not significantly alter the solutions until the amount of eroded Mesaverde section is about 4,000 ft, an amount that is not geologically reasonable.

Reconstructing a burial history for surface samples in the Uinta basin is much more uncertain because no trace of the surface of the basin prior to the onset of downcutting about 10 Ma remains. The best results from near the

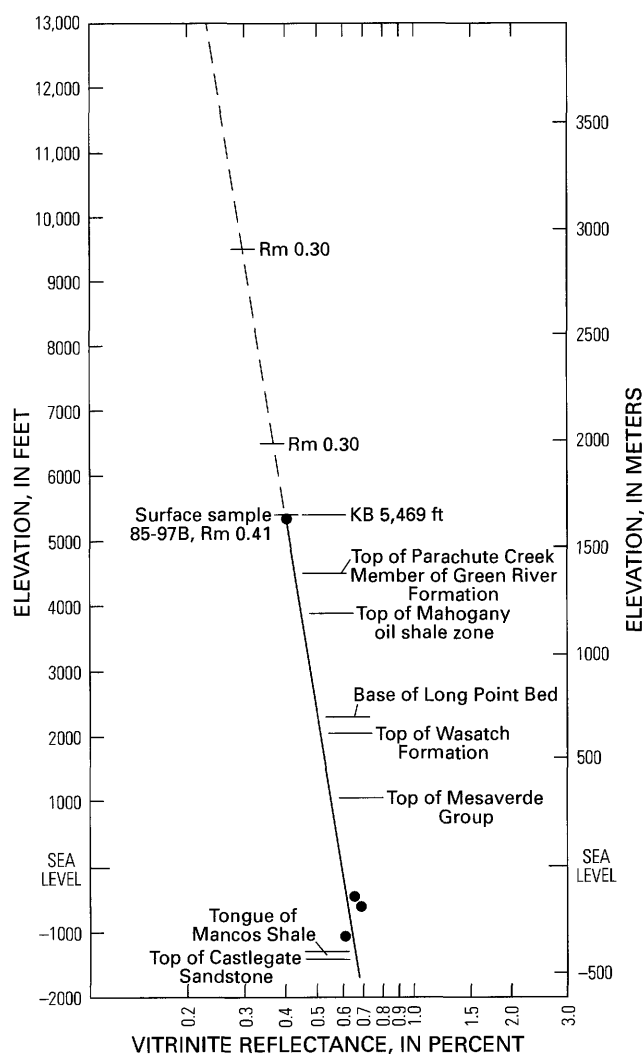


Figure 14. Vitritine reflectance profile using subsurface data from Mid-America 1 Unit well (sec. 24, T. 9 S., R. 24 E.) and surface sample 85-97B located nearby (fig. 1, plate 1). Selected geologic contacts and extrapolations (dashed line) to vitritine reflectance values of 0.20 and 0.30 percent are shown.

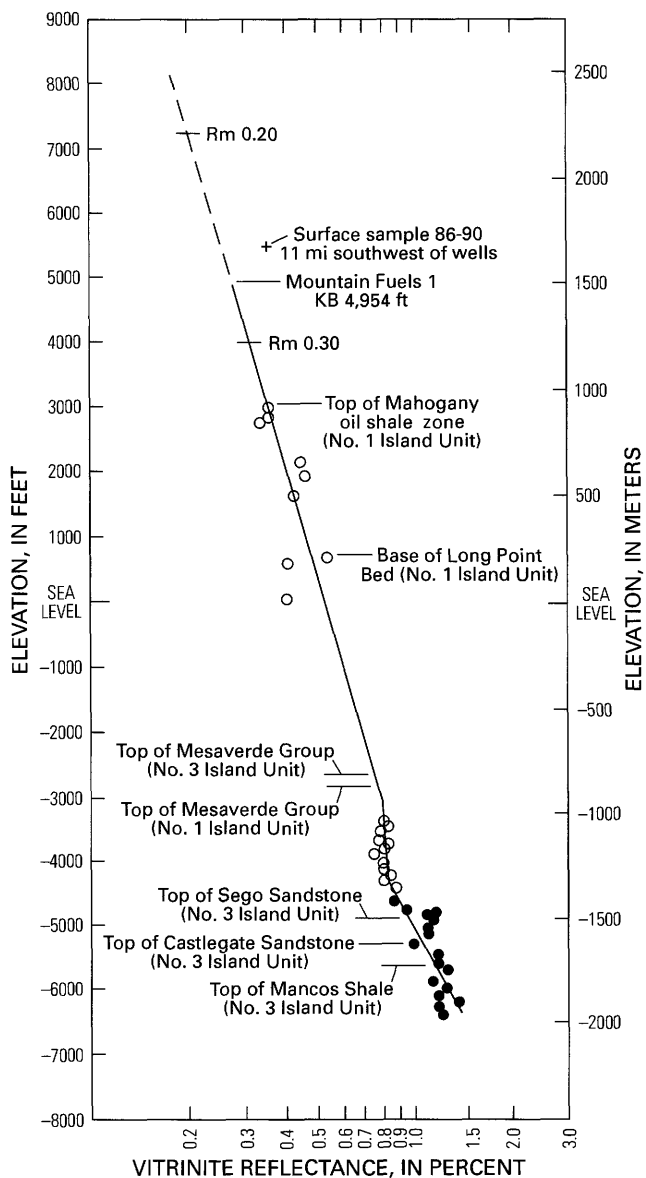


Figure 15. Vitritine reflectance profile using subsurface data from Mountain Fuels 1 Island Unit well (sec. 7, T. 10 S., R. 20 E.) (open circles), Mountain Fuels 3 Island Unit well (sec. 8, T. 10 S., R. 20 E.) (solid circles), and surface sample 86-9D (plus symbol), about 11 mi to southwest (sec. 22, T. 11 S., R. 19 E.) (fig. 1, plate 1). Selected geologic contacts and extrapolations (dashed line) to vitritine reflectance values of 0.20 and 0.30 percent are shown.

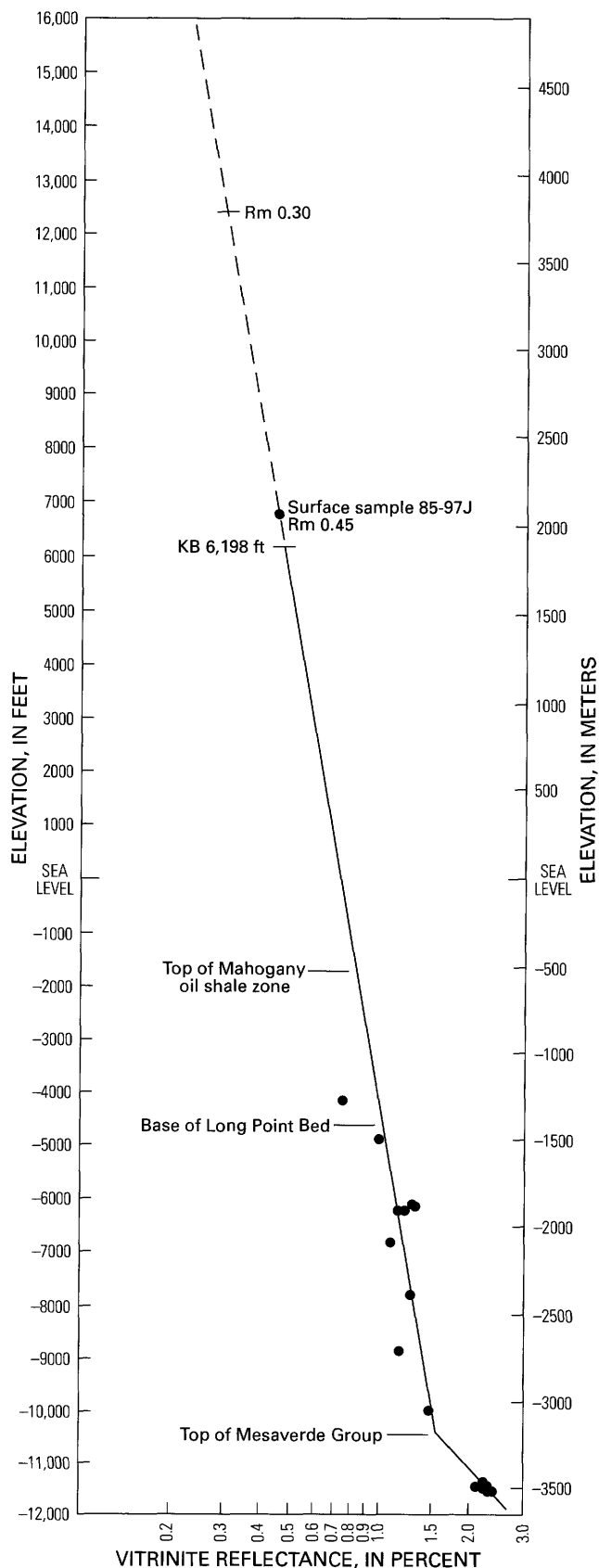


Figure 16 (facing column). Vitritine reflectance profile using subsurface data from Shell 1-11-B4 Brotherson well (sec. 11, T. 2 S., R. 4 W.) and surface sample 85-97J (sec. 24, T. 1 S., R. 5 W.) (fig. 1, plate 1). Selected geologic contacts and extrapolations (dashed line) to vitritine reflectance values 0.20 and 0.30 percent are shown.

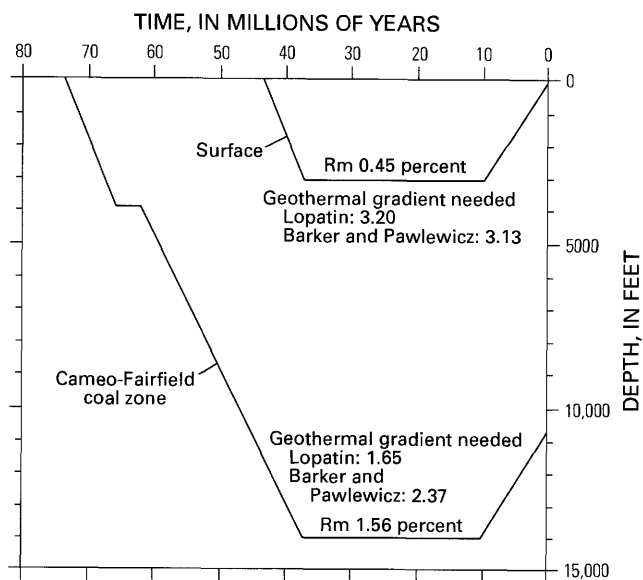


Figure 17. Burial curves for sample of Cameo-Fairfield coal zone in Mobil T-52-19G well (sec. 19, T. 2 S., R. 96 W.) (fig. 1, plate 1). Surface vitrinite reflectance of 0.45 is average of several surface samples in vicinity of well. Reconstruction assumes that present-day 10,000-ft level was level of maximum basin aggradation. Geothermal gradients ($^{\circ}\text{F}/100\text{ ft}$) are those needed to attain observed vitrinite reflectance (Rm) values using models of Lopatin (1971) and Barker and Pawlewicz (1986a).

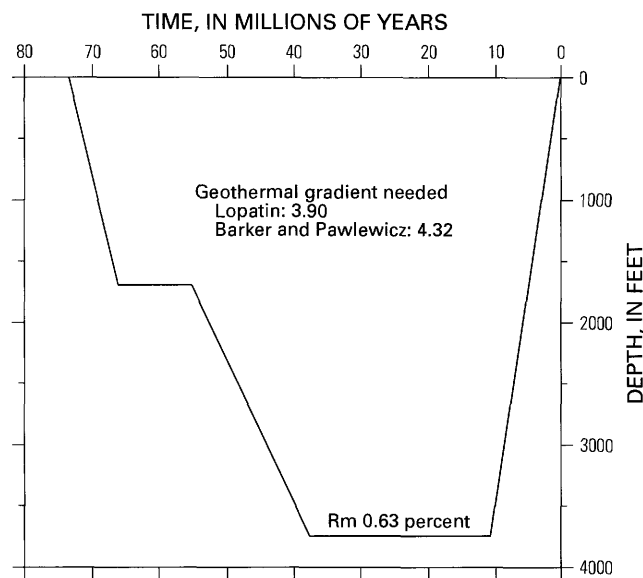


Figure 18. Burial curves for typical surface sample (83-163B) of Mesaverde Group on Douglas Creek arch (plate 1). Reconstruction assumes that present-day 10,000-ft level was level of maximum basin aggradation. Geothermal gradients ($^{\circ}\text{F}/100\text{ ft}$) are those needed to attain observed vitrinite reflectance (Rm) value using models of Lopatin (1971) and Barker and Pawlewicz (1986a).

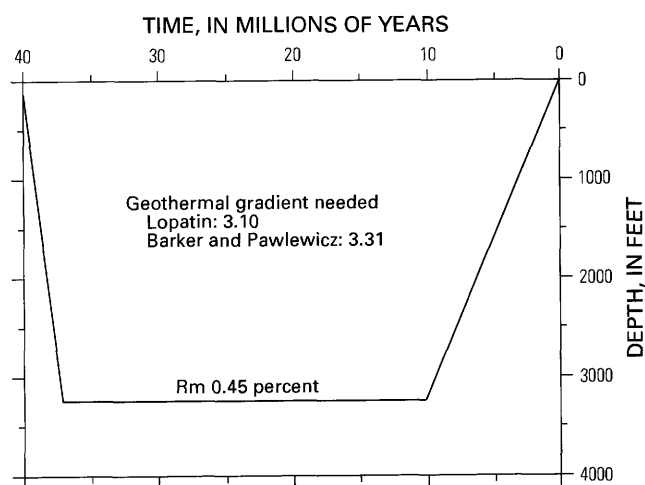


Figure 19. Burial curve for surface sample 85-97J of Duchesne Formation collected in area of Altamont-Bluebell oil field (fig. 1, plate 1). Reconstruction assumes present-day 10,000-ft level was level of maximum basin aggradation. Geothermal gradients ($^{\circ}\text{F}/100\text{ ft}$) are those needed to attain observed vitrinite reflectance (Rm) value using models of Lopatin (1971) and Barker and Pawlewicz (1986a).

trough of the Uinta basin were obtained from samples 85-97J and 85-73A, both of which yielded Rm values of 0.45 percent. If the present-day 10,000-ft level prior to downcutting is used for sample 85-97J, then both models seriously underpredict the surface vitrinite reflectance (fig. 19). Using the Lopatin model a geothermal gradient of $3.10^{\circ}\text{F}/100\text{ ft}$ ($57^{\circ}\text{C}/\text{km}$) is required, whereas using the Barker and Pawlewicz model a geothermal gradient of $3.31^{\circ}\text{F}/100\text{ ft}$ ($59^{\circ}\text{C}/\text{km}$) is required. These gradients compare with a present-day geothermal gradient of only about $1.10^{\circ}\text{F}/100\text{ ft}$ ($20^{\circ}\text{C}/\text{km}$) for the area (Willett and Chapman, 1983; Chapman and others, 1984).

The thickness of overburden and geothermal gradients required by the two coalification models in order to explain the observed vitrinite reflectance values at the four sites is shown in figure 20. In figure 21, the same curves have been repositioned on the x- and y-coordinates so that a comparison can be made between the "excess overburden above the 10,000-ft level needed" and the "excess above the present-day thermal gradient needed" at the four locations; the closer a curve is to the zero point on the x-y axis, the smaller the discrepancy between the predicted and measured vitrinite reflectance value. Figure 21 shows that, for the four samples considered, the coalification models underpredict the observed surface vitrinite reflectance value along the trough of the Uinta basin by the most and underpredict the two observed surface vitrinite reflectance values in the Piceance basin by the least. The sample on the Douglas Creek arch is between the two. These results are qualitatively similar to estimates of overburden removed made by extrapolating Rm versus depth profiles. The profiles estimate that a con-

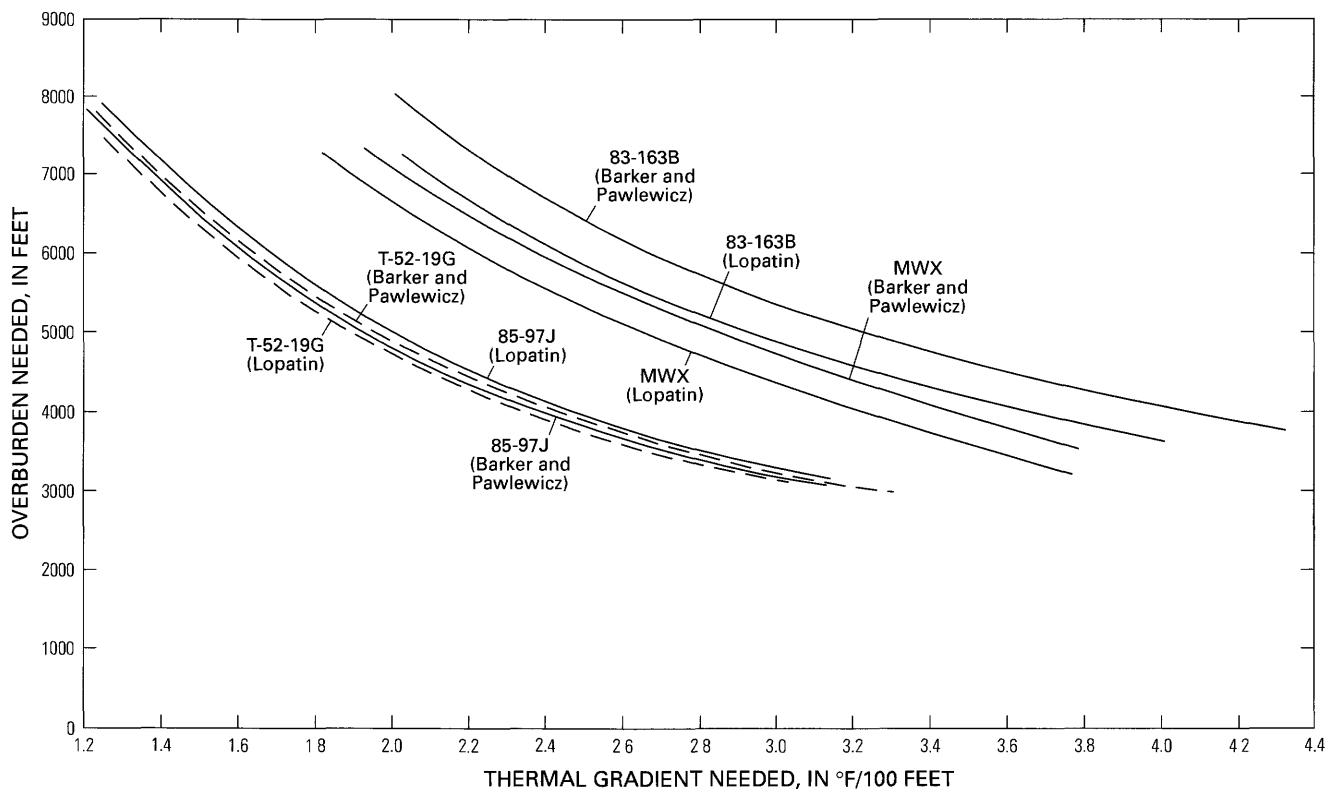


Figure 20. Overburden and geothermal gradients needed to explain observed vitrinite reflectance values at locations in Uinta and Piceance basins and on Douglas Creek arch using models of Lopatin (1971) and Barker and Pawlewicz (1986a).

siderable thickness of overburden above the present-day 10,000-ft level has been removed from the trough of the Uinta basin (fig. 16), whereas the present-day 10,000-ft level more closely approximates the surface of maximum aggradation near the trough of the Piceance basin (figs. 5, 6, 8).

IMPLICATIONS FOR THE STRUCTURAL DEVELOPMENT OF LARAMIDE UPLIFTS USING SURFACE VITRINITE REFLECTANCE SAMPLES

Surface vitrinite reflectance samples were collected from three uplifts in the area: the Wasatch uplift, San Rafael Swell, and White River uplift (fig. 1). No attempt was made to generate a burial reconstruction for the Wasatch uplift, a complex zone of imbricated thrust sheets that formed during the Cretaceous and Paleocene. Four vitrinite reflectance profiles were collected through the upturned Cretaceous and lower Tertiary strata exposed along the Grand Hogback, which forms the eastern margin of the White River uplift: at the Piceance Creek water gap, Harvey Gap, Fourmile Creek, and Marble (plate 1). Burial profiles were constructed for the Piceance Creek water gap (fig. 22) and Harvey Gap (fig. 23).

No attempt was made to reconstruct the burial history at Marble because heating from nearby intrusions has obviously affected the vitrinite reflectance values. A burial reconstruction at Fourmile Creek was not attempted because of evidence for post-Laramide structural movement in the area that is not well understood at this time. Basalt flows that cap the ridge north of Fourmile Creek dip markedly to the east, possibly due to some collapse of the White River uplift along the hogback fault in this area or due to salt tectonics associated with the underlying Pennsylvanian evaporites (Grout and Abrams, 1988). A vitrinite reflectance profile at Fourmile Creek was plotted next to the profile for the TRW Sunlight Federal 2 well (fig. 13), drilled just west of the hogback along Fourmile Creek. The surface samples were plotted at the same stratigraphic position as samples in the TRW well. For example, surface sample 87-78 is from near the base of the Cameo-Fairfield coal zone and was plotted adjacent to subsurface samples collected from near the base of the coal zone. Although burial reconstructions were not attempted, the plot does show that coal ranks for a given stratigraphic position increase markedly from surface outcrops to the nearby subsurface.

The Grand Hogback is underlain by a west-thrusting reverse fault that carried the White River uplift westward over the eastern margin of the Piceance basin during the Laramide orogeny (Perry and Grout, 1988). Where seismic

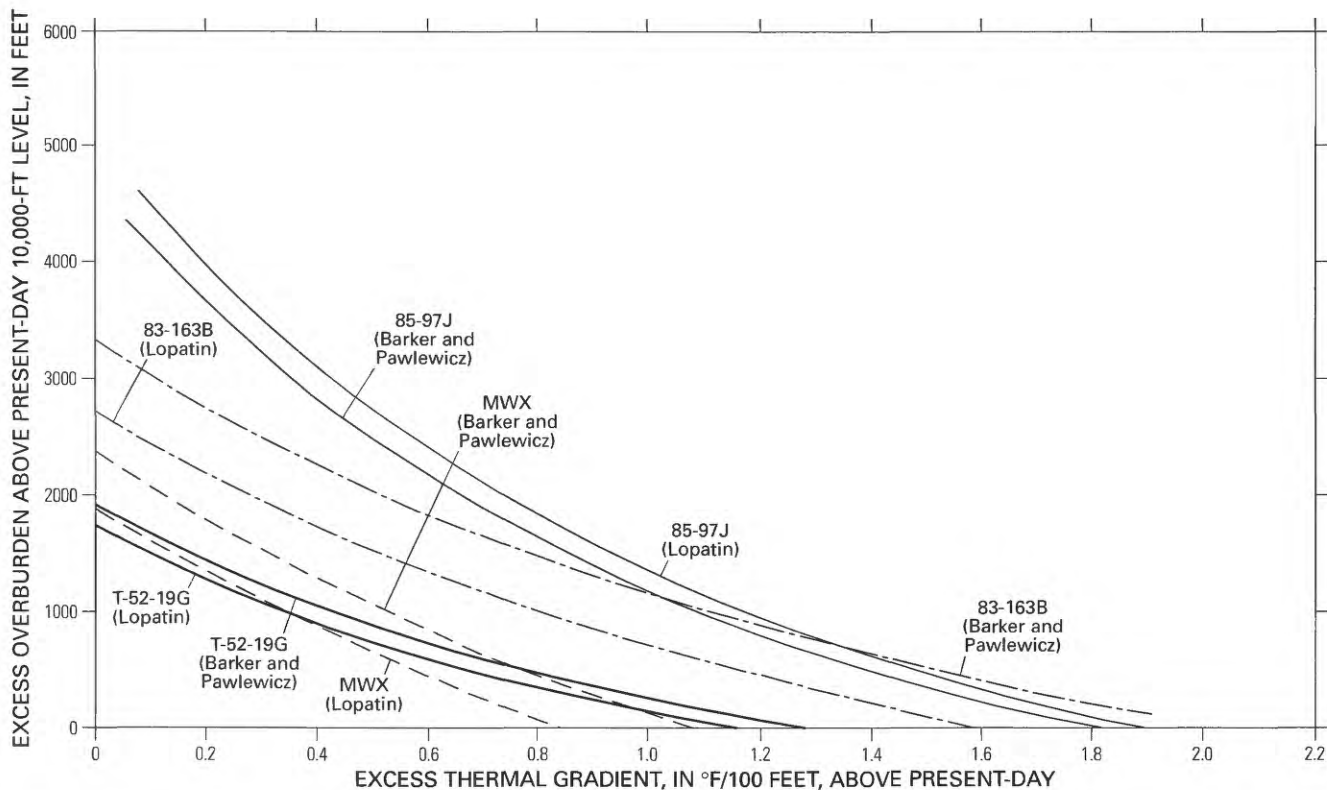


Figure 21. Excess overburden above 10,000-ft level versus excess thermal gradient above present-day needed to explain observed vitrinite reflectance values at locations in Uinta and Piceance basins and on Douglas Creek arch using models of Lopatin (1971) and Barker and Pawlewicz (1986a).

data are available, the inferred amount of thrusting is about 6–10 mi. The hogback thrust is somewhat unique among Laramide reverse faults in that most of the movement was absorbed by the incompetent Upper Cretaceous Mancos Shale (fig. 24). Units below the Mancos Shale are cut by the fault, whereas overlying units are sharply upturned but generally not faulted. Movement on the hogback fault probably began during the Paleocene. The Upper Cretaceous Mesaverde Group does not thin toward the hogback, whereas the overlying Paleocene-age Atwell Gulch Member of the Wasatch Formation thins markedly from more than 2,500 ft thick near the structural trough of the Piceance basin a few miles west of the hogback (Johnson and Finn, 1986) to about 880 ft at the Piceance Creek water gap and about 950 ft at Harvey Gap. Burial reconstructions for the Piceance Creek water gap and Harvey Gap again assume that the present-day 10,000-ft level approximates maximum burial, that the Cretaceous-Tertiary hiatus was from 66 to 62 Ma, that no erosion occurred during this hiatus, and that the two areas were under maximum burial from the end of the Laramide orogeny about 37 Ma to about 10 Ma when downcutting began. The gradients needed to generate the observed vitrinite reflectance values using the models of Lopatin (1971) and Barker and Pawlewicz (1986a) are

shown on the burial diagrams. Gradients needed for the two lower Mesaverde coals at Piceance Creek gap are 2.40°F/100 ft (44°C/km) using Lopatin and 2.00°F/100 ft (37°C/km) using Barker and Pawlewicz. These are close to the present-day gradient of about 2.00°F/100 ft (37°C/km) (Johnson and Nuccio, 1986). The upper Mesaverde coals, however, require significantly higher gradients of 3.70°F–4.58°F/100 ft (67°C–83°C/km). For Harvey Gap coals, gradients needed to generate the observed R_m values are 3.45°F–3.90°F/100 ft (60°C–71°C/km) using Lopatin and 3.76°F–4.84°F/100 ft (68°C–88°C/km) using Barker and Pawlewicz, considerably higher than the present-day gradient of about 2.00°F/100 ft (37°C/km) (Johnson and Nuccio, 1986). The range, however, is much less than at the Piceance Creek water gap.

The San Rafael uplift south of the Uinta basin (plate 1) was extensively sampled. The San Rafael Swell is a large northeast-trending anticlinal structure that, unlike the White River uplift, has gently dipping flanks and may never have been a major topographic high. Uplift began during the late Campanian (Franczyk and Nichols, 1988) and continued until about the end of the Eocene. A burial reconstruction was attempted for the northeast flank of the uplift near surface samples 86–5G and 86–5H (fig. 25). The R_m values of

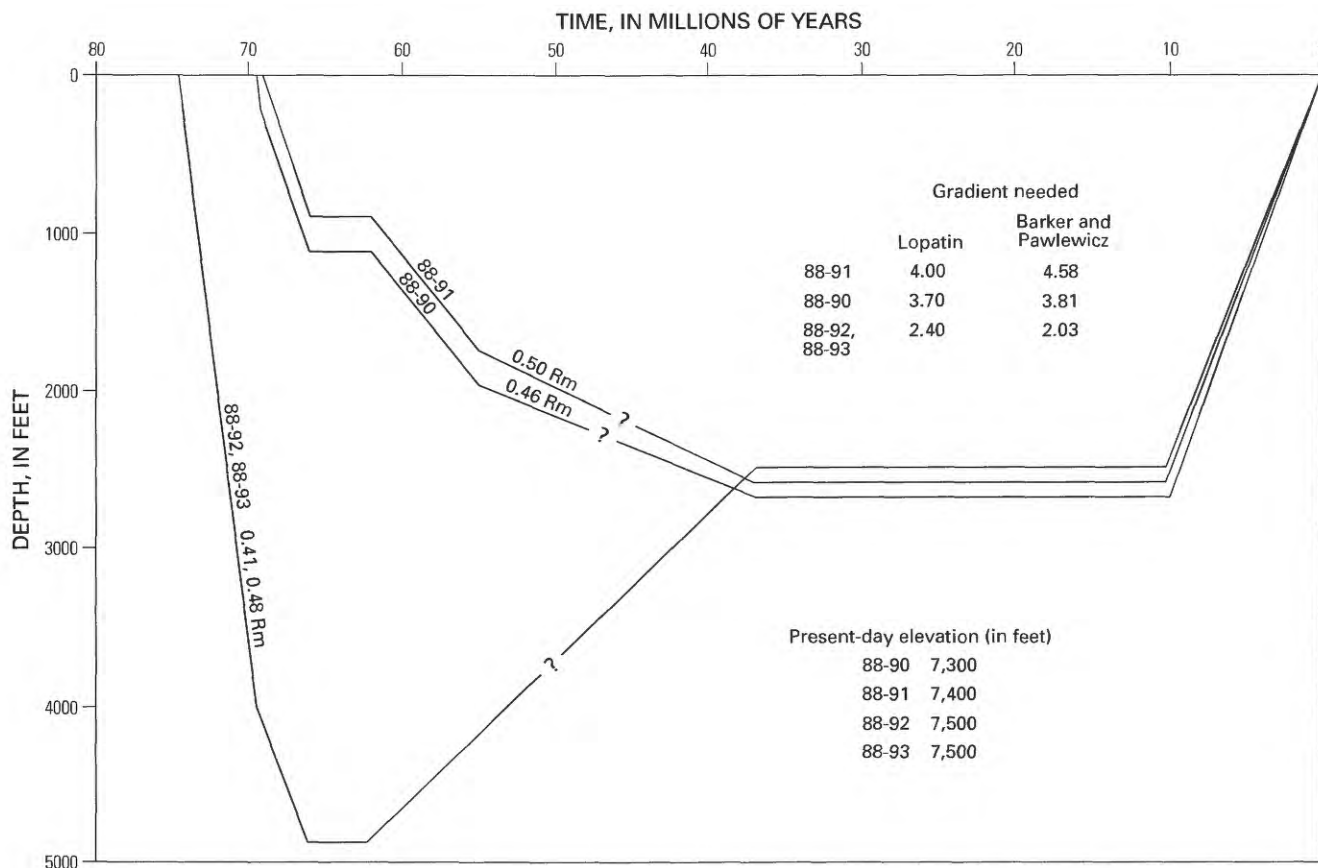


Figure 22. Burial curves for surface samples of Mesaverde Group collected along Piceance Creek water gap (plate 1). Reconstructions assume that present-day 10,000-ft level was level of maximum basin aggradation. Geothermal gradients ($^{\circ}\text{F}/100\text{ ft}$) are those needed to attain observed vitrinite reflectance (Rm) values using models of Lopatin (1971) and Barker and Pawlewicz (1986a).

0.62 and 0.49 percent are typical of those for this area. Sample 86-5G is from about 750 ft above the top of the Dakota Sandstone and sample 86-5H from about 1,100 ft above. The interval from the top of the Dakota Sandstone to the top of the Castlegate Sandstone is estimated to be 4,610 ft from the Forest Oil and Lone Star 25-1 Govt. Arnold well in sec. 25, T. 16 S., R. 14 E. The thickness from the top of the Castlegate Sandstone to the Cretaceous-Tertiary unconformity was estimated to be 650 ft by Fouch and others (1983), and it is assumed that no Cretaceous section was removed during the Cretaceous-Tertiary hiatus. The thickness of 515 ft for the lower Tertiary section was obtained by assuming that the present-day 10,000-ft level approximates the level of maximum aggradation. A geothermal gradient of $2.50^{\circ}\text{F}/100\text{ ft}$ ($46^{\circ}\text{C}/\text{km}$) is needed using Lopatin (1971) and $2.86^{\circ}\text{F}/100\text{ ft}$ ($53^{\circ}\text{C}/\text{km}$) using Barker and Pawlewicz (1986a) to explain the average Rm value for the two samples of 0.56 percent. These gradients are considerably higher than the present-day geothermal gradient of about $1.4^{\circ}\text{F}/100\text{ ft}$ ($26^{\circ}\text{C}/\text{km}$) in the area (Geothermal Gradient Map of the United States, 1976).

SUMMARY

The problems with interpreting surface vitrinite reflectance results from this study form two general categories. The first category is the inability to obtain reliable vitrinite reflectance readings because of (1) a scarcity of suitable rock types, a problem with most of the units sampled in this study; (2) natural variations in vitrinite reflectance between different types of vitrinite; (3) reworking of older vitrinite; (4) confusing vitrinite with other macerals such as fusinite, which may, in part, explain the high readings from the coal chips in the Wasatch channel sandstones; (5) suppression of vitrinite reflectance in shale sequences such as the Mancos Shale; (6) oxidation during diagenesis such as the coal chips in the Wasatch channel sandstones; and (7) recent oxidation from near-surface weathering, which could explain many of the anomalously high readings obtained from many units sampled in this study. The second category of problems involves interpreting the results once reliable readings are obtained because (1) different coalification models predict different results; (2) there is no accepted minimum value of

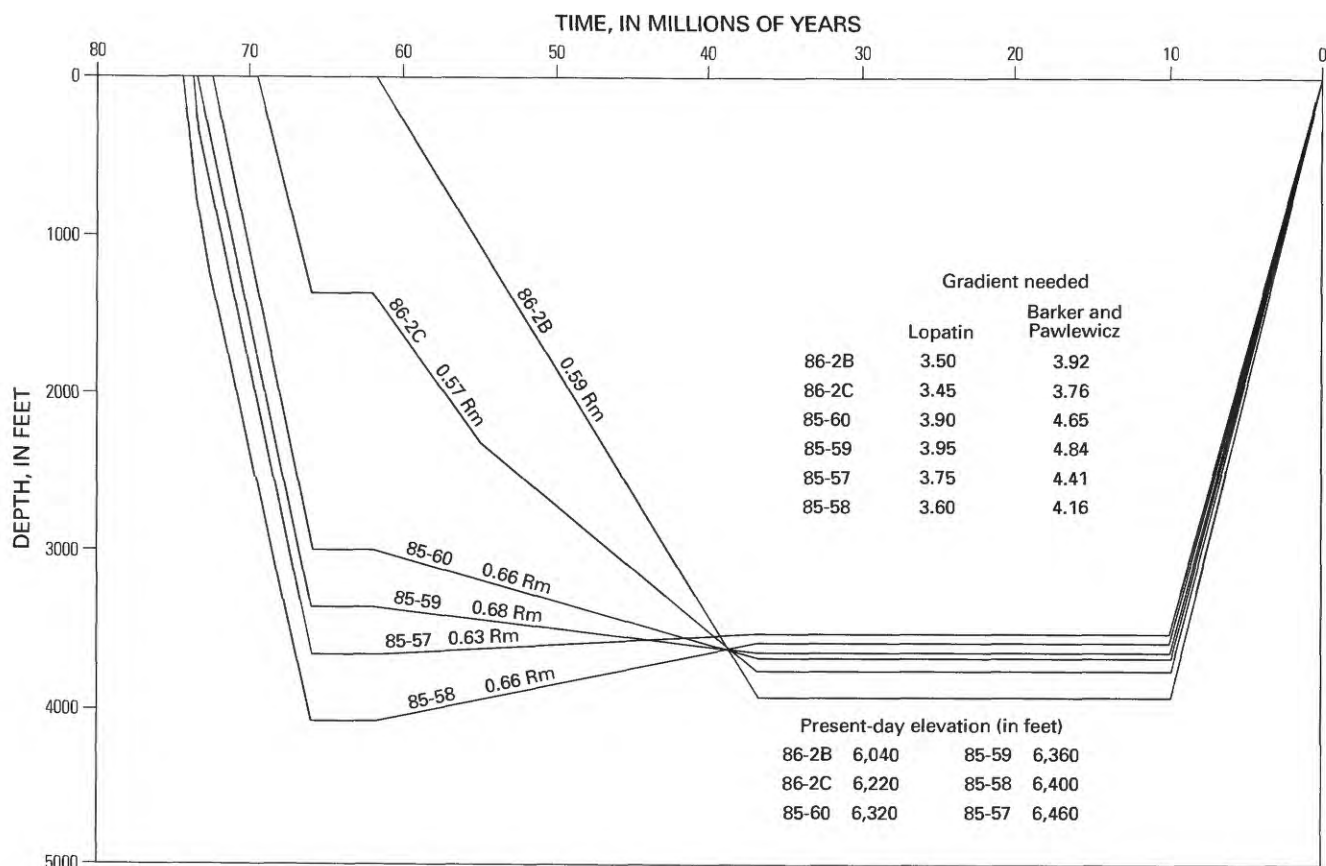


Figure 23. Burial curves for surface samples of Mesaverde Group collected from Harvey Gap (fig. 1, plate 1). Reconstructions assume that present-day 10,000-ft level was level of maximum basin aggradation. Geothermal gradients ($^{\circ}\text{F}/100\text{ ft}$) are those needed to attain observed vitrinite reflectance (R_m) values using models of Lopatin (1971) and Barker and Pawlewicz (1986a).

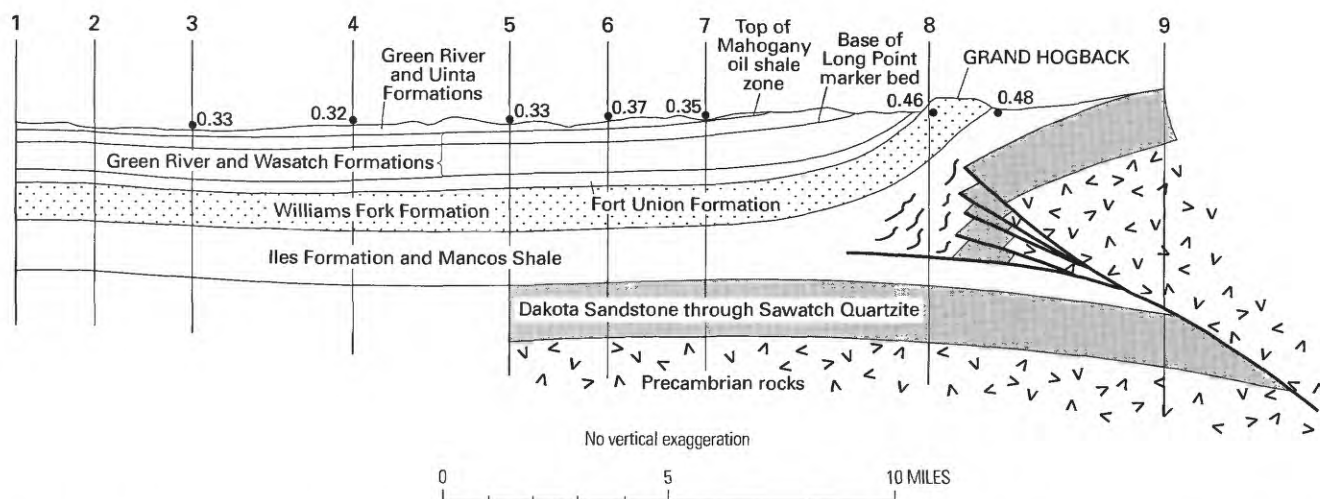


Figure 24. Geologic cross section across Grand Hogback at Piceance Creek water gap constructed using surface information and seismic information from areas to south. Location of cross section shown on plate 1. Vitrinite reflectance values (percent R_m) are given along top of section.

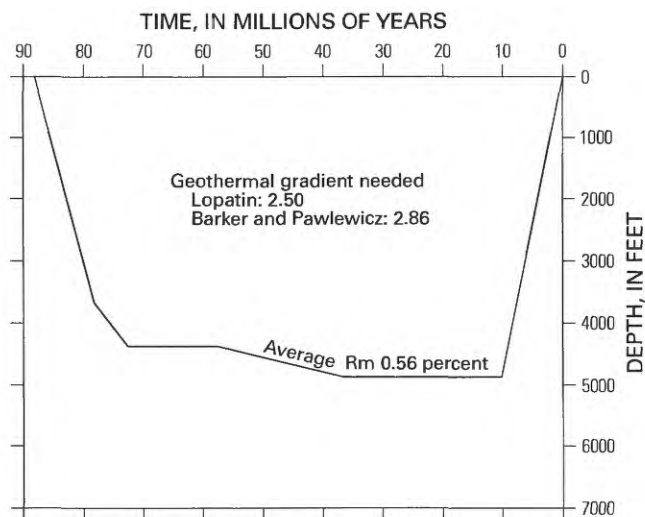


Figure 25. Burial curve for area of samples 86-5G and 86-5H on northeast flank of San Rafael Swell (fig. 1, plate 1). Reconstruction assumes that no erosion occurred at Cretaceous-Tertiary unconformity and that present-day 10,000-ft level was level of maximum aggradation. Geothermal gradients ($^{\circ}\text{F}/100$ ft) are those needed to attain observed vitrinite reflectance (R_m) value using models of Lopatin (1971) and Barker and Pawlewicz (1986a).

vitrinite reflectance for the near-surface environment in a basin under maximum aggradation; (3) the timing of various events needed to construct a burial history is commonly poorly constrained; (4) the lithology of the eroded section is generally not known; and (5) we are unable to recognize kinks in vitrinite reflectance profiles.

Because of these problems, only general observations are offered here. Estimates of overburden removed from the Piceance basin made by extrapolating R_m versus depth plots to R_m values of 0.20 and 0.30 percent bracket the 10,000-ft level, estimated by geologic inference to have been the surface of the basin prior to the onset of downcutting at 10 Ma in all areas studied in the Piceance basin except at the Mobil T-52-19G (fig. 6) and Tenneco 20-4 wells (fig. 12). These results suggest that there may never have been much thickness of section above this 10,000-ft level; however, the 2,500-5,000-ft difference between the extrapolation for R_m values of 0.20 and 0.30 percent is substantial. Extrapolation of vitrinite reflectance plots for the Uinta basin gave widely varying results. Extrapolation to 0.20 and 0.30 percent at the Mountain Fuels site (fig. 15) in the southern Uinta basin suggests that little erosion has occurred and that the present-day land surface elevation of around 5,000 ft is close to the surface of maximum burial. In contrast, extrapolation to 0.20 and 0.30 percent at the Brotherson well near the trough of the basin suggests that the surface of maximum aggradation was between 12,400 ft and about 17,500 ft; however, there is an 11,000-ft gap between the surface sample and shallowest sample in the

subsurface. A major problem with these extrapolations is the inability to recognize kinks or changes in slope in the profiles because of these large gaps in the data. The profile for the Mountain Fuels site is fairly complete, however, and a major unrecognized kink most likely is not present. The 5,000-ft elevation approximates the surface of maximum aggradation only if the Uinta basin has recently tilted to the north because the south rim of the basin south of the Brotherson well has elevations as high as 10,000 ft. This tilting would have to have occurred after the course of the Green River was established because the river flows toward the south across the basin. Another possibility is that kinks once may have been present in the eroded section. Such kinks would be impossible to detect today but would significantly change the estimates of overburden removed.

Estimates of overburden using burial reconstructions generally underpredict observed reflectance values except possibly on the San Rafael anticline. In the Piceance basin, the size of the discrepancy is greater on the Grand Hogback and Douglas Creek arch than in the central part of the basin, consistent with previously published subsurface studies which show that planes of equal vitrinite reflectance dip toward the trough of the basin. In other words, a given thermal maturity level is at higher elevations on the Douglas Creek arch and Grand Hogback than along the trough of the basin.

A major discovery made during this study is that the coalification models used here generally overpredict vitrinite reflectance values in the subsurface and underpredict values for surface samples. This unusual relationship was previously discovered at the MWX site in the south-central part of the Piceance basin (Nuccio and Johnson, 1989b). If this relationship is real and not related to one of the many problems previously discussed with surface samples, then the thermal regime of the Piceance basin may be considerably different today than in the past, and in the past shallow areas of the basin probably were warmer than expected. Increasing estimates of overburden removed or increasing geothermal gradients in the past could explain the surface results but would make the discrepancy between predicted and observed results for the deep subsurface even greater. It is unlikely that the basalt flows that once covered much of the Piceance basin could have produced the high surface vitrinite reflectance values. The surface sample collected near MWX was more than 4,600 ft below the base of the basalt flows, much too thick a column of rock for a surface basalt flow to have heated. One possibility is that heat flow in the past was by both conduction, the dominant process today, and convection. Convective heat flow by the expulsion of hot formation water upward has been suggested as the mechanism that created the vertical segment in the vitrinite profile at the MWX site (Law and others, 1989). The expulsion of hot formation waters would increase temperatures in the shallower areas of the basin and create higher than expected reflectance values near the surface. Law and others

suggested that hydrocarbon generation, mainly gas, was the expulsion mechanism, but compaction may have also been a factor during active basin subsidence.

Conduits for fluid movement may have been natural fractures and permeable formations. Because it is unlikely that such convective processes could uniformly heat the near-surface areas of the basin, there should be significant variations in observed vitrinite reflectance values for surface samples today. One area where such variations occur is the north-central part of the Piceance basin. An area of unusually high surface R_m values of 0.47–0.56 percent extends northwestward from the Piceance Creek dome (plate 1). The R_m versus depth plot for the area has a near-vertical segment near the present-day land surface because the R_m value of 0.73 percent is at a depth of about 5,000 ft in the area (fig. 6). Surface reflectance values in the surrounding areas are between 0.32 and 0.43 percent. Another possible paleo-exit point for basin fluids is the Grand Hogback. The upturned strata on the hogback have probably been exposed on the surface since before the end of basin subsidence at about the end of the Eocene. Hot mineral springs still are present along the hogback today. As previously discussed, surface reflectance values along the hogback are generally much higher than values predicted using the coalification models and geological inference. Burial reconstructions for the Uinta basin were hindered by the lack of suitable surface samples for vitrinite reflectance analysis, and only one reconstruction was attempted (fig. 19). Similar to the Piceance basin, coalification models underpredict the observed reflectance values in the Uinta basin.

In summary, there are many uncertainties related to interpreting surface vitrinite reflectance results. Our results do suggest that the thermal regime of at least the Piceance basin and the adjacent White River uplift has changed significantly, and it is unlikely that a simple increase or decrease in conductive heat flow can explain the results. Estimates of the thickness of overburden removed by extrapolating R_m versus depth plots are very approximate, but much of the problem results from uncertainties in what values to extrapolate the plots. Once this problem is resolved, much better estimates of overburden removed can be made. Interpretations for the Uinta basin are difficult because of the lack of vitrinite-rich surface samples.

REFERENCES CITED

- Barker, C.E., 1989, Temperature and time in the thermal maturation of sedimentary organic matter, in Naeser, N.D., and McCulloh, T.H., eds., *Thermal history of sedimentary basins—Methods and case histories*: New York, Springer-Verlag, p. 73–98.
- Barker, C.E., and Pawlewicz, M.J., 1986a, The correlation of vitrinite reflectance with maximum temperature in humid organic matter, in Buntebarth, G., and Stegena, L., eds., *Paleogeothermics*: Berlin, Springer-Verlag, p. 79–93, 205–228.
- , 1986b, A surface vitrinite reflectance anomaly related to the Bell Creek oil field, Montana, U.S.A., in Davidson, M.J., ed., *Unconventional methods for exploration*: Dallas, Southern Methodist Press, p. 125–146.
- Bertrand, R., and Heroux, Y., 1987, Chitinozoan, graptolite, and scolecodont reflectance as an alternative to vitrinite and pyrobitumen reflectance in Ordovician and Silurian strata, Anticosti Island, Quebec, Canada: *American Association of Petroleum Geologists Bulletin*, v. 71, p. 951–957.
- Bostick, N.H., 1979, Microscopic measurements of the level of catagenesis of solid organic matter in sedimentary rocks to aid in exploration for petroleum and to determine former burial temperatures—A review, in Scholle, P.A., and Schluger, P.R., eds., *Aspects of diagenesis*: Society of Economic Paleontologists and Mineralogists Special Publication 26, p. 17–43.
- Bostick, N.H., and Freeman, V.L., 1984, Tests of vitrinite reflectance and paleotemperature models at the Multiwell Experiment Site, Piceance Creek Basin, Colorado, in Spencer, C.W., and Keighin, C.W., eds., *Geologic studies in support of the U.S. Department of Energy Multiwell Experiment, Garfield County, Colorado*: U.S. Geological Survey Open-File Report 84–757, p. 110–120.
- Bradley, W.H., 1936, Geomorphology of the north flank of the Uinta Mountains (Utah): U.S. Geological Survey Professional Paper 185–I, p. 163–199.
- Bustin, R.M., 1986, Organic maturity of Late Cretaceous and Tertiary coal measures, Canadian Arctic Archipelago: *International Journal of Coal Geology*, v. 6, p. 71–106.
- Bustin, R.M., Cameron, A.R., Grieve, D.A., and Kalkreuth, W.D., 1983, Coal petrology—Its principals, methods, and application: *Geological Association of Canada Short Course Notes*, v. 3, 229 p.
- Chancellor, R.E., and Johnson, R.C., 1986, Geologic and engineering implications of production history from five wells in central Piceance Creek basin, northwest Colorado: *Society of Petroleum Engineers Unconventional Gas Technology Symposium*, Louisville, SPE Paper 15237, Proceedings, p. 351–364.
- , 1988, Geologic and engineering implications of production history from five Mesaverde wells in central Piceance Creek basin, northwest Colorado: *Society of Petroleum Engineers Formation Evaluation*, v. 3, no. 2, p. 307–314.
- Chandra, D., 1962, Reflectance and microstructure of weathered coals: *Fuel*, v. 41, p. 185–193.
- Chapman, D.S., Keho, T.H., Bauer, M.S., and Picard, M.D., 1984, Heat flow in the Uinta basin determined from bottom hole temperature (BHT) data: *Geophysics*, v. 49, p. 453–466.
- Donnell, J.R., 1969, Paleocene and lower Eocene units in the southern part of the Piceance Creek Basin, Colorado: *U.S. Geological Survey Bulletin* 1274–M, 18 p.
- Dow, W.G., 1977, Kerogen studies and geological interpretations: *Journal of Geochemical Exploration*, v. 7, p. 79–99.
- Fouch, T.D., 1976, Revision of the lower part of the Tertiary System in the central and western Uinta basin, Utah: *U.S. Geological Survey Bulletin* 1405–C, 7 p.
- Fouch, T.D., Lawton, T.F., Nichols, D.J., Cashion, W.B., and Cobban, W.A., 1983, Patterns and timing of synorogenic sedimentation in Upper Cretaceous rocks of central and northeast Utah, in Reynolds, M.W., and Dolly, E.D., eds., *Mesozoic paleogeography of west-central United States: Rocky Mountain Section*, Society of Economic Paleontologists and Mineralogists, p. 305–336.

- Franczyk, K.J., and Nichols, D.J., 1988, Depositional systems reflecting foreland to intermountain basin deposition in Campanian to Paleocene time, Book Cliffs and Wasatch Plateau, Utah: Geological Society of America Abstracts With Programs, p. A212.
- Freeman, V.A., 1979, Preliminary report on rank of deep coals in part of the southern Piceance Creek basin, Colorado: U.S. Geological Survey Open-File Report 79-725, 10 p.
- Goodarzi, F., 1984, Organic petrography of graptolite fragments from Turkey: Marine and Petroleum Geology, v. 1, p. 202-210.
- Goodarzi, F., and Norford, B.S., 1985, Graptolites as indicators of temperature histories of rocks: Journal of the Geological Society of London, v. 142, p. 1089-1099.
- Grout, M.A., and Abrams, G.A., 1988, Mid-Tertiary shallow decollement and imbricate thrusting, northeastern Colorado Plateau, Piceance Basin, Colorado: Geological Society of America Abstracts with Programs, p. A384.
- Hansen, W.R., 1965, Geology of the Flaming Gorge area, Utah-Colorado-Wyoming: U.S. Geological Survey Professional Paper 490, 196 p.
- 1969, Development of the Green River drainage system across the Uinta Mountains, in Geologic guidebook of the Uinta Mountains: Intermountain Association of Geologists Annual Field Conference, 16th, p. 93-100.
- 1984, Post-Laramide tectonic history of the eastern Uinta Mountains, Utah, Colorado, and Wyoming: The Mountain Geologist, v. 21, p. 5-29.
- Hood, A., Gutjahr, C.C.M., and Heacock, R.L., 1975, Organic metamorphism and the generation of petroleum: American Association of Petroleum Geologists Bulletin, v. 59, p. 986-996.
- Hunt, C.B., 1969, Geological history of the Colorado River: U.S. Geological Survey Professional Paper 669, p. 59-130.
- Hunt, J.M., 1979, Petroleum geochemistry and geology: San Francisco, Freeman, 617 p.
- Hutton, A.C., and Cook, A.C., 1980, Influence of alginite on the reflectance of vitrinite from Joadja, New South Wales, and some other coals and oil shales containing alginite: Fuel, v. 59, p. 711-714.
- Ingram, G.R., and Rimstidt, J.D., 1984, Natural weathering of coal: Fuel, v. 63, p. 292-296.
- Izett, G.A., 1975, Late Cenozoic deformation in northern Colorado and adjoining areas: Geological Society of America Memoir 144, p. 179-210.
- Johnson, R.C., 1985, Early Cenozoic history of the Uinta and Piceance Creek basins, Utah and Colorado, with special reference to the development of Eocene Lake Uinta, in Kaplin, S.S., and Flores, R.M., eds., Cenozoic paleogeography of the west-central United States: Rocky Mountain Section, Society of Economic Paleontologists and Mineralogists, p. 247-275.
- 1989, Detailed cross section correlating the Upper Cretaceous and lower Tertiary rocks between the Uinta basin of eastern Utah and western Colorado and the Piceance basin of western Colorado: U.S. Geological Survey Miscellaneous Investigations Map I-1974.
- Johnson, R.C., Crovelli, R.A., Spencer, C.W., and Mast, R.F., 1987, An assessment of gas resources in low-permeability sandstones of the Upper Cretaceous Mesaverde Group, Piceance Basin, Colorado: U.S. Geological Survey Open-File Report 87-357, 165 p.
- Johnson, R.C., and Finn, T.M., 1986, Cretaceous through Holocene history of the Douglas Creek arch, Colorado and Utah, in Stone, D.S., ed., New interpretations of northwest Colorado geology: Rocky Mountain Association of Geologists, p. 77-95.
- Johnson, R.C., and Johnson, S.Y., 1991, Stratigraphic and time-stratigraphic cross sections, of Phanerozoic rocks along line B-B', Uinta and Piceance basin area, western-central Uinta basin, Utah, to eastern Piceance basin, Colorado: U.S. Geological Survey Miscellaneous Investigations Series Map I-2184-B.
- Johnson, R.C., and Nuccio, V.F., 1986, Structural and thermal history of the Piceance Creek Basin, western Colorado, in relation to hydrocarbon occurrence in the Mesaverde Group, in Spencer, C.W., and Mast, R.F., eds., Geology of tight gas reservoirs: American Association of Petroleum Geologists Studies in Geology 24, p. 165-206.
- Karweil, J., 1955, Die metamorphose der Kohlen vom Standpunkt der physikalischen Chemie: Zeitschrift der Deutschen Geologischen Gesellschaft, v. 107, p. 132-139.
- Katz, B.J., Pfeifer, R.N., and Schunk, D.J., 1988, Interpretation of discontinuous vitrinite reflectance profiles: American Association of Petroleum Geologists Bulletin, v. 72, p. 926-931.
- Law, B.E., Nuccio, V.F., and Barker, C.E., 1989, Kinky vitrinite reflectance profiles—Evidence of paleopore pressure in low-permeability gas-bearing sequences in Rocky Mountain foreland basins: American Association of Petroleum Geologists Bulletin, v. 73, p. 999-1010.
- Lopatin, N.V., 1971, Temperature and geologic time as factors in coalification: Akademiya Nauk SSSR, Izvestiya Seriya Geologicheskaya, no. 3, p. 95-106.
- Marchioni, D.L., 1983, The detection of weathering in coal by petrographic, rheologic and chemical methods: International Journal of Coal Geology, v. 2, p. 231-259.
- Naeser, C.W., 1979, Thermal history of sedimentary basins; fission-track dating of subsurface rocks, in Scholle, P.A., and Schluger, P.R., eds., Aspects of diagenesis: Society of Economic Paleontologists and Mineralogists Special Publication 26, p. 109-112.
- 1981, The fading of fission tracks in the geologic environment—Data from deep drill holes: Nuclear Tracks, v. 5, p. 248-250.
- Narr, W., and Currie, J.B., 1982, Origin of fracture porosity—Example from Altamont Field, Utah: American Association of Petroleum Geologists Bulletin, v. 66, p. 1231-1247.
- Nuccio, V.F., and Johnson, R.C., 1983, Thermal maturity map of the Cameo-Fairfield or equivalent coal zone through the Piceance Creek basin, Colorado—A preliminary report: U.S. Geological Survey Miscellaneous Field Study Map MF-1575, scale: 1:253,400.
- 1984a, Thermal maturation and burial history of the Upper Cretaceous Mesaverde Group, including the Multiwell Experiment (MWX), Piceance Creek Basin, Colorado: U.S. Geological Survey Open-File Report 84-757, 8 p.
- 1984b, Retardation of vitrinite reflectance in Green River oil shales, Piceance Creek Basin, northwestern Colorado [abs.]: American Association of Petroleum Geologists Bulletin, v. 68, p. 513.
- 1986, Thermal maturity of the lower part of the Upper Cretaceous Mesaverde Group, Uinta Basin, Utah: U.S. Geological Survey Miscellaneous Field Studies Map MF-1842, scale 1:250,000.
- 1988, Surface vitrinite reflectance map of the Uinta, Piceance and Eagle Basins area, Utah and Colorado: U.S. Geological Survey Miscellaneous Field Studies Map MF-2008-B, 1 plate, 19 p., scale 1:500,000.
- 1989a, Variations in vitrinite reflectance for the Upper Cretaceous Mesaverde Group, southeastern Piceance

- Creek Basin, northwestern Colorado—Implications for burial history and potential hydrocarbon generation: U.S. Geological Survey Bulletin 1787-H, 10 p.
- 1989b, Thermal history of selected coal beds in the Upper Cretaceous Mesaverde Group and Tertiary Wasatch Formation, Multiwell Experiment site, Colorado, in relation to hydrocarbon generation, in Law, B.E., and Spencer, C.W., eds., *Geology of tight gas reservoirs in Pinedale anticline area, Wyoming, and Multiwell Experiment site, Colorado*: U.S. Geological Survey Bulletin 1886-L, 11 p.
- Nuccio, V.F., and Schenk, C.J., 1986, Thermal maturity and hydrocarbon source-rock potential of the Eagle Basin, northwestern Colorado, in Stone, D.S., ed., *New interpretations of northwestern Colorado geology*: Rocky Mountain Association of Geologists, p. 259–264.
- 1987, Burial reconstruction of the Belden Formation, Gilman area, Eagle Basin, northwestern Colorado: U.S. Geological Survey Bulletin 1787-C, 6 p.
- Perry, W.J., Jr., and Grout, M.A., 1988, Wedge model for late Laramide basement-involved thrusting, Grand Hogback monocline and White River uplift, western Colorado: Geological Society of America Abstracts with Programs, p. A384–385.
- Pitman, J.K., Fouch, T.D., and Goldhaber, M.B., 1982, Depositional setting and diagenetic evolution of some Tertiary unconventional reservoir rocks, Uinta Basin, Utah: *American Association of Petroleum Geologists Bulletin*, v. 66, p. 1581–1596.
- Pitman, J.K., Franczyk, K.J., and Anders, D.E., 1987, Marine and nonmarine gas-bearing rocks in Upper Cretaceous Blackhawk and Neslen Formations, eastern Uinta basin, Utah—Sedimentology, diagenesis, and source rock potential: *American Association of Petroleum Geologists Bulletin*, v. 71, p. 76–94.
- Pollastro, R.M., and Barker, C.E., 1986, Application of clay-mineral, vitrinite reflectance, and fluid inclusion studies to the thermal and burial history of the Pinedale Anticline, Green River Basin, Wyoming, in Gautier, D.L., ed., *Roles of organic matter in sediment diagenesis*: Society of Economic Paleontologists and Mineralogists Special Publication 38, p. 73–83.
- Price, L.C., and Barker, C.E., 1984, Suppression of vitrinite reflectance in amorphous rich kerogen—A major unrecognized problem: *Journal of Petroleum Geology*, v. 8, p. 59–84.
- Robert, P., 1988, Organic metamorphism and geothermal history: Dordrecht, Holland, D. Reidel. 311 p.
- Roedder, E., 1984, Fluid inclusions: Mineralogical Society of America Reviews in Mineralogy, v. 12, 644 p.
- Sales, J.K., 1983, Collapse of Rocky Mountain basement uplifts, in Löwell, J.D., ed., *Rocky Mountain foreland basins and uplifts*: Rocky Mountain Association of Geologists, p. 79–97.
- Sears, J.D., 1924, Relations of the Browns Park Formation and the Bishop Conglomerate and their role in the origin of the Green and Yampa Rivers: *Geological Society of America Bulletin*, v. 635, no. 2, p. 279–304.
- Suggate, R.P., 1982, Low-rank sequences and scales of organic metamorphism: *Journal of Petroleum Geology*, v. 4, p. 377–392.
- Tissot, B., Deroo, G., and Hood, A., 1978, Geochemical study of the Uinta basin—Formation of petroleum from the Green River Formation: *Geochimica et Cosmochimica Acta*, v. 42, p. 1469–1485.
- Walker, A.L., McCulloh, T.H., Peterson, N.F., and Stewart, R.J., 1983, Anomalous low reflectance of vitrinite in comparison with other petroleum source-rock maturation indices, from the Miocene Modelo Formation in the Los Angeles basin, California, in Isaacs, C.M., ed., *Petroleum generation and occurrence in the Miocene Monterey Formation, California*: Los Angeles, Society of Economic Paleontologists and Mineralogists, p. 185–190.
- Waples, D.W., 1980, Time and temperature in petroleum formation; application of Lopatin's method to petroleum exploration: *American Association of Petroleum Geologists Bulletin*, v. 64, p. 916–926.
- 1985, *Geochemistry in petroleum exploration*: Boston, International Human Resources Development Corporation, 232 p.
- Whitney, J.W., and Andrews, E.D., 1983, Past and present geomorphic activity in the Piceance Creek drainage basin, northwestern Colorado, in Gary, J.H., ed., *Sixteenth Oil Shale Symposium proceedings*: Golden, Colorado School of Mines, p. 566–577.
- Whitney, J.W., Verbeek, E.R., and Grout, M.A., 1984, Late Tertiary consequent drainage in the Piceance Creek drainage basin, northwestern Colorado: Geological Society of America Abstracts with Programs, v. 16, p. 260.
- Willett, S.D., and Chapman, D.S., 1987, Temperatures, fluid flow and thermal history of the Uinta basin, in Dologez, B., ed., *Migration of hydrocarbons in sedimentary basins*: Paris, Editions Techniques, p. 533–551.
- Yeend, W.E., 1969, Quaternary geology of the Grand and Battlement Mesas area, Colorado: U.S. Geological Survey Professional Paper 617, 50 p.

Published in the Central Region, Denver, Colorado
 Manuscript approved for publication October 17, 1991
 Graphics by Roger Highland
 Cover art by Art Isom
 Type composed by Marie Melone
 Appendix composed by Judith Stoesser
 Edited by Judith Stoesser

Appendix. Location, formation, age, and vitrinite reflectance data for surface samples from the Uinta, Piceance, and Eagle basins, Utah and Colorado

[Sample locality shown by sample number on plate 1. Type of preparation: mac, macerated. Lithostratigraphic units are formations unless otherwise designated; Mesaverde can be Group or Formation, depending on location; Wasatch Formation is Eocene at some locations and Paleocene and Eocene at other locations. Rm, mean random vitrinite reflectance (in percent); No., number of measurements; S.D., standard deviation of measurement. Leader (—) indicates data not available]

Location	Sample number (type of prep.)	Lithostratigraphic unit	Age	Sample description	Rm	No.	S.D.	Comments on reflectance analysis
Toole County, Utah								
Center, sec. 35, T. 8 S., R. 100 W.	86-3Q (mac)	Salt Lake	Miocene and Pliocene	Micaceous clayey sandstone in limestone sequence	0.58	7	0.11	Organic matter scarce but has consistent reflectance values.
NW¼ sec. 2, T. 9 S., R. 5 W.	86-3P (mac)	Oquirrh Group	Late Mississippian to Early Permian	Gray and red mudstone	—	—	—	Barren of vitrinite.
SW¼ sec. 36, T. 8 S., R. 5 W.	86-3R (mac)	Ochre Mountain Limestone or Woodman	Late Miss. or Early and Late Mississippian	Dark-gray mudstone	—	—	—	Barren of vitrinite.
NW¼ sec. 5, T. 9 S., R. 4 W.	86-3S (mac)	Alluvium	Quaternary	Gray claystone	—	—	—	Barren of vitrinite.
Juab County, Utah								
NE¼ sec. 8, T. 13 S., R. 3 W.	86-3T (mac)	Alluvium	Quaternary	Varicolored mudstone	—	—	—	Barren of vitrinite.
NW¼ sec. 18, T. 13 S., R. 3 W.	86-3U (mac)	Alluvium	Quaternary	Brown mudstone	—	—	—	Barren of vitrinite.
NW¼ sec. 34, T. 13 S., R. 4 W.	86-3V (mac)	Pogonip Group	Early and Middle Ordovician	Black limestone	—	—	—	Barren of vitrinite.
NW¼NW¼ sec. 2, T. 13 S., R. 1 E.	86-3W (mac)	San Rafael Group	Middle Jurassic	Gray calcareous shale	0.55	8	0.16	Vitrinite grains very scarce.
NE¼ sec. 2, T. 13 S., R. 1 E.	86-3X (mac)	San Rafael Group	Middle Jurassic	Dark-gray shale	—	—	—	Barren of vitrinite.
NE¼NE¼ sec. 1, T. 13 S., R. 1 E.	86-3Y (mac)	San Rafael Group	Middle Jurassic	Dark-gray shale from base of coarsening-upward cycle	0.84	26	0.11	Vitrinite abundant, majority reworked.
NE¼NW¼ sec. 6, T. 13 S., R. 2 E.	86-3Z (mac)	San Rafael Group	Middle Jurassic	Dark-gray shale	0.65	21	0.14	Measured lowest reflectance material. Vitrinite grains small. Measured lowest reflectance population.
Salt Lake County, Utah								
SW¼ sec. 24, T. 1 S., R. 1 E.	86-3A (mac)	Twin Creek Limestone	Middle Jurassic	Black limestone	—	—	—	Barren of vitrinite.
Sec. 19, T. 1 S., R. 2 E.	86-3B (mac)	Twin Creek Limestone	Middle Jurassic	Dark-gray clayey limestone	—	—	—	Barren of vitrinite.
Center, sec. 9, T. 1 S., R. 2 E.	86-3C (mac)	Twin Creek Limestone	Middle Jurassic	Dark-gray limestone	—	—	—	Barren of vitrinite.
NE¼ sec. 13, T. 1 S., R. 2 E.	86-3D (mac)	Kelvin	Early Cretaceous	Medium-gray silty shale with shell fragments	1.06	14	0.11	Vitrinite scarce; measured lowest reflectance population.
Utah County, Utah								
NE¼ sec. 7, T. 6 S., R. 3 E.	86-4A (mac)	Unknown	Mississippian?	Black shale	—	—	—	Barren of vitrinite.
SE¼ sec. 23, T. 5 S., R. 3 E.	86-4B (mac)	Phosphoria	Early Permian	Black shale	0.79	6	0.16	Vitrinite scarce. Both low-reflectance material and higher reflectance reworked material.
SW¼ sec. 24, T. 10 S., R. 7 E.	86-5R (mac)	Colton	Paleocene and Eocene	Dark-gray mudstone from variegated sequence	1.46	34	0.18	Wide range of reflectances. Measured lowest population.
SE¼ sec. 21, T. 10 S., R. 7 E.	86-5S (mac)	Green River Green River	Eocene	Dark-gray carbonaceous shale	1.32	45	0.17	Organics abundant but have weathered appearance.
SE¼ sec. 24, T. 10 S., R. 6 E.	86-5T (mac)	Green River	Eocene	Dark-gray shale from interbedded gray shale and marlstone sequence	0.47	15	0.07	Not a lot of vitrinite, some large, low-reflectance grains.
NW¼ sec. 24, T. 10 S., R. 6 E.	86-5U (mac)	Green River	Eocene	Gray silty shale from shale and sandstone sequence	—	—	—	Barren of vitrinite.
SE¼SW¼ sec. 10, T. 10 S., R. 6 E.	86-5V (mac)	Green River	Eocene	Gray silty shale from shale and marlstone sequence	0.32	14	0.07	Barren of vitrinite.
SE¼ sec. 1, T. 10 S., R. 5 E.	86-5W (mac)	Green River	Eocene	Dark-gray silty shale	0.40	37	0.09	Vitrinite scarce, some good low-reflectance grains.
SW¼ sec. 27, T. 9 S., R. 4 E.	86-5X (mac)	Colton	Paleocene and Eocene	Gray siltstone	—	—	—	Large low-reflectance vitrinite population.
Center sec. 28, T. 9 S., R. 4 E.	86-5Y (mac)	Jurassic, undiff.	Jurassic	Gray shale	0.51	16	0.15	Wide range of reflectances, measured lowest.
SW¼ sec. 35, T. 8 S., R. 3 E.	86-5Z (mac)	Pennsylvanian and Permian, undiff.	Pennsylvanian and Permian	Black shaley limestone	0.32	7	0.06	Wide range. Higher population in 1.00–2.00 range.

San Pete County, Utah									
NW¼ sec. 26, T. 15 S., R. 2 E.	86-4A (mac)	Flagstaff Limestone	Paleocene and Eocene	Gray claystone from claystone and sandstone sequence	0.41	4	0.05	Some amorphous organic matter. A few vitrinite grains	
SW¼NW¼ sec. 27, T. 15 S., R. 2 E.	86-4B (mac)	Flagstaff Limestone	Eocene	Gray shale from variegated shale and sandstone sequence	0.54	17	0.18	Wide range. Measured lowest population.	
SE¼ sec. 7, T. 18 S., R. 3 E.	86-4C (mac)	Flagstaff Limestone or North Horn	Paleocene and Eocene or Late Cretaceous	Greenish-gray shale	—	—	—	Barren.	
Sevier County, Utah									
SE¼ sec. 33, T. 21 S., R. 1 E.	86-4D (mac)	Flagstaff Limestone or North Horn	Paleocene and Eocene or Late Cretaceous	Gray claystone from variegated claystone sequence	—	—	—	Barren.	
SW¼ sec. 6, T. 22 S., R. 2 E.	86-4E (coal)	Price River	Late Cretaceous	Sandstone containing coal chips	0.48	9	0.08	Coal almost all fusinite. A few vitrinite grains.	
NW¼ sec. 8, T. 22 S., R. 2 E.	86-4F (coal)	Price River	Late Cretaceous	Coal chips from base of channel sandstone	0.86	18	0.14	Not a good sample. Vitrinite shows signs of weathering.	
NW¼ sec. 9, T. 22 S., R. 2 E.	86-4G (coal)	Price River	Late Cretaceous	Carbonaceous shale containing channel sandstone	0.47	50	0.05	Good coal.	
SE¼NE¼ sec. 9, T. 22 S., R. 2 E.	86-4H (coal)	Price River	Late Cretaceous	1.5-ft-thick coal bed below 15-ft-thick channel sandstone	0.57	50	0.05	Good coal.	
NW¼ sec. 14, T. 22 S., R. 2 E.	86-4I (coal)	Price River	Late Cretaceous	1-ft-thick coal bed below 20-ft-thick channel sandstone	0.51	52	0.04	Good coal. Mineral matter associated with vitrinite.	
NE¼ sec. 13, T. 22 S., R. 2 E.	86-4J (coal)	Price River	Late Cretaceous	6-in.-thick coal in carbonaceous shale	0.54	50	0.05	Good coal.	
NW¼ sec. 20, T. 22 S., R. 3 E.	86-4K (coal)	Price River	Late Cretaceous	Thin coal stringer in carbonaceous shale	0.40	40	0.04	Good coal.	
NW¼ sec. 21, T. 22 S., R. 3 E.	86-4L (coal)	Price River or Blackhawk	Late Cretaceous	1-ft-thick coal at base of channel sandstone	0.54	50	0.06	Good coal.	
NW¼SW¼ sec. 13, T. 23 S., R. 3 E.	86-4M (coal)	Blackhawk?	Late Cretaceous	Thin coal in carbonaceous shale with 1-3-ft-thick sandstone beds	0.41	50	0.05	Good coaly shale.	
SW¼ sec. 34, T. 23 S., R. 4 E.	86-4N (coal)	Blackhawk?	Late Cretaceous	Carbonaceous shale with coal stringers.	0.42	50	0.05	Good, consistent, coaly shale.	
SE¼ sec. 34, T. 23 S., R. 5 E.	86-4O (mac)	Mancos Shale	Late Cretaceous	Dark-gray shale	0.43	45	0.07	Good sample. Large low-reflectance population.	
Wayne County, Utah									
Sec. 34, T. 28 E., R. 8 E.	39-12 (coal)	Mancos Shale	Late Cretaceous	Coal	0.52	—	—	—	
Sec. 19, T. 28 S., R. 10 E.	39-11 (coal)	Tununk Member of Mancos Shale	Late Cretaceous	Coal	0.60	—	—	—	
Sec. 13, T. 28 S., R. 10 E.	39-14 (coal)	Dakota Sandstone	Late Cretaceous	Coal	0.52	—	—	—	
Emery County, Utah									
NW¼NE¼ sec. 30, T. 23 S., R. 6 E.	86-4P (coal)	Mancos Shale	Late Cretaceous	3-ft-thick coal beneath 18-ft-thick channel sandstone	0.51	48	0.04	Good coal.	
NW¼ sec. 21, T. 23 S., R. 6 E.	86-4Q (coal)	Mancos Shale	Late Cretaceous	2-ft-thick coal beneath 8-ft-thick channel sandstone	0.54	49	0.06	Fair coal.	
SW¼ sec. 14, T. 23 S., R. 6 E.	86-4R (mac)	Mancos Shale	Late Cretaceous	Dark-gray shale	0.45	40	0.10	Vitrinite abundant.	
NE¼ sec. 18, T. 23 S., R. 7 E.	86-4S (mac)	Dakota Sandstone	Late Cretaceous	Gray shale from base of conglomeratic channel	0.50	20	0.07	Not a lot of vitrinite, but quality is good.	
SW¼ sec. 4, T. 23 S., R. 8 E.	86-4T (mac)	Jurassic, undiff.	Jurassic	Gray silty sandstone	0.64	10	0.16	Low-reflectance population scarce. A higher reflectance, reworked population.	
NW¼ sec. 2, T. 23 S., R. 9 E.	86-4U (mac)	Glen Canyon Group	Early Jurassic	Gray shale from maroon, gray, and green sandstone and shale sequence	1.43	48	0.20	Organic matter abundant. Measured lowest reflectance population.	
SE¼ sec. 29, T. 22 S., R. 11 E.	86-4V (mac)	Moenkopi	Early and Middle? Triassic	Gray shale from maroon and gray sandstone and shale sequence	0.68	7	0.19	Vitrinite grains scarce and small.	
NW¼NE¼ sec. 9, T. 22 S., R. 13 E.	86-4W (mac)	Moenkopi	Early and Middle? Triassic	Gray sandy shale	—	—	—	Barren.	
SW¼ sec. 3, T. 22 S., R. 13 E.	86-4X (mac)	Moenkopi	Middle? Triassic	Gray silty shale from coarsening-upward sandstone and shale cycle	—	—	—	Barren.	
SW¼ sec. 35, T. 21 S., R. 13 E.	86-4Y (mac)	Moenkopi	Early and Middle? Triassic	Gray shale	—	—	—	Barren.	
NW¼NW¼ sec. 1, T. 22 S., R. 14 E.	86-4Z (mac)	Mancos Shale	Late Cretaceous	Black shale just above Dakota	0.53	49	0.07	Good sample. Large low-reflectance vitrinite population.	
SE¼ sec. 15, T. 21 S., R. 15 E.	86-5A (mac)	Mancos Shale	Late Cretaceous	Dark-gray shale	0.49	15	0.11	Few good vitrinite grains.	
NW¼ sec. 5, T. 21 S., R. 15 E.	86-5B (mac)	Mancos Shale	Late Cretaceous	Dark-gray shale	0.64	34	0.14	Wide range of organic matter, measured lowest vitrinite population.	
SW¼ sec. 23, T. 20 S., R. 14 E.	86-5C (mac)	Mancos Shale	Late Cretaceous	Dark-gray shale	0.43	33	0.10	Fairly large low-reflectance population.	
NW¼SW¼ sec. 34, T. 19 S., R. 14 E.	86-5D (mac)	Mancos Shale	Late Cretaceous	Dark-gray shale	0.51	31	—	Large low-reflectance population.	
Center, sec. 3, T. 19 S., R. 14 E.	86-5E (mac)	Mancos Shale	Late Cretaceous	Dark-gray shale	0.52	31	0.10	Large, fairly consistent low-reflectance population.	

Appendix. Location, formation, age, and vitrinite reflectance data for surface samples from the Uinta, Piceance, and Eagle basins, Utah and Colorado—Continued

Location	Sample number (type of prep.)	Lithostratigraphic unit	Age	Sample description	Rm	No.	S.D.	Comments on reflectance analysis
Emery County, Utah—Continued								
SE $\frac{1}{4}$ sec. 4, T. 18 S., R. 14 E.	86-5F (mac)	Mancoos Shale	Late Cretaceous	Dark-gray shale	0.51	26	0.11	Fairly good low-reflectance population.
Sec. 17, T. 17 S., R. 14 E.	86-5G (mac)	Mancoos Shale	Late Cretaceous	Dark-gray shale	0.62	30	0.14	Wide range. Measured lowest population.
NW $\frac{1}{4}$ sec. 9, T. 16 S., R. 13 E.	86-5H (mac)	Mancoos Shale	Late Cretaceous	Dark-gray shale	0.49	50	0.09	Very good sample.
Sec. 3, T. 16 S., R. 14 E.	U86-KF-3VR (coal)	Blackhawk	Late Cretaceous	Coal	0.58	50	0.05	Good coal.
Sec. 23, T. 17 S., R. 15 E.	U86-19-KF-Tt (coal)	North Horn and Flagstaff Limestone, undiff.	Late Cretaceous to Eocene	Coal	1.28	51	0.12	Sample looks weathered.
Carbon County, Utah								
SW $\frac{1}{4}$ sec. 14, T. 15 S., R. 12 E.	86-5I (mac)	Mancoos Shale	Late Cretaceous	Dark-gray shale	0.61	48	0.08	Large, low-reflectance population.
NE $\frac{1}{4}$ sec. 2, T. 15, R. 11 S.,	86-5J (mac)	Mancoos Shale	Late Cretaceous	Dark-gray shale from base of coarsening-upward cycle	0.58	50	0.06	Very good sample.
NW $\frac{1}{4}$ sec. 22, T. 14 S., R. 10 E.	86-5K (mac)	Mancoos Shale	Late Cretaceous	Dark-gray shale	0.58	47	0.08	Good sample.
NE $\frac{1}{4}$ sec. 1, T. 14 S., R. 9 S.	86-5L (mac)	Mancoos Shale	Late Cretaceous	Dark-gray shale	0.59	50	0.07	Good sample. Vitrinite abundant and consistent.
SE $\frac{1}{4}$ NE $\frac{1}{4}$ sec. 11, T. 13 S., R. 9 E.	86-5M (mac)	Mancoos Shale	Late Cretaceous	Dark-gray shale	0.55	36	0.05	Good consistent low-reflectance population.
NW $\frac{1}{4}$ sec. 1, T. 13 S., R. 9 E.	86-5N (coal)	Blackhawk	Late Cretaceous	3-ft-thick coal bed	0.61	48	0.03	Good coal.
SE $\frac{1}{4}$ sec. 35, T. 12 S., R. 9 E.	86-5O (coal)	Blackhawk	Late Cretaceous	Coal	0.49	41	—	Fair coal.
SE $\frac{1}{4}$ sec. 16, T. 12 S., R. 9 E.	86-5P (coal)	Blackhawk	Late Cretaceous	3-ft-thick coal bed	0.54	50	0.05	Good coal.
SE $\frac{1}{4}$ sec. 5, T. 12 S., R. 9 E.	86-5Q (coal)	Blackhawk	Late Cretaceous	Thin coal bed	0.49	51	0.04	Very good coal.
Sec. 8, T. 12 S., R. 9 E.	U86-KF-1VR (coal)	North Horn	Late Cretaceous	Coal	0.49	54	0.03	Good clean coal.
NE $\frac{1}{4}$ NE $\frac{1}{4}$ sec. 33, T. 13 S., R. 13 E.	U86-KF-1RC (coal)	North Horn and Flagstaff Limestone, undiff.	Late Cretaceous to Eocene	Coal	0.52	47	0.08	Fairly dirty coal. Mineral matter associated with vitrinite.
SE $\frac{1}{4}$ NW $\frac{1}{4}$ sec. 18, T. 13 S., R. 12 E.	UGMS 594 (coal)	Mesaverde	Late Cretaceous	Coal	0.63	66	0.03	—
SE $\frac{1}{4}$ NW $\frac{1}{4}$ sec. 1, T. 13 S., R. 11 E.	UGMS 588 (coal)	Mesaverde	Late Cretaceous	Coal	0.59	69	0.04	—
SE $\frac{1}{4}$ NW $\frac{1}{4}$ sec. 10, T. 13 S., R. 11 E.	UGMS 587 (coal)	Mesaverde	Late Cretaceous	Coal	0.61	57	0.04	—
NW $\frac{1}{4}$ NW $\frac{1}{4}$ sec. 9, T. 13 S., R. 11 E.	UGMS 204 (coal)	Mesaverde	Late Cretaceous	Coal	0.70	46	0.03	—
Wasatch County, Utah								
SW $\frac{1}{4}$ SE $\frac{1}{4}$ sec. 19, T. 3 S., R. 9 W.	85-97G (mac)	Uinta	Eocene	Greenish-gray siltstone	1.06	39	0.10	Vitrinite scarce, some nice pieces.
Summit County, Utah								
NW $\frac{1}{4}$ sec. 35, T. 1 S., R. 3 E.	86-3E (mac)	Morrison	Late Jurassic	Dark-gray silty shale	1.30	12	0.28	Grains scarce and small.
SE $\frac{1}{4}$ sec. 25, T. 1 N., R. 4 E.	86-3F (mac)	Kelvin	Early Cretaceous	Gray shale from shale and conglomeratic sandstone sequence	—	—	—	Barren.
Center, sec. 12, T. 2 N., R. 5 E.	86-3G (mac)	Kelvin	Early Cretaceous	Carbonaceous shale above 4-ft-thick channel sandstone	0.68	50	0.07	Vitrinite abundant; grains slightly weathered.
NW $\frac{1}{4}$ sec. 34, T. 3 N., R. 6 E.	86-3H (coal)	Frontier	Late Cretaceous	1/8-in.-thick coal bed just below sandstone	0.35	35	0.03	Fair coal.
NW $\frac{1}{4}$ sec. 31, T. 3 N., R. 7 E.	86-3I (coal)	Evanson	Late Cretaceous and Paleocene	Coal from Boyer mine	0.47	46	0.04	Good coal.
SW $\frac{1}{4}$ sec. 23, T. 2 S., R. 6 E.	86-3J (mac)	Morgan or Round Valley	Early and Middle Pennsylvanian or Early Penn.	Dark-gray limestone	—	—	—	Barren.
SW $\frac{1}{4}$ sec. 15, T. 2 S., R. 6 E.	86-3K (mac)	Morgan or Round Valley	Early and Middle Pennsylvanian or Early Penn.	Black shaley limestone	—	—	—	Barren.
NW $\frac{1}{4}$ sec. 16, T. 3 S., R. 7 E.	86-3L (mac)	Weber	Middle Pennsylvanian	Dark-purple-gray mudstone from sandstone and mudstone sequence	—	—	—	Barren.
Duchesne County, Utah								
NW $\frac{1}{4}$ sec. 25, T. 1 N., R. 9 W.	86-3M (mac)	Uinta	Eocene	Dark-gray shale from red and gray sandstone and shale sequence	—	—	—	Barren.
SE $\frac{1}{4}$ sec. 4, T. 1 S., R. 8 W.	86-3N (mac)	Uinta	Eocene	Medium-gray shale	0.98	14	0.25	Grains scarce and small. Measured almost everything.
NW $\frac{1}{4}$ NE $\frac{1}{4}$ sec. 17, T. 2 S., R. 7 W.	86-3O (mac)	Uinta	Eocene	—	0.94	36	0.15	Measured lowest reflectance population.

Center, sec. 32, T. 3 S., R. 6 W. NE¼ sec. 36, T. 3 S., R. 6 W. SE¼ sec. 2, T. 4 S., R. 5 W.	85-97E (mac) 85-97E (coal) 85-77 (coal)	Uinta Uinta Uinta	Eocene Eocene Eocene	Dark-gray silty shale Sandstone with carbonized plant fragments Coal from two 1-in.-thick-beds, 8 in. apart, in carbonaceous shale	— 0.47 0.48	— 51 50	— 0.03 0.05	Barren. Fairly good sample. Very good coaly shale.
NW¼ sec. 1, T. 3 S., R. 5 W. NW¼ sec. 12, T. 2 S., R. 5 W.	85-97H (mac) 85-97I (mac)	Uinta Duchesne River	Eocene Paleocene to Oligocene	Dark-greenish-gray silty claystone Green silty claystone	0.75 1.00	13 14	0.13 0.13	Vitrinite scarce. Vitrinite scarce.
SE¼ sec. 24, T. 1 S., R. 5 W.	85-97J (coal)	Duchesne River	Paleocene to Oligocene	Coaly carbonaceous shale	0.45	100	0.05	Very nice coal.
SW¼ sec. 31, T. 3 S., R. 3 W.	85-76A (mac)	Uinta	Eocene	Dark-gray silty claystone	0.60	4	0.10	Grains very small. Abundant low-reflectance population too small to measure accurately, approximately 0.60.
SW¼ sec. 31, T. 3 S., R. 3 W. Sec. 26, T. 11 S., R. 10 E.	85-76B (mac) U86-KF-2VR (coal)	Uinta Green River	Eocene Paleocene and Eocene	Sandstone containing carbonized flakes Coal	1.04 0.49	10 50	0.14 0.03	Vitrinite very lean. Could all be reworked. Very good coal.
SE¼ sec. 34, T. 3 S., R. 3 W. SW¼NW¼ sec. 13, T. 3 S., R. 2 W. SE¼ sec. 8, T. 2 S., R. 1 W.	85-75 (mac) 85-74 (coal) 85-72 (mac)	Uinta Uinta Duchesne River	Eocene Eocene Paleocene to Oligocene	Dark-gray sandy claystone Weathered sandstone containing carbonized fragments Mottled gray and red mudstone	— 0.58 —	— 54 —	— 0.05 —	Barren. Good sample. Barren.
NE¼ sec. 6, T. 1 S., R. 1 W.	85-73A (mac)	Duchesne River	Paleocene to Oligocene	Gray shale	0.45	32	0.05	Coaly shale.
NW¼ sec. 5, T. 1 S., R. 1 W.	85-73B (mac)	Duchesne River	Paleocene to Oligocene	Red and gray mudstone	0.80	20	0.18	Vitrinite scarce and has a wide range. Could all be reworked.
NE¼NE¼ sec. 17, T. 9 S., R. 22 E. NE¼SW¼ sec. 4, T. 9 S., R. 20 E. NW¼SW¼ sec. 28, T. 11 S., R. 19 E.	86-9A (mac) 86-9B (mac) 86-9C (mac)	Uinta Uinta Green River	Eocene Eocene Paleocene and Eocene	Red and gray mudstone Dark-gray silty and sandy mudstone Low-grade oil shale	— 0.88 0.59	— 2 9	— 0.09 0.15	Barren. Organic matter lean. Organic matter lean.

Uintah County, Utah

NW¼NE¼ sec. 32, T. 11 S., R. 19 E.	86-9D (mac)	Green River	Paleocene and Eocene	Calcareous mudstone containing carbonaceous debris	0.35	19	0.08	Low-reflectance population and higher reflectance reworked population.
NE¼NE¼ sec. 32, T. 11 S., R. 19 E.	86-9E (mac)	Green River	Paleocene and Eocene	Calcareous mudstone	—	—	—	Barren.
SW¼ sec. 24, T. 9 S., R. 24 E. NE¼ sec. 35, T. 9 S., R. 24 E. Sec. 8, T. 9 S., R. 23 E. Sec. 6, T. 5 S., R. 21 E.	85-97A (mac) 85-97B (coal) 85-97C (mac) 85-71 (mac)	Uinta Uinta Uinta Duchesne River	Eocene Eocene Eocene Paleocene to Oligocene	Gray silty claystone containing carbonaceous debris Carbonized wood chip in gray to brown sandstone Gray silty claystone Gray silty claystone	0.94 0.41 — 0.76	12 21 — 24	0.13 0.05 — 0.14	Grains small. Fairly good sample. Barren. Organic matter scarce. Wide range of reflectances.
NE¼NE¼ sec. 26, T. 6 S., R. 25 E. NE¼NE¼ sec. 26, T. 6 S., R. 25 E.	84-55A (coal) 84-56 (coal)	Mesaverde Mesaverde	Late Cretaceous Late Cretaceous	10-in.-thick carbonaceous shale containing coal stringers Weathered carbonaceous shale containing coal	0.40 0.46	52 53	0.04 0.08	Good coal. Good coal.

Grand County, Utah

Sec. 23, T. 21 S., R. 16 E. NE¼NE¼NE¼ sec. 29, T. 20 S., R. 20 E.	39-16 UGMS 531 (coal)	Dakota Sandstone Mesaverde	Late Cretaceous Late Cretaceous	Coal Coal	0.57 0.59	— 70	— 0.05	— —
NE¼NW¼ sec. 1, T. 19 S., R. 22 E. Sec. 2, T. 19 S., R. 25 E.	UGMS 191 (coal) UB-86-KF-4VR (coal)	Mesaverde Dakota Sandstone	Late Cretaceous Late Cretaceous	Coal Coal	0.70 0.65	38 48	0.03 0.04	— Good coal.
Sec. 13, T. 22 S., R. 22 E. Sec. 29, T. 22 S., R. 24 E.	39-15 (coal) 39-7 (mac)	Dakota Sandstone Dakota Sandstone	Late Cretaceous Late Cretaceous	Coal Shale	0.75 0.60	— —	— —	— —

San Juan County, Utah

Sec. 34, T. 29 S., R. 24 E. Sec. 24, T. 33 S., R. 22 E. Sec. 24, T. 33 S., R. 26 E.	39-19 (mac) 39-9 (mac) 24-20 (coal)	Dakota Sandstone Dakota Sandstone Dakota Sandstone	Late Cretaceous Late Cretaceous Late Cretaceous	Shale Shale Coal	0.80 1.12 0.60	— — —	— — —	— — —
---	---	--	---	------------------------	----------------------	-------------	-------------	-------------

San Miguel County, Colorado

Sec. 3, T. 42 N., R. 17 W. Sec. 3, T. 43 N., R. 17 W. Sec. 19, T. 45 N., R. 12 W. Sec. 28, T. 46 N., R. 16 W.	24-3 (mac) 24-13 (coal) 24-1 (mac) 39-4 (mac)	Dakota Sandstone Dakota Sandstone Dakota Sandstone Dakota Sandstone	Late Cretaceous Late Cretaceous Late Cretaceous Late Cretaceous	Shale Coal Shale Shale	1.14 0.67 0.78 0.89	— — — —	— — — —	— — — —
--	--	--	--	---------------------------------	------------------------------	------------------	------------------	------------------

Appendix. Location, formation, age, and vitrinite reflectance data for surface samples from the Uinta, Piceance, and Eagle basins, Utah and Colorado—Continued

Sample number (type of prep.)	Location	Lithostratigraphic unit	Age	Sample description	Rm	No.	S.D.	Comments on reflectance analysis
San Miguel County, Colorado—Continued								
24-17 (coal)	Sec. 21, T. 46 N., R. 15 W.	Dakota Sandstone	Late Cretaceous	Coal	0.59	—	—	—
24-14 (coal)	Sec. 6, T. 46 N., R. 15 W.	Dakota Sandstone	Late Cretaceous	Coal	0.55	—	—	—
86-14E (mac)	SE $\frac{1}{4}$ sec. 16, T. 48 N., R. 6 W.	Manos Shale	Late Cretaceous	Dark-gray shale	0.31	50	0.07	Large low-reflectance population.
86-14F (mac)	SE $\frac{1}{4}$ sec. 3, T. 48 N., R. 7 W.	Manos Shale	Late Cretaceous	Dark-gray shale	0.51	38	0.11	Good shale. Measured lowest reflectance population.
86-14G (mac)	NE $\frac{1}{4}$ sec. 6, T. 48 N., R. 7 W.	Manos Shale	Late Cretaceous	Dark-gray shale	0.55	44	0.13	Good sample.
86-81 (coal)	Sec. 7, T. 50 N., R. 6 W.	Dakota Sandstone	Late Cretaceous	Coal chips in sandstone	0.94	39	0.11	Fair coal sample.
Mesa County, Colorado								
86-21 (coal)	SW $\frac{1}{4}$ NE $\frac{1}{4}$ sec. 15, T. 9 S., R. 97 W.	Wasatch	Tertiary	Coal chips from base of channel sandstone	0.78	34	0.09	Not a lot of vitrinite, but good quality.
86-2J (coal)	SW $\frac{1}{4}$ SE $\frac{1}{4}$ sec. 26, T. 9 S., R. 97 W.	Wasatch	Tertiary	Weathered coal chips from base of channel sandstone	1.16	44	0.10	Fair coal.
86-2K (coal)	SW $\frac{1}{4}$ NE $\frac{1}{4}$ sec. 16, T. 10 S., R. 96 W.	Wasatch	Tertiary	Carbonaceous shale containing coal stringers, 20 ft above Mesaverde	0.58	51	0.05	Good coal.
86-2L (mac)	Sec. 21, T. 11 S., R. 96 W.	Wasatch	Tertiary	Red and green mudstone ripups from channel sandstone	—	—	—	Barren of vitrinite.
86-7E (coal)	SE $\frac{1}{4}$ NE $\frac{1}{4}$ sec. 16, T. 8 S., R. 91 W.	Mesaverde	Late Cretaceous	Coal chips from channel sandstone, possibly weathered	0.71	25	0.09	Poor quality coal.
86-7G (mac)	SW $\frac{1}{4}$ SE $\frac{1}{4}$ sec. 15, T. 8 S., R. 91 W.	Mesaverde	Late Cretaceous	Black shale	0.45	44	0.05	Coaly shale.
86-7I (mac)	SE $\frac{1}{4}$ sec. 29, T. 8 S., R. 91 W.	Wasatch	Tertiary	Claystone rip-ups from channel sandstone	—	—	—	Barren.
86-7K (mac)	NE $\frac{1}{4}$ sec. 22, T. 8 S., R. 92 W.	Mesaverde	Late Cretaceous	Brown silty shale collected 5 ft below white channel sandstone	0.81	20	0.15	Measured all but a few of high-reflectance grains.
86-7L (mac)	NE $\frac{1}{4}$ sec. 22, T. 8 S., R. 91 W.	Wasatch	Tertiary	Brown silty shale in variegated shale	—	—	—	Barren.
86-7M (mac)	NE $\frac{1}{4}$ sec. 22, T. 8 S., R. 92 W.	Wasatch	Tertiary	Gray shale in gray and purple shale	0.92	7	0.09	Poor sample. Grains small and have a wide reflectance range.
86-7N (mac)	SW $\frac{1}{4}$ sec. 29, T. 8 S., R. 92 W.	Wasatch	Tertiary	Brown sandy shale from variegated sequence just above white sandstone	0.77	21	0.17	Grains scarce. A few good low-reflectance grains but majority are high reflectance; probably reworked.
86-7O (mac)	Sec. 20, T. 9 S., R. 92 W.	Wasatch	Tertiary	Gray sandy shale from mostly red-bed sequence	0.86	8	0.15	Grains scarce. Measured lowest reflectance population.
86-7P (coal)	SW $\frac{1}{4}$ NW $\frac{1}{4}$ sec. 12, T. 10 S., R. 92 W.	Wasatch	Tertiary	Coalified plant fragments from base of channel sandstone	0.53	29	0.06	Fairly good coal.
86-7Q (coal)	SE $\frac{1}{4}$ NE $\frac{1}{4}$ sec. 25, T. 10 S., R. 92 W.	Wasatch	Tertiary	Weathered coal stringers in sandstone	0.45	50	0.05	Fairly good coal.
Delta County, Colorado								
86-7X (mac)	SE $\frac{1}{4}$ NW $\frac{1}{4}$ sec. 23, T. 12 S., R. 95 W.	Green River	Eocene	Green, micaceous sandy shale just above white micaceous sandstone	0.71	10	0.15	Organic matter scarce. Few relatively low-reflectance grains.
86-7Y (mac)	NW $\frac{1}{4}$ sec. 24, T. 12 S., R. 95 W.	Green River	Eocene	Dark-olive-gray clayey marl	0.49	7	0.13	Organic matter lean. Read almost every grain.
86-7Z (mac)	SE $\frac{1}{4}$ NW $\frac{1}{4}$ sec. 23, T. 12 S., R. 95 W.	Green River	Eocene	Greenish shale or silty marl	0.55	20	0.11	Good sample. Relatively large low-reflectance population.
86-8A (mac)	SE $\frac{1}{4}$ SW $\frac{1}{4}$ sec. 10, T. 12 S., R. 95 W.	Wasatch	Tertiary	Gray shale from variegated maroon and gray shale	0.71	39	0.13	Good sample.
86-8B (mac)	NW $\frac{1}{4}$ sec. 10, T. 12 S., R. 95 W.	Green River	Eocene	Gray mudstone from mudstone and white sandstone sequence	—	—	—	Barren.
86-8C (coal)	Center, sec. 31, T. 14 S., R. 94 W.	Dakota Sandstone	Late Cretaceous	Coal stringer in sandstone	0.62	50	0.04	Good coal sample.
86-8D (mac)	NW $\frac{1}{4}$ NW $\frac{1}{4}$ sec. 33, T. 14 S., R. 94 W.	Manos Shale	Late Cretaceous	Black shale	0.38	49	0.06	Good sample.
86-8E (mac)	Sec. 31, T. 14 S., R. 93 W.	Manos Shale	Late Cretaceous	Black shale from base of coarsening-upward cycle	0.34	44	0.08	Fair sample. Wide range of reflectances. Measured lowest reflectance population.
86-8F (mac)	NE $\frac{1}{4}$ sec. 32, T. 14 S., R. 92 W.	Manos Shale	Late Cretaceous	Dark-gray shale	0.53	23	0.09	Measured lowest reflectance population.
86-8G (mac)	SW $\frac{1}{4}$ SW $\frac{1}{4}$ sec. 25, T. 15 S., R. 92 W.	Manos Shale	Late Cretaceous	Black shale	0.88	53	0.12	Sample shows signs of weathering.
86-8H (mac)	Sec. 31, T. 15 S., R. 91 W.	Manos Shale	Late Cretaceous	Dark-gray shale	0.47	49	0.05	Good sample.
86-7R (mac)	NE $\frac{1}{4}$ sec. 12, T. 11 S., R. 91 W.	Wasatch	Tertiary	Coal chips in sandstone	0.68	15	0.22	Organic matter scarce.
Garfield County, Colorado								
83-163H (coal)	Sec. 23, T. 6 S., R. 104 W.	Mesaverde	Late Cretaceous	Carbonaceous claystone containing coal	0.59	101	0.04	Very good coal.
83-139B (coal)	Sec. 24, T. 6 S., R. 104 W.	Mesaverde	Late Cretaceous	4-ft-thick coal bed	0.64	101	0.04	Very good coal.
83-146 (coal)	Sec. 21, T. 6 S., R. 103 W.	Mesaverde	Late Cretaceous	Coal in carbonaceous shale	0.62	101	0.05	Very good coal.
83-145 (coal)	Sec. 21, T. 6 S., R. 103 W.	Mesaverde	Late Cretaceous	10-in.-thick coal stringer in carbonaceous shale	0.57	17	0.05	Fair coal.
83-147 (coal)	Sec. 5, T. 7 S., R. 103 W.	Mesaverde	Late Cretaceous	8-ft-thick coal bed in carbonaceous shale	0.65	102	0.03	Very good coal.

Sec. 8, T. 6 S., R. 102 W.	VN-6A (coal)	Mesaverde	Late Cretaceous	Coal	0.60	101	0.05	Good coal.
Sec. 8, T. 6 S., R. 102 W.	VN-6B (coal)	Mesaverde	Late Cretaceous	Coal	0.63	101	0.05	Good coal.
Sec. 6, T. 5 S., R. 101 W.	VN-6C (coal)	Green River	Eocene	Coal	0.32	150	0.04	Very good coal.
Sec. 13, T. 5 S., R. 100 W.	C-144 (coal)	Uinta	Eocene	Coal chip in mudstone or sandstone	0.38	101	0.05	Good coal.
Sec. 23, T. 6 S., R. 97 W.	Bar-A-2 (coal)	Uinta	Eocene	Coaly shale	0.45	21	0.07	Coaly shale. Some good vitrinite grains.
Sec. 32, T. 7 S., R. 96 W.	86-2H (coal)	Wasatch	Tertiary	Coalified log at base of channel sandstone	0.87	44	0.04	Nice, clean, consistent coal.
SW $\frac{1}{4}$ sec. 31, T. 5 S., R. 91 W.	86-2A (coal)	Wasatch	Tertiary	Badly weathered coal chips from base of channel sandstone	0.55	20	0.07	Poor-quality coal. Mineral matter associated with vitrinite.
Sec. 25, T. 5 S., R. 92 W.	86-2B (coal)	Mesaverde	Late Cretaceous	Weathered coal chips from channel sandstone	0.59	23	0.08	Poor-quality coal.
Sec. 24, T. 5 S., R. 92 W.	86-2C (coal)	Mesaverde	Late Cretaceous	Carbonaceous shale containing coal stringers	0.57	40	0.06	Fair coal.
NE $\frac{1}{4}$ SE $\frac{1}{4}$ sec. 10, T. 6 S., R. 92 W.	86-2D (coal)	Wasatch	Tertiary	0.25-in.-thick coal stringer in even-bedded sandstone	0.49	45	0.04	Fair to good coal.
NW $\frac{1}{4}$ NE $\frac{1}{4}$ sec. 17, T. 6 S., R. 93 W.	86-2F (coal)	Wasatch	Tertiary	Moderately to badly weathered coalified plant fragments in channel sandstone	0.71	50	0.07	Good clean coal.
SW $\frac{1}{4}$ sec. 22, T. 6 S., R. 94 W.	86-2G (coal)	Wasatch	Tertiary	Coal stringer in carbonaceous shale from fresh roadcut	0.60	47	0.03	Good consistent coal.
SW $\frac{1}{4}$ NE $\frac{1}{4}$ sec. 31, T. 6 S., R. 91 W.	86-1A (mac)	Wasatch	Tertiary	Gray- and rust-mottled mudstone	0.83	5	0.15	Vitrinite almost absent.
Sec. 20, T. 7 S., R. 91 W.	86-1B (coal)	Wasatch	Tertiary	0.5 by 3 in. coalified log from base of channel sandstone	0.55	49	0.06	Fair coal.
Sec. 21, T. 7 S., R. 91 W.	86-1C (coal)	Wasatch	Tertiary	0.25 by 2 in. coalified log from base of channel sandstone; good sample	1.30	51	0.06	Good coal.
NW $\frac{1}{4}$ sec. 31, T. 7 S., R. 91 W.	86-1D (coal)	Wasatch	Tertiary	Coal chips from recently exposed channel sandstone; good sample	1.58	36	0.08	Fair coal.
Sec. 1, T. 8 S., R. 92 W.	86-1E (mac)	Wasatch	Tertiary	Medium-purple-gray claystone	—	—	—	Barren.
Sec. 7, T. 7 S., R. 88 W.	N (mac)	Eagle Valley	Middle and Late Pennsylvanian	Gray mudstone	1.12	50	0.05	Good sample. Organic matter abundant.
SE $\frac{1}{4}$ sec. 13, T. 6 S., R. 92 W.	86-1F (coal)	Wasatch	Tertiary	Fairly weathered coal chips from base of channel sandstone	2.01	50	0.12	Consistent coal.
Sec. 24, T. 7 S., R. 92 W.	86-7A (coal)	Wasatch	Tertiary	Coal chips from base of channel sandstone	0.71	50	0.06	Fair coal.
NW $\frac{1}{4}$ NE $\frac{1}{4}$ sec. 5, T. 8 S., R. 91 W.	86-7B (mac)	Mesaverde	Late Cretaceous	Badly weathered black claystone	0.62	48	0.06	Coaly shale.
NW $\frac{1}{4}$ sec. 4, T. 8 S., R. 91 W.	86-7C (mac)	Mesaverde	Late Cretaceous	Black claystone	0.60	50	0.07	Good coaly shale.
NE $\frac{1}{4}$ sec. 9, T. 8 S., R. 91 W.	86-7D (mac)	Mesaverde	Late Cretaceous	Gray shale	1.05	48	0.12	Fairly consistent shale. Grains abundant and large.
NE $\frac{1}{4}$ sec. 8, T. 6 S., R. 91 W.	86-7H (coal)	Wasatch	Tertiary	Coal chips from base of channel sandstone	0.75	30	0.08	Poor quality coal.
NW $\frac{1}{4}$ SE $\frac{1}{4}$ sec. 7, T. 8 S., R. 91 W.	86-7I (mac)	Wasatch	Tertiary	Brown to dark-gray shale in variegated sandstone and shale sequence	0.88	21	0.20	Wide range of measurements.
NW $\frac{1}{4}$ NE $\frac{1}{4}$ sec. 19, T. 5 S., R. 91 W.	85-51 (coal)	Mesaverde	Late Cretaceous	10-ft-thick coal above sandstone	0.82	76	0.05	Good coal.
NW $\frac{1}{4}$ SW $\frac{1}{4}$ sec. 21, T. 5 S., R. 91 W.	85-56 (coal)	Mesaverde	Late Cretaceous	10-15 ft thick coal just above Rollins, cinklered nearby	1.41	80	0.10	Fair coal.
NE $\frac{1}{4}$ NE $\frac{1}{4}$ sec. 24, T. 5 S., R. 92 W.	85-57 (coal)	Mesaverde	Late Cretaceous	Coal mine sample	0.63	96	0.05	Very good coal.
NE $\frac{1}{4}$ NE $\frac{1}{4}$ sec. 24, T. 5 S., R. 92 W.	85-58 (coal)	Mesaverde	Late Cretaceous	Coal from abandoned mine in Cozzette Sandstone	0.66	96	0.05	Very good coal.
SW $\frac{1}{4}$ NE $\frac{1}{4}$ sec. 24, T. 5 S., R. 92 W.	85-59 (coal)	Mesaverde	Late Cretaceous	Coal from abandoned mine	0.68	61	0.05	Good coal.
SW $\frac{1}{4}$ NE $\frac{1}{4}$ sec. 24, T. 5 S., R. 92 W.	85-60 (coal)	Mesaverde	Late Cretaceous	Coal from abandoned mine	0.63	75	0.03	Good coal.
RS $\frac{1}{4}$ SE $\frac{1}{4}$ sec. 8, T. 3 S., R. 102 W.	87-75 (coal)	Mesaverde	Late Cretaceous	Fairly fresh shale sample	0.88	53	0.15	Coaly shale.
NE $\frac{1}{4}$ SE $\frac{1}{4}$ sec. 8, T. 7 S., R. 89 W.	87-76 (mac)	Mesaverde	Late Cretaceous	Coal from Black Diamond mine	0.52	50	0.03	Good clean coal.
NW $\frac{1}{4}$ NE $\frac{1}{4}$ sec. 34, T. 7 S., T. 89 W.	87-77 (mac)	Mancos Shale	Late Cretaceous	Medium-gray silty clay	0.56	50	0.06	Good sample.
SW $\frac{1}{4}$ NW $\frac{1}{4}$ sec. 34, T. 7 S., R. 89 W.	87-78 (coal)	Mesaverde	Late Cretaceous	Dark-gray silty claystone	0.48	51	0.05	Good sample.
E $\frac{1}{4}$ sec. 33, T. 7 S., R. 89 W.	87-79 (coal)	Mesaverde	Late Cretaceous	Coal from Sunlight Mine	0.65	50	0.03	Good consistent coal.
E $\frac{1}{4}$ sec. 33, T. 7 S., R. 89 W.	87-80 (coal)	Mesaverde	Late Cretaceous	1-3-ft-thick coal	0.61	50	0.04	Fair coal.
Center sec. 33, T. 7 S., R. 89 W.	87-81 (coal)	Mesaverde	Late Cretaceous	6-in.-thick coal	0.48	50	0.04	Fair coal.
SE $\frac{1}{4}$ NW $\frac{1}{4}$ sec. 33, T. 7 S., R. 89 W.	87-82 (coal)	Mesaverde	Late Cretaceous	Carbonaceous shale with coal stringers	0.45	32	0.02	Fair to poor sample.
NW $\frac{1}{4}$ SW $\frac{1}{4}$ sec. 18, T. 5 S., R. 91 W.	87-64 (mac)	Mancos Shale	Late Cretaceous	Carbonaceous shale with coal stringers	0.33	50	0.02	Consistent coal.
SE $\frac{1}{4}$ SW $\frac{1}{4}$ sec. 2, T. 5 S., R. 92 W.	87-66 (mac)	Mancos Shale	Late Cretaceous	Dark-gray shale	0.68	48	0.10	Some signs of weathering.
NW $\frac{1}{4}$ sec. 3, T. 5 S., R. 92 W.	87-67 (mac)	Dakota Sandstone	Late Cretaceous	Dark gray shale	0.50	51	0.09	Good sample.
SW $\frac{1}{4}$ SW $\frac{1}{4}$ sec. 36, T. 4 S., R. 93 W.	87-72 (mac)	Mancos Shale	Late Cretaceous	Carbonaceous shale	0.90	47	0.10	Fair sample.
NW $\frac{1}{4}$ SE $\frac{1}{4}$ sec. 36, T. 4 S., R. 93 W.	87-70 (mac)	Mowry Shale—Frontier Formation	Late Cretaceous	Black shale	0.49	33	0.11	Fair to poor sample.
NE $\frac{1}{4}$ NE $\frac{1}{4}$ sec. 8, T. 5 S., R. 92 W.	87-69 (mac)	Mancos Shale	Late Cretaceous	Dark-gray shale	0.40	50	0.08	Good sample.
SE $\frac{1}{4}$ SW $\frac{1}{4}$ sec. 4, T. 5 S., R. 92 W.	87-68 (mac)	Mancos Shale	Late Cretaceous	Dark-gray shale	0.42	49	0.06	Fair sample.
Center sec. 35, T. 4 S., R. 93 W.	87-73 (mac)	Dakota Sandstone?	Late Cretaceous	Weathered shale	0.43	55	0.07	Good sample.
NE $\frac{1}{4}$ NE $\frac{1}{4}$ sec. 2, T. 5 S., R. 93 W.	87-71 (mac)	Mancos Shale	Late Cretaceous	Silty shale	—	—	—	Barren.
SE $\frac{1}{4}$ sec. 13, T. 5 S., R. 91 W.	87-63 (mac)	Mancos Shale	Late Cretaceous	Silty shale	0.51	40	0.09	Several populations.
SW $\frac{1}{4}$ NW $\frac{1}{4}$ sec. 3, T. 4 S., R. 94 W.	88-90 (coal)	Mesaverde	Late Cretaceous	Coal from spoil pile	0.46	52	0.04	Good sample.
SW $\frac{1}{4}$ NW $\frac{1}{4}$ sec. 3, T. 4 S., R. 94 W.	88-91 (coal)	Mesaverde	Late Cretaceous	Coal from spoil pile	0.46	50	0.03	Very good coal.
NE $\frac{1}{4}$ SW $\frac{1}{4}$ sec. 35, T. 3 S., R. 94 W.	88-92 (coal)	Mesaverde	Late Cretaceous	Thin coal	0.50	50	0.03	Very good coal.
					0.41	40	0.04	Very good coal.

Appendix. Location, formation, age, and vitrinite reflectance data for surface samples from the Uinta, Piceance, and Eagle basins, Utah and Colorado—Continued

Location	Sample number (type of prep.)	Lithostratigraphic unit	Age	Sample description	Rm	No.	S.D.	Comments on reflectance analysis
Garfield County, Colorado—Continued								
NE $\frac{1}{2}$ SW $\frac{1}{4}$ sec. 35, T. 3 S., R. 94 W.	88-93 (coal)	Mesaverde	Late Cretaceous	2-ft-thick coal	0.48	50	0.04	Fair coal.
Rio Blanco County, Colorado								
Center sec. 28, T. 1 N., R. 94 W.	89-1 (coal)	Mesaverde Group (Iles Formation)	Late Cretaceous	Coal and carbonaceous shale	0.46	40	0.04	Good coal.
NW $\frac{1}{2}$ SW $\frac{1}{4}$ sec. 28, T. 1 N., R. 94 W.	89-2 (coal)	Mesaverde Group (Iles Formation)	Late Cretaceous	Coal from Fairfield Mine	0.53	40	0.03	Good coal.
NW $\frac{1}{2}$ SE $\frac{1}{4}$ sec. 8, T. 2 N., R. 94 W.	89-3 (mac)	Mesaverde	Late Cretaceous	Carbonaceous shale	0.45	35	0.04	Good sample.
SE $\frac{1}{2}$ NE $\frac{1}{4}$ sec. 8, T. 2 N., R. 94 W.	89-4 (coal)	Mesaverde	Late Cretaceous	Carbonaceous shale and coal	0.39	40	0.03	Good coal.
NE $\frac{1}{2}$ sec. 4, T. 2 N., R. 94 W.	89-5 (coal)	Mesaverde Group (Iles Formation)	Late Cretaceous	Coal	0.50	40	0.03	Good coal.
NE $\frac{1}{2}$ NE $\frac{1}{4}$ sec. 16, T. 2 S., R. 101 W.	84-40 (coal)	Mesaverde	Late Cretaceous	5-ft-thick coal bed	0.40	61	0.04	Fairly good coal.
SE $\frac{1}{2}$ SE $\frac{1}{4}$ sec. 31, T. 1 S., R. 100 W.	84-9A (coal)	Mesaverde	Late Cretaceous	Carbonaceous shale containing coal	0.36	21	0.05	Fair coal. Mineral matter associated with vitrinite.
NW $\frac{1}{2}$ NW $\frac{1}{4}$ sec. 32, T. 1 S., R. 100 W.	84-36A (coal)	Green River	Eocene	Thin coal in carbonaceous shale	0.26	65	0.02	Fair coal. Polish poor due to softness.
NE $\frac{1}{2}$ NE $\frac{1}{4}$ sec. 31, T. 1 S., R. 100 W.	84-27G (coal)	Green River	Eocene	Thin coal in carbonaceous shale	0.43	53	0.04	Coal is all vitrinite.
SW $\frac{1}{2}$ NE $\frac{1}{4}$ sec. 18, T. 4 S., R. 100 W.	83-144P (coal)	Green River	Eocene	Coalified plant fragments in rich oil shale	0.35	70	0.03	Vitrinite grains scarce but large. Good cell structure.
SW $\frac{1}{2}$ NW $\frac{1}{4}$ sec. 2, T. 2 S., R. 101 W.	84-2C (coal)	Mesaverde	Late Cretaceous	4-6-in.-thick coal bed	0.56	58	0.05	Very good trimacerallic coal.
SE $\frac{1}{2}$ SW $\frac{1}{4}$ sec. 13, T. 1 S., R. 101 W.	85-70A (coal)	Mesaverde	Late Cretaceous	Thin coal in carbonaceous shale just above white sandstone	0.66	8	0.17	Poor sample. Material looks weathered.
NW $\frac{1}{2}$ NE $\frac{1}{4}$ sec. 3, T. 1 S., R. 102 W.	84-47 (coal)	Mesaverde	Late Cretaceous	3-ft-thick coal	0.38	53	0.03	Good trimacerallic coal.
NW $\frac{1}{2}$ SE $\frac{1}{4}$ sec. 30, T. 1 N., R. 101 W.	84-43B (coal)	Mesaverde	Late Cretaceous	3-6 in.-thick coal	0.52	59	0.05	Very good coal.
NW $\frac{1}{2}$ NW $\frac{1}{4}$ sec. 26, T. 1 N., R. 101 W.	84-46 (coal)	Mesaverde	Late Cretaceous	1-2-ft-thick dirty coal	0.43	62	0.04	Fair coal.
SE $\frac{1}{2}$ NW $\frac{1}{4}$ sec. 13, T. 1 N., R. 101 W.	84-45A (coal)	Mesaverde	Late Cretaceous	1-ft-thick coal in carbonaceous shale	0.42	65	0.03	Good coal.
NE $\frac{1}{2}$ NE $\frac{1}{4}$ sec. 12, T. 1 N., R. 103 W.	84-48C (coal)	Mesaverde	Late Cretaceous	5-in.-thick coal	0.47	64	0.04	Good trimacerallic coal.
SW $\frac{1}{2}$ NW $\frac{1}{4}$ sec. 11, T. 1 N., R. 101 W.	84-44C (coal)	Mesaverde	Late Cretaceous	10-ft-thick coal	0.44	76	0.04	Good coal.
SW $\frac{1}{2}$ NW $\frac{1}{4}$ sec. 7, T. 2 N., R. 103 W.	84-53 (coal)	Mesaverde	Late Cretaceous	6-ft-thick coal from prospect pit	0.41	65	0.04	Good coal.
NW $\frac{1}{2}$ NW $\frac{1}{4}$ sec. 7, T. 2 N., R. 103 W.	84-49 (coal)	Mesaverde	Late Cretaceous	6-in.-thick dirty coal	0.37	55	0.04	Fair coal.
NW $\frac{1}{2}$ sec. 19, T. 3 N., R. 103 W.	84-54A (coal)	Mesaverde	Late Cretaceous	2-3-ft-thick coal from prospect pit	0.36	54	0.03	Fair coal.
Sec. 29, T. 2 N., R. 99 W.	USGS CH-9 (coal)	Green River	Eocene	Coal chip in 3 gallon per ton oil shale at depth of 87 ft	0.43	101	0.05	Good coal.
Sec. 12, T. 1 N., R. 100 W.	USGS CH-9A (coal)	Green River	Eocene	Coal chip at depth of 30 ft	0.36	72	0.05	Good coal.
NE $\frac{1}{2}$ NE $\frac{1}{4}$ sec. 25, T. 2 N., R. 97 W.	85-64 (mac)	Wasatch	Tertiary	Carbonaceous shale	0.62	50	0.07	Good organic-rich shale.
NW $\frac{1}{2}$ NW $\frac{1}{4}$ sec. 14, T. 1 S., R. 98 W.	C-155 (coal)	Uinta	Eocene	Coal chip in sandstone or mudstone	0.51	101	0.05	Good coal.
Sec. 28, T. 1 S., R. 98 W.	C-153 (coal)	Uinta	Eocene	Coal chip in sandstone or mudstone	0.56	101	0.07	Good coal.
Sec. 29, T. 1 S., R. 97 W.	C-299 (coal)	Green River	Eocene	Coal chip in sandstone or mudstone	0.50	59	0.06	Fair to good coal.
SE $\frac{1}{2}$ NW $\frac{1}{4}$ sec. 16, T. 2 S., R. 97 W.	85-44 (coal)	Uinta	Eocene	Coal chip in sandstone	0.24	20	0.03	Poor coal sample.
SE $\frac{1}{2}$ NW $\frac{1}{4}$ sec. 31, T. 2 S., R. 96 W.	85-45 (coal)	Uinta	Eocene	Coal chip in sandstone	0.33	50	0.05	Good coal. Nice cell structure.
SE $\frac{1}{2}$ SE $\frac{1}{4}$ sec. 3, T. 3 S., R. 96 W.	85-46 (coal)	Uinta	Eocene	Coal chip in sandstone	0.32	100	0.05	Good coal.
Center SW $\frac{1}{4}$ sec. 8, T. 3 S., R. 95 W.	85-47 (coal)	Uinta	Eocene	Coal chip in sandstone	0.33	60	0.03	Good coal. Some nice spores.
Center NE $\frac{1}{4}$ sec. 15, T. 3 S., R. 95 W.	85-48 (coal)	Uinta	Eocene	Coal chip in sandstone	0.37	50	0.04	Fair coal.
SE $\frac{1}{2}$ NW $\frac{1}{4}$ sec. 24, T. 3 S., R. 95 W.	USGS CH-2 (coal)	Green River	Eocene	Coal chip in marlstone	0.35	108	0.05	Good coal.
Sec. 26, T. 2 S., R. 95 W.	USGS CH-3A (coal)	Green River	Eocene	Coal chip in marlstone	0.43	150	0.05	Very good coal.
Sec. 14, T. 2 S., R. 95 W.	USGS CH-3 (coal)	Green River	Eocene	Coal chip in marlstone	0.51	102	0.06	Good coal.
Sec. 9, T. 1 S., R. 95 W.	USGS CH-4 (coal)	Green River	Eocene	Coal chip in marlstone	0.41	85	0.06	Fair coal. Mineral matter associated with vitrinite.
Sec. 3, T. 1 S., R. 93 W.	2U (mac)	Mancos Shale	Late Cretaceous	Dark-gray mudstone	1.07	60	0.15	Vitrinite abundant.
Sec. 8, T. 1 S., R. 91 W.	2Q (mac)	Eagle Valley	Middle and Late Pennsylvanian	Mudstone	0.73	43	0.14	Grains scarce and full of mineral matter.
Sec. 15, T. 1 N., R. 90 W.	2W (mac)	Maroon	Middle Permian	Sandstone	0.81	8	0.13	Grains scarce and small.
Sec. 21, T. 2 N., R. 88 W.	2Y (mac)	Mancos Shale	Early Permian	Dark-brown mudstone	0.42	50	0.17	Large low-reflectance population.

Sec. 36, T. 3 N., R. 88 W.	2Z (mac)	Mancos Shale	Late Cretaceous	Dark-brown mudstone	0.52	71	0.07	Vitrinite abundant. Large low-reflectance population.
NW¼SE¼ sec. 29, T. 9 N., R. 90 W.	85-117B (mac)	Wasatch	Tertiary	Medium-gray-green silty shale	1.07	49	0.19	Organic matter abundant. Only one population.
SW¼NW¼ sec. 2, T. 10 N., R. 91 W.	85-117D (mac)	Wasatch	Tertiary	Gray silty shale from purple and gray outcrop	—	—	—	Barren.
SE¼NW¼ sec. 17, T. 12 N., R. 91 W.	85-117E (mac)	Fort Union	Paleocene	Black claystone	—	—	—	Barren of vitrinite. Some signs of bitumen.
NW¼NE¼ sec. 30, T. 12 N., R. 92 W.	85-117G (mac)	Wasatch	Tertiary	Gray silty claystone	0.52	8	0.08	Vitrinite grains scarce but consistent.
Moffat County, Colorado								
Sec. 29, T. 2 N., R. 94 W.	85-117H (mac)	Upper Wasatch or Tipton Shale Mbr. of Green River	Eocene	Gray silty claystone	0.55	20	0.12	Organic matter scarce.
NW¼NE¼ sec. 5, T. 11 N., R. 96 W.	85-117I (mac)	Wasatch	Tertiary	Gray silty claystone	0.61	21	0.17	Some vitrinite spanning a wide range. Some bitumen.
NE¼NE¼ sec. 21, T. 12 N., R. 99 W.	85-117M (mac)	Tipton Shale Mbr. of Green River	Eocene	Gray silty shale	0.45	24	0.06	Good sample. Some bitumen.
NE¼SW¼ sec. 29, T. 12 N., R. 101 W.	85-117Q (coal)	Luman Tongue of Green River	Eocene	Carbonaceous shale with coal stringers	0.53	40	0.06	Fair coal.
NW¼SE¼ sec. 8, T. 11 N., R. 101 W.	85-117R (coal)	Luman Tongue of Green River	Eocene	6-in.-thick coal	0.53	50	0.06	Fair coal. Mineral matter associated with vitrinite.
Roott County, Colorado								
Sec. 31, T. 3 N., R. 85 W.	3F (mac)	Mancos Shale	Late Cretaceous	Dark-brown mudstone	0.48	52	0.05	Good sample. Large low-reflectance population.
Sec. 23, T. 2 N., R. 85 W.	3G (mac)	Mancos Shale	Late Cretaceous	Gray mudstone	0.57	40	0.11	Grains small. Measured lowest population.
Sec. 16, T. 1 N., R. 84 W.	3H (mac)	Mancos Shale	Late Cretaceous	Mudstone	0.57	52	0.09	Grains small. Good sample.
Sec. 10, T. 1 S., R. 84 W.	3M (mac)	Minturn	Middle Penn.	Mudstone	0.69	45	0.05	Good sample.
Eagle County, Colorado								
Sec. 2, T. 2 S., R. 84 W.	3O (mac)	Minturn	Middle Pennsylvanian	Dark-gray mudstone	0.82	100	0.09	Good sample.
Sec. 17, T. 2 S., R. 84 W.	3T (mac)	Mancos Shale	Late Cretaceous	Gray mudstone	0.96	61	0.11	Grains scarce but large.
Sec. 16, T. 2 S., R. 83 W.	8 (mac)	Minturn	Middle Pennsylvanian	Mudstone	1.20	81	0.10	Good sample. Two populations; measured lower one.
Sec. 6, T. 3 S., R. 85 W.	3V (mac)	Maroon	Middle Penn. to Early Permian	Red mudstone	0.66	24	0.07	Grains scarce.
Sec. 15, T. 3 S., R. 83 W.	7 (mac)	Mancos Shale	Late Cretaceous	Dark-gray mudstone	0.50	67	0.04	Very good sample.
Sec. 9, T. 4 S., R. 86 W.	3X (mac)	Belden	Early and Middle Pennsylvanian	Dark-gray mudstone	2.47	60	0.19	Good sample. Vitrinite abundant.
Sec. 24, T. 4 S., R. 84 W.	18 (mac)	Eagle Valley	Middle Pennsylvanian	Mudstone	1.18	50	0.10	Good sample. Measured lowest population.
Sec. 15, T. 4 S., R. 83 W.	4 (mac)	Dakota Sandstone	Late Cretaceous	Black mudstone	0.74	65	0.09	Good sample.
Sec. 31, T. 4 S., R. 86 W.	3Z (mac)	Belden	Early and Middle Pennsylvanian	Dark-gray mudstone	2.68	52	0.22	Good sample. Vitrinite abundant.
Sec. 4, T. 5 S., R. 85 W.	21 (mac)	Eagle Valley	Middle and Late Pennsylvanian	Dark mudstone	1.86	102	0.25	Coaly mudstone.
Sec. 5, T. 5 S., R. 84 W.	4H (mac)	Eagle Valley	Middle and Late Pennsylvanian	Black gypsum	1.55	62	0.14	Good sample. Vitrinite abundant.
Sec. 24, T. 5 S., R. 84 W.	4J (mac)	Eagle Valley	Pennsylvanian	Gray mudstone	1.08	45	0.18	Measured lowest population.
Sec. 11, T. 5 S., R. 82 W.	L (mac)	Eagle Valley	Pennsylvanian	Gray mudstone	1.35	53	0.11	Poor quality, looks weathered.
Sec. 15, T. 5 S., R. 81 W.	C (mac)	Minturn	Middle and Late Pennsylvanian	Mudstone	1.03	74	0.10	Organic matter abundant.
Sec. 20, T. 5 S., R. 79 W.	B (mac)	Minturn	Pennsylvanian	Sandstone	0.94	31	0.24	Poor sample. Grains scarce.
Sec. 29, T. 5 S., R. 86 W.	4E (mac)	Eagle Valley	Pennsylvanian	Mudstone	0.53	34	0.07	Lowest reflectance population scarce.
Sec. 5, T. 6 S., R. 85 W.	4G (mac)	Maroon	Middle Penn. to Early Permian	Sandstone	0.91	50	0.09	Good sample. Vitrinite consistent.
Sec. 16 T. 6 S., R. 86 W.	4C (mac)	Eagle Valley	Middle and Late Pennsylvanian	Gypsum	1.30	60	0.14	Vitrinite of poor quality.

Appendix. Location, formation, age, and vitrinite reflectance data for surface samples from the Uinta, Piceance, and Eagle basins, Utah and Colorado—Continued

Location	Sample number (type of prep.)	Lithostratigraphic unit	Age	Sample description	R _m	No.	S.D.	Comments on reflectance analysis
Eagle County, Colorado—Continued								
Sec. 12 T. 6 S. R. 81 W.	2 (mac)	Belden	Early and Middle Pennsylvanian	Sandstone	3.72	80	0.23	Good sample. Fairly consistent for high level of maturity.
Sec. 12 T. 8 S. R. 87 W.	R (mac)	Mancos Shale	Late Cretaceous	Dark-brown mudstone	0.74	63	0.09	Large low-reflectance population.
Sec. 10, T. 8 S., R. 84 W.	Z (mac)	Belden	Early and Middle Pennsylvanian	Dark mudstone	3.70	78	0.27	Large high-reflectance population only. Consistent.
Pitkin County, Colorado								
Sec. 33, T. 8 S., R. 86 W.	2B (mac)	Mancos Shale	Late Cretaceous	Dark-gray mudstone	1.66	56	0.14	Vitrinite abundant but small.
Sec. 28, T. 9 S., R. 85 W.	2D (mac)	Mancos Shale	Late Cretaceous	Dark mudstone	1.27	51	0.11	Fair sample.
Gunnison County, Colorado								
Sec. 12, T. 11 S., R. 89 W.	2G (mac)	Mesaverde	Late Cretaceous	Black mudstone	0.71	49	0.07	Very good coaly mudstone.
SE $\frac{1}{4}$ sec. 5, T. 11 S., R. 90 W.	86-7S	Mesaverde	Late Cretaceous	2-in.-thick coal stringer in sandstone	0.53	50	0.04	Good coal.
Sec. 19, T. 11 S., R. 89 W.	86-7T (coal)	Mesaverde	Late Cretaceous	Coalfied log in sandstone	0.80	50	0.06	Most of sample is cell structure.
SE $\frac{1}{4}$ SW $\frac{1}{4}$ sec. 5, T. 12 S., R. 89 W.	86-7U (mac)	Mesaverde	Late Cretaceous	Dark shale stringer in sandstone	0.65	50	0.09	Fairly coaly shale.
NW $\frac{1}{4}$ sec. 17, T. 12 S., R. 89 W.	86-7V (mac)	Mesaverde	Late Cretaceous	Carbonaceous shale	0.75	65	0.07	Good-quality shale. Organic matter abundant.
Sec. 4, T. 13 S., R. 89 W.	86-7W (coal)	Mesaverde	Late Cretaceous	6-in.-thick coal bed	0.47	7	0.04	Majority of sample is high reflectance grains. A few low-reflectance grains.
NE $\frac{1}{4}$ sec. 11, T. 13 S., R. 87 W.	86-13B (mac)	Mesaverde	Late Cretaceous	Dark-gray silty shale	1.35	16	0.29	Wide range of material. Measured lowest reflectance population.
SW $\frac{1}{4}$ NW $\frac{1}{4}$ sec. 19, T. 13 S., R. 86 W.	86-12J (mac)	Mesaverde	Late Cretaceous	Dark-gray silty shale	4.24	49	0.39	Good-quality sample.
SW $\frac{1}{4}$ NW $\frac{1}{4}$ sec. 19, T. 13 S., R. 86 W.	86-12N (mac)	Mesaverde	Late Cretaceous	Dark-gray silty shale	1.21	46	0.19	Good shale. Measured lowest population.
NE $\frac{1}{4}$ NE $\frac{1}{4}$ sec. 18, T. 15 S., R. 86 W.	86-14A (coal)	Mesaverde	Late Cretaceous	Coal from spoil pile of abandoned Baldwin mine	0.51	50	0.03	Very good coal.
SW $\frac{1}{4}$ NE $\frac{1}{4}$ sec. 8, T. 15 S., R. 86 W.	86-14B (coal)	Mesaverde	Late Cretaceous	1-ft-thick coal seam	0.46	50	0.05	Fair coal.
NW $\frac{1}{4}$ SE $\frac{1}{4}$ sec. 5, T. 15 S., R. 86 W.	86-14C (coal)	Mesaverde	Late Cretaceous	Coal from spoil pile of abandoned Kubler mine	0.58	50	0.04	Good consistent coal.
NE $\frac{1}{4}$ NW $\frac{1}{4}$ sec. 29, T. 15 S., R. 84 W.	86-8R (mac)	Mancos Shale	Late Cretaceous	Dark-gray shale	1.05	51	0.13	Fair shale. No low-reflectance grains.
SE $\frac{1}{4}$ sec. 20, T. 13 S., R. 86 W.	86-8Q (coal)	Mesaverde	Late Cretaceous	Coal from spoil pile of abandoned Smith Hill mine	2.81	50	0.17	Very good coal.
NW $\frac{1}{4}$ SE $\frac{1}{4}$ sec. 28, T. 13 S., R. 86 W.	86-8P (coal)	Mesaverde	Late Cretaceous	Coal from spoil pile of abandoned Peanut mine	2.77	52	0.17	Very good coal.
SE $\frac{1}{4}$ NE $\frac{1}{4}$ sec. 33, T. 13 S., R. 86 W.	86-8Q (coal)	Mesaverde	Late Cretaceous	Coal from spoil pile of abandoned mine	1.87	50	0.10	Very good coal.
SW $\frac{1}{4}$ SE $\frac{1}{4}$ sec. 11, T. 13 S., R. 86 W.	86-14H (mac)	Mancos Shale	Late Cretaceous	Dark-gray shale	0.67	41	0.09	Measured lowest population.
NW $\frac{1}{4}$ sec. 27, T. 12 S., R. 86 W.	86-14I (mac)	Mancos Shale	Late Cretaceous	Dark-gray shale	0.78	16	0.13	Organic matter lean.
SE $\frac{1}{4}$ sec. 18, T. 12 S., R. 86 W.	86-14J (mac)	Mancos Shale	Late Cretaceous	Dark-gray shale	0.52	2	0.02	Grains very scarce. Measured two low-reflectance grains.
NW $\frac{1}{4}$ sec. 27, T. 48 N., R. 5 W.	86-14D (mac)	Mancos Shale	Late Cretaceous	Dark-gray shale	0.53	39	0.12	Fair shale.
Sec. 29, T. 49 N., R. 5 W.	86-8J (mac)	Morrison	Late Jurassic?	Light-green-gray mudstone in maroon and gray sequence	—	—	—	Barren.
Sec. 33, T. 49 N., R. 4 W.	86-8K (mac)	Morrison	Late Jurassic?	Dark-red mudstone in all red sequence	—	—	—	Barren.
Sec. 35, T. 49 N., R. 4 W.	86-8L (mac)	Dakota Sandstone	Late Cretaceous	Black mudstone	1.08	9	0.13	Poor sample. Grain small.
Sec. 21, T. 41 N., R. 3 W.	86-8M (coal)	Dakota Sandstone	Late Cretaceous	Coaly carbonaceous shale from sandstone cliff	0.47	50	0.05	Fair coal. Full of mineral matter.
NW $\frac{1}{4}$ sec. 30, T. 49 N., R. 2 W.	86-8N (mac)	Dakota Sandstone	Late Cretaceous	Dark material from base of highly weathered sandstone	—	—	—	Barren.
NW $\frac{1}{4}$ sec. 1, T. 12 S., R. 88 W.	87-9R (mac)	Mancos Shale	Late Cretaceous	Dark-gray shale	4.82	50	0.44	Very good sample.
NW $\frac{1}{4}$ sec. 1, T. 12 S., R. 88 W.	87-9S (mac)	Mancos Shale	Late Cretaceous	Dark-gray shale	4.50	50	0.34	Very good sample.
SE $\frac{1}{4}$ NE $\frac{1}{4}$ sec. 2, T. 12 S., R. 88 W.	87-100 (mac)	Mancos Shale	Late Cretaceous	Dark-gray shale	3.75	50	0.23	Very good sample.
SE $\frac{1}{4}$ NE $\frac{1}{4}$ sec. 2, T. 12 S., R. 88 W.	87-101 (mac)	Mancos Shale	Late Cretaceous	Dark-gray shale	3.40	50	0.20	Very good sample.
SE $\frac{1}{4}$ NE $\frac{1}{4}$ sec. 2, T. 12 S., R. 88 W.	87-102 (mac)	Mancos Shale	Late Cretaceous	Dark-gray shale	1.55	35	0.14	Two populations; measured lower one.
NE $\frac{1}{4}$ SE $\frac{1}{4}$ sec. 2, T. 12 S., R. 88 W.	87-103 (mac)	Mancos Shale	Late Cretaceous	Dark-gray shale	1.29	60	0.11	Fair sample.
NE $\frac{1}{4}$ SE $\frac{1}{4}$ sec. 2, T. 12 S., R. 88 W.	87-104 (mac)	Mancos Shale	Late Cretaceous	Dark-gray shale	3.06	53	0.27	Good sample.
SE $\frac{1}{4}$ sec. 2, T. 12 S., R. 88 W.	87-105 (mac)	Mancos Shale	Late Cretaceous	Sandy shale	1.25	50	0.09	Fair sample.
SE $\frac{1}{4}$ sec. 2, T. 12 S., R. 88 W.	87-107 (mac)	Mancos Shale	Late Cretaceous	Gray shale	1.43	42	0.16	Measured lowest population.
SE $\frac{1}{4}$ sec. 2, T. 12 S., R. 88 W.	87-108 (mac)	Mancos Shale	Late Cretaceous	Gray shale	1.77	35	0.23	Two populations; measured lower one.

